CRP40: CLINICAL IMPLICATIONS IN PARKINSON'S DISEASE

CATECHOLAMINE REGULATED PROTEIN 40 (CRP40): CLINICAL IMPLICATIONS IN PARKINSON'S DISEASE

By SARAH E. GROLEAU

A Thesis Submitted to the School of Graduate Studies
in Partial Fulfillment of the Requirements for
the Degree of
Doctor of Philosophy, McMaster University

DOCTOR OF PHILOSOPHY (2013) Neuroscience

McMaster University Hamilton, Ontario

Title: Catecholamine Regulated Protein 40 (CRP40): Clinical Implications in Parkinson's Disease

Author: Sarah E. Groleau, B.Sc. (Hons) University of Western Ontario

Supervisor: Dr. J.P. Gabriele

Committee: Dr. R.K. Mishra,
Dr. J. Rosenfeld,
Dr. L. Doering

Number of pages: xv, 197

Abstract:

Parkinson's disease (PD) is characterized by progressive cell death of the dopaminergic neurons of nigrostriatal pathway. Several causes have been implicated for PD via neurochemical research including mitochondrial dysfunction, oxidative stress, and protein misfolding, to list a few. The novel Catecholamine Regulated Protein 40 (CRP40) has certain dopaminergic and neuroprotective features that implicate its importance for PD research. Recent studies using post-mortem brain tissue of patients with PD found MOT-2/CRP40 depletion in the frontal cortex and substantia nigra. MOT-2/CRP40 reduction is also observed in striatal brain tissue samples from a hemi-lesioned preclinical animal model of PD. Most recently, work done at the University of Laval in collaboration McMaster University suggests that levels of CRP40 mRNA are in deficit in blood platelet samples from a primate model of PD.

The studies presented in this thesis suggest that the CRP40 protein has a dual function with regards to PD. The full-length CRP40 binds dopamine and, upon injection at the striatum of 6-hydroxydopamine hemi-lesioned rats, alleviates behavioural symptoms for up to 7 days. On the other hand, a 7kDA fragment of CRP40 does not bind dopamine, but does confer the same alleviatory effect upon intra-striatal injection in 6-hydroxydopamine hemi-lesioned rats. Not only has a protein now been identified with novel potential as a therapeutic agent for PD, but also the approximate region of the CRP40 protein responsible for behavioural effects.

The later studies of this thesis show that CRP40 is found dysregulated in platelets of PD patients and lymphocytes of SCZ patients. This evidence has revealed CRP40 as a novel PD biomarker, for which on going studies are now in place to explore the potential of CRP40 as a diagnostic for PD.

Acknowledgements:

My first and sincere appreciation goes to Dr. Joseph Gabriele, my thesis supervisor, for all I have learned from him and for his support over the last four years.

I would also like to express my gratitude and respect to Drs. Ram Mishra and Eva Werstiuk whose advice and insight were invaluable to me during my graduate studies.

In addition, my greatest appreciation and thanks goes to Nancy Thomas for sharing her expertise in the laboratory, and for teaching me the skills I needed to become the scientist that I am today.

I would like to thank my family, especially my Mother and Father, for always believing in me, as well as for their continuous love and support.

Thanks, also, to the students of Dr. Mishra's laboratory who made the lab a friendly and fun environment to work in.

Table of Contents:

Lists of Figures:

Lists of Tables:

List of Abbreviations and Symbols:

%PPI	Percent prepulse inhibition
[3H]-DA	Tritiated dopamine
3-MT	3-methoxytyramine
6-OHDA	6-hydroxydopamine
AD	Alzheimer's disease
AIF	Apoptosis inducing factor
ANOVA	Analysis of variance
ATP	Adenosine triphosphate
CAF	Central Animal Facility
cAMP	Cyclic adenosine monophosphate
CNS	Central nervous system
COMT	Catechol-o-methyltransferase
CQDM	Quebec Consortium for Drug Discovery
CRP40	Catecholamine Regulated Protein (40kDa)
DA	Dopamine
DAT	Dopamine transporter
DJ-1	Parkinson’s disease protein 7
dB	Decibels
DNA	Deoxyribonucleic acid
DOPAC	Dihydroxyphenylacetic acid

DSM-IV	Diagnostic Statistical Manual of Mental Disorders
Ep	Epinephrine
ETC	Electron transport chain
GFP	Green fluorescent protein
HPLC	High performance liquid chromatography
HSP47	Heat shock protein (47kDA)
HSP70	Heat shock protein (70kDA)
HVA	Homovanillic acid
L-DOPA	Levodopa (L-3,4-dihydroxyphenylalanine)
LB	Lysogeny broth
MAO	Monoamine oxidase
MMP	Mitochondrial membrane potential
MMSE	Mini mental-state examination
MOT-2	Mortalin protein
MPTP	1-methyl-4-phenyl-1,2,3,6-tetrahydropyridine
mRNA	Messenger ribonucleic acid
MWM	Morris Water Maze
NA	Nucleus Accumbens
NMDA	*N*-methyl-D-aspartate
NorEp	Norepinephrine
p53	Tumor suppressor protein
PD	Parkinson's disease

PET	Positron emission tomography
PFC	Prefrontal cortex
PPI	Prepulse inhibition
ROS	Reactive oxygen species
RpoC	RNA Polymerase β' Subunit
RT-PCR	Reverse transcription polymerase chain reaction
SCZ	Schizophrenia
SN	Substantia Nigra
TH	Tyrosine hydroxylase
TTX	Tetrodotoxin
UCM	Umbilical cord matrix
VTA	Ventral tegmental area
WT	Wildtype

Declaration of Academic Achievement:

CHAPTER 4: CRP40 PROTEIN ALLEVIATES BEHAVIOURAL SYMPTOMS IN A RAT MODEL OF PARKINSON'S DISEASE

Dr. Joe Gabriele and myself designed experiments described in this chapter. Nancy Thomas and myself performed the studies from cloning to animals to HPLC. Dr. Mark Ferro and myself are writing the manuscript in preparation for publication of these results.

CHAPTER 5: CLONED FRAGMENTS OF CRP40 ALLEVIATE BEHAVIOURAL SYMPTOMS IN A RAT MODEL OF PARKINSON'S DISEASE (PILOT STUDY)

Dr. Joe Gabriele and myself designed experiments described in this chapter. Drs. Zdenek Pristupa, Ram Mishra, and Joe Gabriele designed the fragments to be used in the animal studies. Jovana Lubarda and Nancy Thomas cloned and purified the protein fragments used for animal studies. Nancy Thomas and myself performed the animal studies. Dr. Mark Ferro and myself are writing the manuscript in preparation for publication of these results.

CHAPTER 6: EFFECTS OF CRP40 ON MEMORY AND COGNITION IN A MOUSE MODEL OF ALZHEIMER'S DISEASE (CONTROL STUDY)

Dr. Joe Gabriele and myself designed experiments described in this chapter. Dr. Monica Marchese trained me to perform the eight-day Morris Water Maze paradigm. Nancy Thomas and myself performed the studies from cloning to animals. Dr. Henry Szechtman and myself performed the statistical analysis of the Morris Water Maze results.

CHAPTER 7: HUMAN BLOOD ANALYSIS REVEALS DIFFERENCES IN GENE EXPRESSION OF CRP40 IN PARKINSON'S DISEASE

Dr. Joe Gabriele designed experiments described in this chapter. Nancy Thomas, Jovana Lubarda, and myself performed the studies from blood separation to RT-PCR. Jovana Lubarda, Dr. Mark Ferro, and myself wrote the manuscript for publication of these results.

CHAPTER 8: APPLICATIONS FOR SCHIZOPHRENIA: HUMAN BLOOD ANALYSIS REVEALS DIFFERENCES IN GENE EXPRESSION OF CRP40

Dr. Joe Gabriele designed experiments described in this chapter. Nancy Thomas performed the studies from blood separation to RT-PCR. Jovana Lubarda, Dr. Mark Ferro, and myself wrote the manuscript for publication.

CHAPTER 1

INTRODUCTION TO DOPAMINE

1.0 Dopamine

Dopamine (DA) is one of three neurotransmitters termed catecholamines. These compounds are named for their structure: benzene with two hydroxyl side groups (catechol ring) and an ethylamine arm (Fitzgerald, 2011). This category also includes epinephrine (Ep) and norepinephrine (NorEp). Catecholamines are present both as neurotransmitters in the central nervous system (CNS) and as hormones in the peripheral systems of the body. Of the total catecholamine concentration found in the CNS, DA is the most abundant, constituting approximately 80%. DA can be found in various brain regions; the striatum, nucleus accumbens (NA), substantia nigra (SN), ventral tegmental area (VTA), olfactory tubercle, cortex, amygdala, subthalamic nucleus, pituitary, hypothalamus, thalamus, hippocampus, and cerebellum (Vallone et al., 2000). Only about 1% of the brain's synapses are dopaminergic, and over 80% of brain DA is located within the basal ganglia (Cowan et al., 2001; Siegel et al., 1994). DA is involved in pathways that regulate motor control, memory, motivation, reward and desire, addiction, and maternal behavior.

1.1 Dopamine synthesis and metabolism

DA synthesis occurs at the VTA and SN. Phenylalanine is first acquired through diet, and is hydroxylated to the amino acid tyrosine, which can cross the blood-brain barrier (Kopin, 1968; Siegel et al., 1994). Conversion of tyrosine by rate-limiting enzyme tyrosine hydroxylase (TH) results in levodopa (L-3,4-dihydroxyphenylalanine; L-DOPA), which is then converted by the enzyme DOPA decarboxylase to DA (Figure 1a) (Kopin, 1968; Siegel et al., 1994). Hydroxylation of DA produces NorEp, which can be methylated to form Ep (Figure 1b) (Kopin, 1968; Siegel et al., 1994).

DA is taken up from the cytosol and concentrated in storage vesicles in the nerve terminal, where it either remains DA or is further processed into NorEp (Siegel et al., 1994). From there, NorEp can be released into the cytosol where it is processed into Ep (Siegel et al., 1994).

Excess synaptic DA is collected and deposited into surrounding cells by the 12-transmembrane domain DA transporter (DAT), where it is either recycled into vesicles or metabolized (Schultz, 1998; Torres, 2003). This mechanism of re-uptake silences the signal of DA until the next wave of vesicular release. Amphetamine and cocaine are DA receptor agonists that inhibit the reuptake of catecholamines from the synaptic cleft (Siegel et al., 1994). Cocaine inhibits DAT, while amphetamine competes with DA by binding DAT (Siegel et al., 1994).

DA metabolism occurs by function of two catabolic enzymes: monoamine oxidase (MAO) and catechol-o-methyltransferase (COMT). MAO, located on the outer membrane of mitochondria, inactivates catecholamines that are free within the nerve terminal (Siegel et al., 1994). Specifically, oxygen is used to remove the amine group from DA, converting DA to 3,4-Dihydroxyphenylacetic acid (DOPAC) (Kopin, 1968; Siegel et al., 1994; Edmondson, 2004). DOPAC is further metabolized by COMT to form homovanillic acid (HVA), which can be excreted from the body via urination (Figure 2) (Matsumoto, 2003). COMT also acts on extraneuronal DA by introducing a methyl group, converting DA to 3-methoxytyramine (3-MT) (Siegel et al., 1994; Matsumoto, 2003). 3-MT is further metabolized by MAO to HVA (Figure 2) (Kopin, 1968; Siegel et al., 1994; Matsumoto, 2003).

1.2 Dopamine receptors

Release of DA into the synapse from presynaptic vesicular storage occurs by calcium-mediated exocytosis. Action potentials that reach the presynaptic terminal mediate fusion of vesicles with the neuronal membrane, thereby releasing DA into the synaptic cleft (Figure 3) (Siegel et al., 1994; Sudhof, 1995). Once released, DA acts as a ligand for one of five receptor types, depending on the brain region and intended function (Vallone et al., 2000).

DA receptors act indirectly via second messenger systems to bring about a post-synaptic response by coupling with G-proteins (Siegel et al., 1994). The five 7-transmembrane domain receptors (D1, D2, D3, D4, D5) can be separated into two distinct groups: D1-like receptors (D1 and D5) and D2-like receptors (D2, D3, and D4). Members of the D1-like group are responsible for activation of adenylyl cyclase, thereby increasing concentrations of cyclic adenosine monophosphate (cAMP), mobilizing calcium stores, and decreasing concentrations of arachidonic acid (Siegel et al., 1994; Vallone et al., 2000). Conversely, D2-like receptors are responsible for inhibition of adenylyl cyclase, thereby decreasing concentrations of cAMP, dampening calcium channel activity, and increasing concentrations of arachidonic acid (Siegel et al., 1994; Vallone et al., 2000). Each receptor is localized to specific brain regions (Table 1), and can be found on both the pre-synaptic and post-synaptic neurons.

It is the D2 receptor group, specifically, that is implicated in movement and locomotion (Vallone et al., 2000). D2 receptors have been implicated in psychosis, movement disorders, and neurodegenerative disease. Psychotic disorders may be the result of overstimulation of D2 receptors, while understimulation of D2 receptors is responsible for locomotor symptoms in neurodegenerative movement disorders like Parkinson's disease (PD) (Siegel et al., 1994).

1.3 Dopaminergic tracts and connectivity

There are four dopaminergic neural pathways: nigrostriatal, mesolimbic, mesocortical, and tuberoinfundibular. The nigrostriatal pathway is responsible for modulating movement and locomotion via binding of DA to D1 and D2 receptors. This pathway originates in the SN, sending axons to the striatum (Figure 4) (Siegel et al., 1994). The nigrostriatal pathway is degenerated in PD patients. The mesolimbic pathway influences motivated behaviour and is implicated in addiction. This pathway originates in VTA and sends axons to NA (Figure 4) (Siegel et al., 1994). The mesocortical pathway, involved in aspects of learning and memory, originates in the VTA and sends axons to the NA and frontal cortex (Figure 4) (Siegel et al., 1994). DA imbalances in the mesolimbic/mesocortical pathways have been implicated in Schizophrenia (SCZ) and other psychotic diseases. The tuberoinfundibular pathway is involved in the stimulation of milk production via connections with the mammary glands (Vallone et al., 2000). This pathway originates in the hypothalamus, sending axons to pituitary, median eminence. It is responsible for regulation of pituitary hormones like prolactin (Siegel et al., 1994).

The neurotoxin 6-hydroxydopamine (6-OHDA) has been found to deplete the neurotransmitter content of dopaminergic neurons, effectively causing anterograde degeneration of the entire neuron (Ungerstedt, 1968). In experiments by Thompson and Moss (1995), 6-OHDA lesioning at the

prefrontal cortex (PFC) caused an 80% decrease in the number of TH-containing cells. Interestingly, this PFC lesion caused a nearly 3-fold increase in DA abundance at the NA compared to non-lesioned controls. After reproduction and confirmation, this observable fact has become known as the DA connectivity phenomenon; where a decrease in cortical DA causes an increase in subcortical DA, and vice versa (Thompson and Moss, 1995). Karreman and Moghaddam (1996) performed experiments using a DA receptor agonist and various inhibitory compounds to further elucidate the mechanisms of the DA connectivity phenomenon. Their results suggest that the PFC regulates DA concentrations at the striatum (as predicted by the DA connectivity phenomenon) via mediatory signalling from the VTA (Karreman and Moghaddam, 1996).

1.4 Dopamine cytotoxicity

Free DA (molecules of DA not stored in vesicles) can be oxidized to DA quinones (Van Laar et al., 2007; Graham et al., 1978). Quinones are a form of reactive oxygen species (ROS) and are detrimental to cellular and genetic health. There are multiple pathways that result in the production of DA quinones including spontaneous oxidation, protein mediated oxidation, and oxidation by a metal catalyst (Stokes et al., 1999). For example, the natural breakdown of DA by MAO produces hydrogen peroxide, a ROS. Further, hydrogen peroxide can react with transition metals, like iron, to produce hydroxyl radicals (Stokes et al., 1999). Some naturally occurring proteins can use DA as an electron donor, converting DA to different species of electron-deficient DA quinones (Stokes et al., 1999).

The toxicity of DA quinones lies in their ability to target sulfhydryl groups on cellular proteins and use them in nucleophilic addition reactions. These groups are often found at protein active sites, any modification to which can lead to protein inactivation and aggregation (Stokes et al., 1999). DA quinones also have genotoxic abilities; they can covalently modify DNA and can cause DNA strand breaks. Extensive inactivation of proteins or DNA damage can ultimately lead to DA-induced apoptosis of the neuron (Stokes et al., 1999). Dopaminergic neurons in culture show extensive cell death following exposure to DA at physiologically-similar concentrations between 50–200 μM (Michel and Hefti, 1990; Simantov et al., 1996;

Shinkai et al., 1997; Zhang, 1998). Specifically, DA enhances the translocation of cytochrome c from the mitochondrion to the cytosol and activates caspase-3; two important proteins with activational functions in the intrinsic apoptotic pathway (Figure 5) (Pirger et al., 2009).

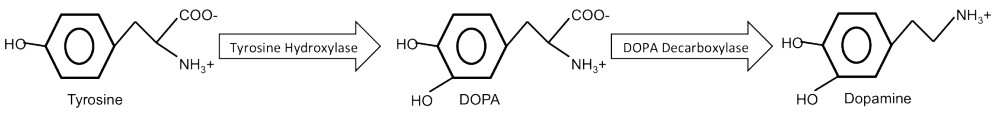

Figure 1a: DA synthesis from tyrosine via DOPA (adapted from Siegel et al., 1994).

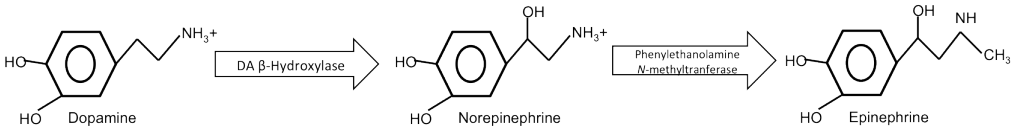

Figure 1b: DA conversion to NorEp, and NorEp conversion to Ep (adapted from Siegel et al., 1994).

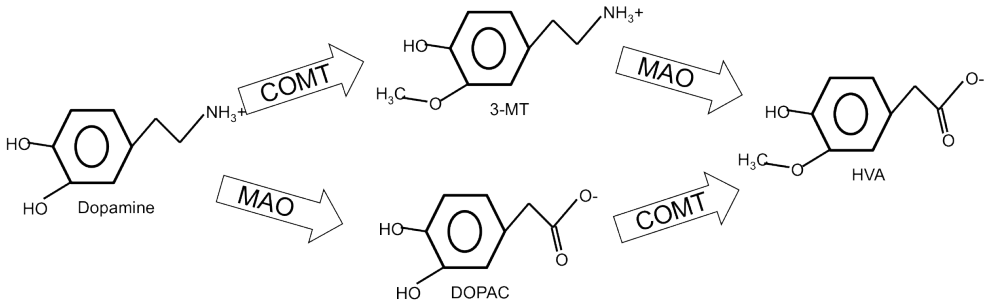

Figure 2: DA degradation pathways– conversion to HVA via either 3-MT or DOPAC (adapted from Siegel et al., 1994).

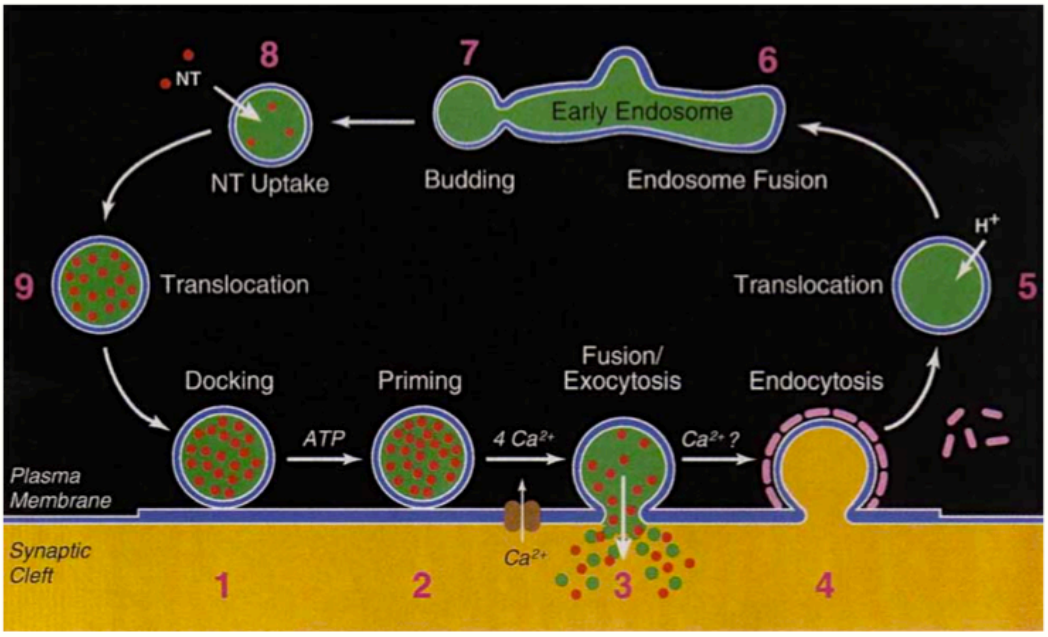

Figure 3: Synaptic vesicle cycling at the presynaptic terminal (from Sudhof, 1995).

Receptor	**Receptor Localization**
D1	Striatum, NA, Olfactory Tubercle, Cortex, Amygdala, Subthalamic Nucleus
D2	Striatum, NA, Olfactory Tubercle, SN, VTA, Pituitary (Non-CNS Tissue Localization: Retina, Kidney, Vasculature)
D3	Hypothalamus, Thalamus, Cerebellum, SN
D4	Frontal Cortex, Amygdale, Olfactory Bulb, Hippocampus, Hypothalamus, Mesencephalon
D5	Thalamus, Hypothalamus

Table 1: Localization of specific DA receptors to different brain regions.

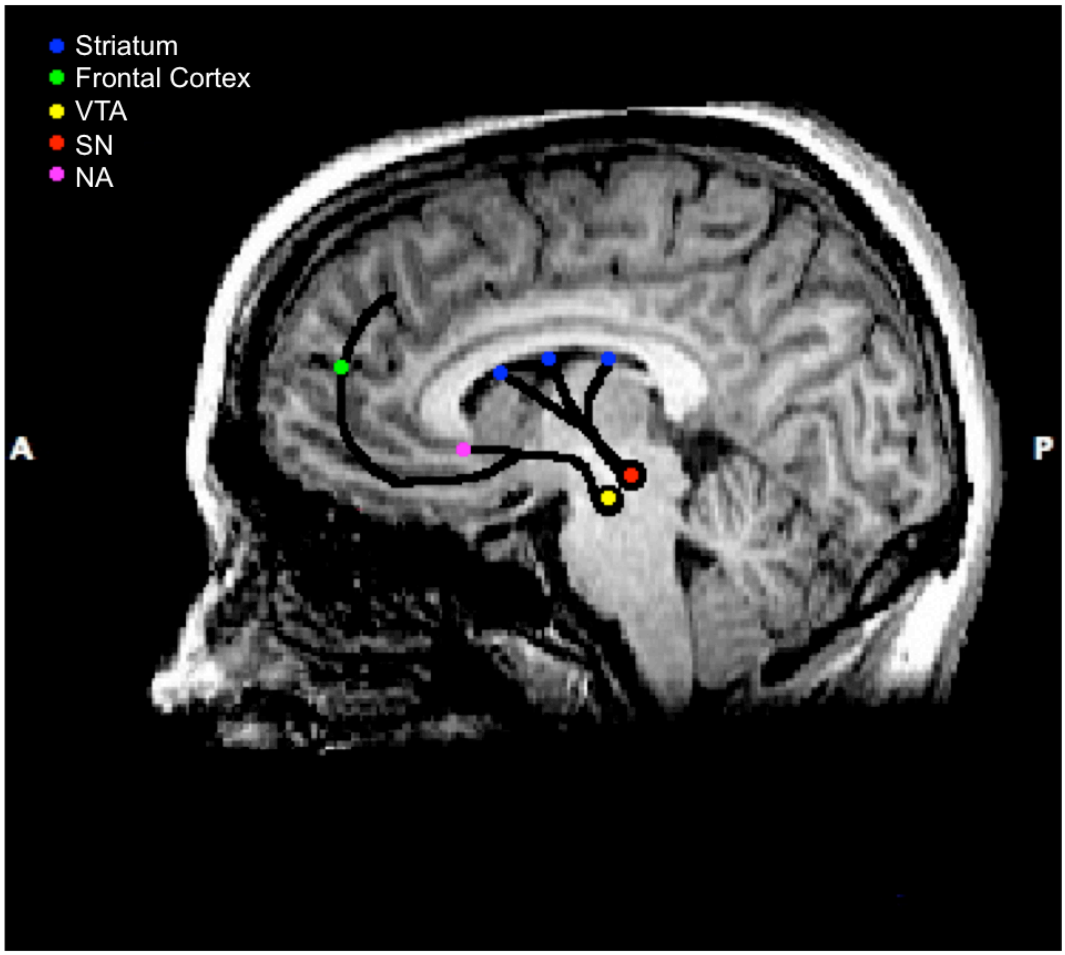

Figure 4: Dopaminergic tracts of the human brain (Groleau, 2013).

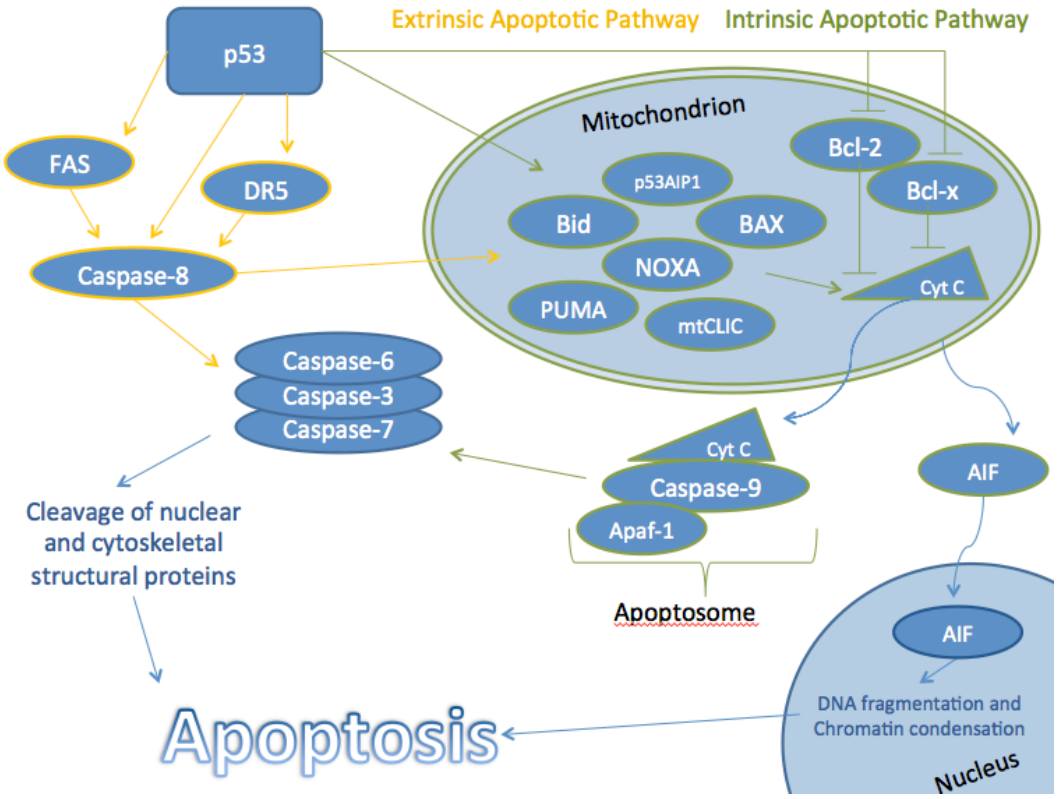

Figure 5: Extrinsic and intrinsic apoptotic pathways.

CHAPTER 2

INTRODUCTION TO CATECHOLAMINE REGULATED PROTEIN 40

2.0 Heat shock proteins and molecular chaperones

Molecular chaperones are a class of proteins whose main function is to ensure the correct folding and functional maturation of other cellular proteins (Ellis, 1987). They can also disassemble misfolded proteins and interfere with detrimental protein interactions (Ellis, 1987). Molecular chaperones function by forming transient complexes with their target proteins (Schlesinger, 1990). In some cases, the protein-chaperone interaction occurs under the cooperation of multiple chaperones (Hendrick and Hartl, 1993).

Molecular chaperones prevent the aggregation of newly translated polypeptides. The chaperone proteins ensure new peptides stay soluble by binding their hydrophobic regions; thereby preventing improper folding that could occur before synthesis is complete (Hendrick and Hartl, 1993; Becker and Craig, 1994). The chaperone will then disengage by hydrolysis of adenosine triphosphate (ATP), and the peptide can fold into its final conformation.

Chaperones also encourage the breakdown of proteins that are either no longer needed or damaged past the point of rescue. To target proteins for degradation, chaperones work closely with ubiquitin pathways, as well as pathways of lysosomal proteolysis and degradation specific to individual organelles (Hayes and Dice, 1996).

Heat Shock Proteins of size 70kDa (HSP70) are a family of highly conserved molecular chaperones containing an amino-terminal ATPase domain and a variable peptide-binding site at the carboxyl terminal. Some HSP70s are constitutive, but all are inducible by cell stress (Hendrick and Hartl, 1993; Becker and Craig, 1994). HSP70s have the ability to protect the structure and function of cellular proteins by binding the threatened proteins under conditions of cellular stress. As the concentration of unbound HSP70s decreases, the cell responds by upregulating HSP70s to replenish its stock (Becker and Craig, 1994). By binding the exposed hydrophobic regions of proteins under denaturing stress, these 70kDa chaperones prevent endangered proteins from precipitating in the cell, giving them the chance to be reconfigured post-stress (Becker and Craig, 1994).

2.1 Mortalin-2: mitochondrial HSP70

Mortalin-2 (MOT-2, HSPA9, GRP75, mtHSP70; chromosome 5q31.1), a ubiquitously expressed mitochondrial HSP70 with catecholamine binding abilities, has many functions within the cell. It is involved in the import of mitochondrial proteins, production of ATP, rescue of misfolded proteins, and detection of oxidative stress (Kaul et al., 2007; Deocaris et al., 2008; Kaul et al., 2012). MOT-2 has two functional domains: an N-terminal nucleotide-binding domain (ATPase domain), and a C-terminal substrate-binding domain (Domanico et al., 1993). This mitochondrial chaperone has been implicated in such diseases as SCZ, Ischemia, PD, and carcinoma, as well as in Alzheimer's (AD) and Huntington's (Kaul, 2007; Deocaris et al., 2008).

MOT-2 is an important player in the transfer of mitochondrial proteins from the cytosol to the mitochondrial matrix. Here, the proteins targeted for transfer must stay partially hydrophobic to be accepted into the matrix and intermembrane space by mitochondrial membrane pores. MOT-2 prevents these proteins from conforming into their tertiary and quaternary structures until they are safely translocated (Hendrick and Hartl, 1993; Becker and Craig, 1994). Further, MOT-2 can catalyze the disassembly of damaged or unused mitochondrial proteins within the organelle (Hayes and Dice, 1996).

Studies using human fibroblasts revealed that normal aging causes a time-dependant decrease in neuronal concentrations of MOT-2 (Deocaris et al., 2008). Other factors leading to loss of functional MOT-2 protein in neurons include environmental toxins and exacerbation of oxidative stress (Deocaris et al., 2008).

Results from studies overexpressing MOT-2 in mouse astrocytes under glucose deprivation confirm previous hypotheses that MOT-2 protects against ischemic astrocyte injury *in vitro* in the following ways: a) control cells showed a four-fold increase in ROS compared to MOT-2 treated cells; b) control cells displayed a 15% mitochondrial membrane depolarization, whereas MOT-2 treated cells maintained full mitochondrial membrane potential (MMP); c) control cells exhibited 30% more ATP depletion compared to MOT-2 treated cells and; d) total astrocytic cell death was 25% in control cells, while MOT-2 treated cells only suffered a total of 5% cell death (Volobоueva et al., 2008).

Xu and colleagues (2009) overexpressed MOT-2 to study its protective effect against ischemia *in vivo*. MOT-2 treated animals showed a 42% reduction in size of infarction following middle cerebral artery occlusion compared to controls. They also showed significantly less damage by oxidative stress compared to controls (Xu et al., 2009). Post-occlusion activity of mitochondrial complexes was measured. Results showed more preservation of function of complex IV in animals treated with MOT-2 than

any other group or control (Xu et al., 2009). Further, MOT-2 treated animals suffered 30% more ATP depletion compared to controls and other treatments. This result compliments those found by Voloboueva and colleagues– MOT-2 protects against mitochondrial-specific ischemic brain injury *in vivo*, displaying impressive neuroprotective properties (Sun et al., 2006; Voloboueva et al., 2008; Xu et al., 2009).

To date, many publications exist that detail MOT-2's involvement in carcinogenesis (Deocaris et al., 2008). Functional MOT-2 binds the tumour suppressor protein (p53) in the cytoplasm, tethering it there. *In vivo*, during high stress, MOT-2 is recruited to the mitochondria for damage control, leaving p53 unbound and free to induce apoptotic signalling (Londono et al., 2012) (Figure 5). Underexpression of MOT-2 causes activation of the p53-Bax apoptotic pathway, while overexpression of MOT-2 causes complete inactivation of p53 leading to constitutive cell division, immortalization of cells, and carcinomas (Walker et al., 2006; Bottger et al., 2008).

Specific implications of MOT-2 in PD and SCZ have been growing robustly over the last decade. These important relationships will be discussed in sections 3.3 and 8.1.

2.3 Catecholamine Regulated Protein 40kDa

2.3.1 Bovine CRP40

Nair and Mishra (2001) were the first to clone and characterize the novel Catecholamine Regulated Protein of size 40kDa (CRP40; chromosome 5q31.1). This protein of bovine origin that shares homology with HSP70 and MOT-2 (Nair and Mishra, 2001). The bovine CRP40 was found to covalently associate with DA, Ep, and NorEp, but not with serotonin or other amines, which implicates its functional specificity to catecholamines (Nair and Mishra, 2001). It was discovered that bovine CRP40 is induced by DA when its expression was significantly increased in SH-SY5Y cells incubated with excess DA (Nair and Mishra, 2001). This increased expression at high concentrations of DA is inhibited by treatment of cells with antioxidants, implicating CRP40 in the response pathways associated with oxidative stress resulting from the oxidation of excess DA (Nair and Mishra, 2001). Interestingly, after heat shock, cells treated with bovine CRP40 displayed decreased protein denaturation and aggregation compared to controls, drawing similarity between the functions of CRP40 and other heat shock proteins/molecular chaperones, including MOT-2 (Nair and Mishra, 2001).

2.3.2 Human CRP40

More recently, a human CRP40 that shows significant homology with the bovine strain was cloned and characterized by Gabriele and colleagues (2009). Messenger ribonucleic acid (mRNA) and protein sequencing revealed that the human CRP40 is 100% homologous to the C-terminus substrate-binding domain of human MOT-2 (from exon 10 to exon 17 with an independent promoter region found at intron 9) (Gabriele et al, 2009) (Figure 6a & Figure 6b). The human CRP40 protein will be discussed and examined throughout the remainder of this dissertation.

Covalent affinity labelling was used to localize CRPs to specific regions of the brain. The relative concentrations of CRPs, conforms to the following trend from areas of greatest concentration to areas of lower concentration: Striatum > NA > Olfactory Tubercle > Frontal Cortex > Hypothalamus > Hippocampus > Cerebellum (Ross et al., 1995). Non-CNS tissues were also probed; all were negative for CRP labelling including heart, liver, kidney, skin, spleen, and muscle (Ross et al., 1995).

2.3.3 Dopaminergic implications of CRP40

Human CRP40 displays DA binding capabilities with low affinity and high capacity (Figure 7) (Gabriele et al., 2009). Localization studies by Goto and colleagues (2001) exhibit TH in co-localization with CRP40, corroborating the theory that CRP40 has catecholamine-specific functions (Goto et al., 2001).

In SH-SY5Y neuroblastoma, cell treatment with haloperidol (a commonly used D2 receptor antagonist for treatment of SCZ) caused increased free synaptic DA and a subsequent increase in the expression of human CRP40 compared to untreated cells (Gabriele et al., 2009). This result parallels the bovine finding– CRP40 expression is inducible by high concentrations of DA.

Further, immunofluorescence results have localized human CRP40 to the cytoplasm in healthy post-mortem human NA, as well as in drug naive schizophrenic NA tissue, but to the nucleus in haloperidol-treated schizophrenic post-mortem tissue. Interestingly, this nuclear translocation occurs in response to apoptotic pathways set in motion by DA oxidative stress which strengthens the theory that CRP40 is a neuroprotective agent (Gabriele et al., 2009). Further implications of CRP40 in the pathogenesis of SCZ will be discussed in section 8.1, and implications of CRP40 in PD, another DA-related neurodegenerative disease, will be discussed in section 3.3.

In studies using DA D1 and D2 receptor antagonist treatments in rats, Sharan and colleagues (2000) found that antagonists of each receptor caused a differential modulation of CRP40 protein expression *in vivo*. In animals treated with Haloperidol, a D2 receptor antagonist, there was a marked increase in striatal CRP40. Haloperidol blocks the D2 receptor DA binding site, causing an increase in free extracellular DA, in response to which CRP40 expression was induced. In animals treated with SCH23390, a D1 receptor antagonist, there was a significant decrease in striatal CRP40. SCH23390 blocks the D1 receptor DA binding site, thereby also causing an increase in free extracellular DA. Interestingly, however, this scenario does not cause an increase in CRP40 protein. It is possible that D1 receptors have a role in the inducing pathway of CRP40, but that they cannot carry out such functions when blocked by an antagonist (Sharan et al., 2000).

Many further studies have been done to tease apart the DA-inducibility of CRP40. According to experiments by Gabriele and colleagues (2002), chronic, but not acute, amphetamine treatment causes a marked increase in CRP40 expression in both the striatum and the NA in rats. The modulatory effects of amphetamine are specific to CRP40 expression since the experiments were repeated to investigate expression of HSP70, with no change found (Gabriele et al., 2002). Similar experiments by Sharan and colleagues (2003) showed that acute treatment with cocaine,

which increases extracellular DA, caused a significant increase in CRP40 expression in the striatum and NA of rats. Chronic cocaine treatment caused a significant CRP40 increase as well, but only in the NA. Further, cocaine treatment accompanied by anisomycin treatment, which blocks protein synthesis, inhibited the increase in CRP40 (Sharan et al., 2003). This finding shows that the increase in CRP40 caused by cocaine exposure is via upregulation and increased expression, as opposed to protein translocation. The modulatory effects of cocaine on CRP40 expression are also CRP40 specific since the experiments were repeated to investigate expression of HSP70, with no change found (Sharan et al., 2003). In another study, Gabriele and colleagues (2003) found that chronic Quinpirole (a high affinity D2/D3 receptor agonist) treatment leads to decreased CRP40 at the striatum, VTA, and PFC, but increased CRP40 at the NA, as predicted by the DA connectivity phenomenon.

2.3.4 Neuroprotective functions of CRP40

Cells incubated with human CRP40 showed decreased protein denaturation and aggregation following heat shock, implicating the human strain of this protein as a heat shock protein and molecular chaperone (Gabriele et al., 2009). Previously, a MOT-2 mutant was used to study the function of the carboxyl terminal (CRP40) in protecting against ischemic brain injury. CRP40 protected against ischemic brain injury almost as well as the MOT-2 wildtype (WT) in the following ways: a) primary astrocytes were protected against ischemic insults *in vitro*; b) infarct size and neurological dysfunctions were reduced *in vivo*; c) protein aggregation (measured by ubiquitin tagging) was decreased and; d) apoptosis inducing factor (AIF) translocation to the nucleus was inhibited (Sun et al., 2006). These results suggest that CRP40 (the carboxyl terminal of MOT-2) possesses the impressive neuroprotective properties previously exhibited by MOT-2 (Sun et al., 2006). This chaperone-like protein has become an exciting new target for studying neurodegeneration and exploring new avenues for therapeutics thereof.

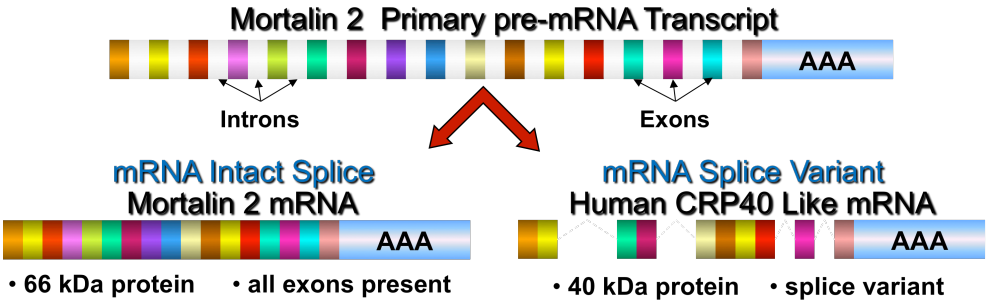

Figure 6a: Alternative splice variance from the *Mortalin* gene (Gabriele et al., 2009).

Figure 6b: Crystal structure of MOT-2 substrate binding domain, which is homologous to CRP40 (Protein Data Bank, 2013)

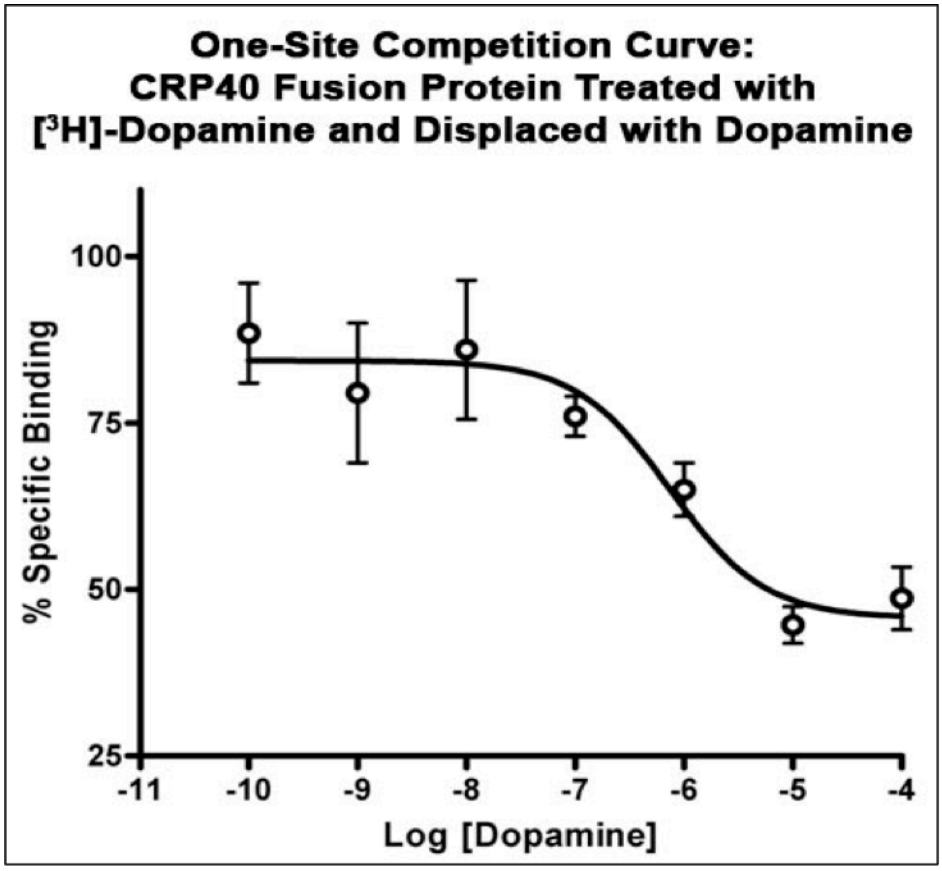

Figure 7: Competition curve indicating that CRP40 binds to DA in a low affinity and high-capacity manner with an approximate IC50 of 25μM (Gabriele et al., 2009).

CHAPTER 3

INTRODUCTION TO PARKINSON'S DISEASE

3.0 Global statistics

PD is a universal disease, affecting people of both sexes and of all ethnicities. PD affects approximately 1% of the population over the age of 65, making it one of the most frequent neurodegenerative disorders (WHO, 2006). About 0.3% of the general population is affected, which translates into approximately 100,500 Canadians (Lang and Lozano, 1998). The World Health Organization reports PD at an incidence rate of roughly 4.5–19 per 100,000 population per year (WHO, 2006). Others report age-adjusted rates of prevalence in the range of 72–258.8 per 100,000 persons (Marras and Tanner, 2004). Recent data show a higher proportion of males affected by this disorder compared to females (1.9 males per 1 female), which is in contrast to the previously accepted theory that PD affects individuals of both sexes equally (Van Den Eeden et al., 2003).

3.1 Symptoms and pathophysiology

PD is characterized by progressive cell death specific to the dopaminergic neurons of the SN. This disease can cause major (>90%) loss of basal ganglia neurons in its late stages (Siegel et al., 1994). The resulting loss of DA neurotransmission in the nigrostriatal tract (Figure 4) is associated with impairments in movement and locomotion. Cardinal symptoms include muscle tone rigidity, akinesia, postural decline, and tremor at rest (Lang and Lozano, 1998). Some patients with PD will also suffer from cognitive and psychiatric dysfunction (Moore et al., 2005). Dementia is becoming increasingly recognized as a major symptom of PD, and contributes greatly to shortened life in patients with this disease (Lang and Lozano, 1998).

Currently, diagnosis is confirmed only by clinical criteria, based on how a patient's symptoms have manifested (Hughes et al., 2001). There is no definitive biological marker to confirm PD diagnosis, and approximately 25% of patients are misdiagnosed (Rajput et al., 1991; Tolosa et al., 2006).

Another major characteristic of PD, though not visible until autopsy or post-mortem study, is the presence of Lewy bodies– plaque-like structures in the brain. These proteinaceous inclusions form only in the cytoplasm of surviving dopaminergic neurons (Moore et al., 2005; Londono et al., 2012). Recent findings suggest that Lewy bodies may be the result of the

body's attempt to protect the brain against the progression of PD by sequestering toxic insoluble proteins in one place so they may be rendered less harmful (Lang and Lozano, 1998).

The PD pattern of deterioration starts at the ventro-lateral SN and progresses to the medial-ventral SN. This trend is highly specific to PD, and is opposite of trends observed in normal aging (Lang and Lozano, 1998).

Several causes have been implicated for PD pathophysiology via neurochemical research. Those most relevant to the current study include: mitochondrial dysfunction, oxidative stress, and protein misfolding; however, others include: excitotoxins, neurotrophic deficiencies, and abnormal immune response mechanisms (Schapira et al., 1992; Lang and Lozano, 1998; Hastings, 2009; Sajjad et al., 2010).

Mitochondrial dysfunction in PD occurs as a significant decrease in activity levels of Complex I proteins in the SN (Moore et al., 2005; Lang and Lozano, 1998; Hastings, 2009). A defect of this magnitude could be responsible for energy failure leading to apoptosis, or a weakening of the cell against such insults as toxins, oxidative stress, or mutagens.

ROS are natural by-products of the electron transport chain (ETC) responsible for ATP biogenesis in the mitochondria. When the cell and mitochondria are healthy, these natural toxins are disposed of by various, highly conserved processes (Lang and Lozano, 1998). However, as

discussed earlier, if these ROS are not properly controlled, they can react with proteins, and other cellular molecules, altering their structures and leading to cell damage or death. Specifically, oxidative stress leads to rapid proteolytic degradation (Deocaris et al., 2008). Loss of important chaperones in this manner would ultimately leave unfolded or misfolded proteins in a non-functional state, creating chaos in a system that requires intricate balance and homeostasis. As the natural oxidation of excess DA forms DA quinones, this pathway is of particular interest when conducting research in the realm of PD.

Genetics have been greatly implicated in the pathophysiology of PD. Proteins of particular interest to the current research are discussed below. Variability in the promoter region of gene *SNCA* has been correlated with predisposition for sporadic PD as it causes a change in cellular concentrations of α-synuclein protein. Work with knockout animals suggests that α-synuclein may be associated with vesicular cycling and DA neurotransmission by interaction with the DAT (Moore et al., 2005). α-synuclein overexpression has been shown to cause PD-like symptoms in animal models since its interaction with DAT causes increased synaptic DA, which leads to DA-induced apoptosis. Further, α-synuclein can be found highly aggregated in Lewy bodies, suggesting that an excess of this protein triggers its precipitation and inclusion (Moore et al., 2005). Finally, Complex I inhibition *in vivo* and *in vitro* causes accumulation of α-

synuclein aggregates similar to aggregates found in Lewy Bodies. This result suggests that Lewy body protein inclusions may result from mitochondrial dysfunction (Moore et al., 2005).

Insoluble forms of the Parkinson's disease protein 7 (DJ-1) are also found in excess in brain tissues of patients with sporadic PD. Studies show that DJ-1 may have some chaperone-like functions, and may also act as an antioxidant by scavenging ROS. *In vitro*, cells treated with excess DJ-1 were protected against oxidative damage (Taira et al., 2004). Oxidative stress causes the localization of DJ-1 to the mitochondria where it confers some protection against mitochondria-induced apoptosis.

The PD-associated protein Parkin is also known to translocate to the mitochondria in times of oxidative stress (Yang et al., 2011). Parkin has been implicated in neuroprotection by sustaining mitochondrial function and suppressing apoptotic pathways (Kuroda et al., 2006; Yang et al., 2011; Yu et al., 2011). Overexpression of WT Parkin in SH-SY5Y cells decreased ROS production, while mutant Parkin enhanced ROS production (Kuroda et al., 2006). WT Parkin also prevented apoptosis and conserved mitochondrial membrane potentials in cells under oxidative stress (Kuroda et al., 2006).

3.2 Treatment and prevention

Current options for PD treatment include pharmaceutical therapy and surgical intervention therapy (National Parkinson Foundation, 2013). Complimentary treatment options can include exercise and physical therapy, support groups, occupational therapy, and speech therapy (National Parkinson Foundation, 2013).

L-DOPA is the most commonly prescribed medicinal treatment for PD. Unfortunately, L-DOPA fails to stop disease progression and also fails to treat symptoms after long-term use due to desensitization to the drug's effects (Hattoria et al., 2009). Further, L-DOPA, like DA, can auto-oxidize to a harmful Quinone molecule, which can be dangerous in a system that is already suffering from oxidative damage and could exacerbate the neurodegeneration associate with PD progression (Hattoria et al., 2009).

Currently, there are no valid preventions for PD (Nutt and Wooten, 2005). The most important pipeline now is the search for specific diagnostic tools that could detect PD in its earliest stages.

3.3 Implications of MOT-2 and CRP40 in Parkinson's disease

MOT-2/CRP40 have become an important link between chaperone protein functions and the pathophysiology of PD. The gene for both MOT-2 and CRP40 is found within chromosome 5q31.1, a putative PD locus (Foroud et al., 2006).

Rotenone, an insecticide/pesticide, is known to interfere with the ETC at the mitochondria. This neurotoxin can be used to create models of PD in cells (Jin et al., 2006), and in rats (Sherer, et al., 2003). Recently, it was discovered that rotenone targets MOT-2 and causes apoptosis triggered by oxidative stress (Jin et al., 2006).

In cell studies by Yang and colleagues (2011), knockdown of MOT-2 in HeLa cells caused truncation and fragmentation of mitochondria, as well as an increased rate of apoptosis. Specifically, apoptotic pathways were activated by ROS accumulation and decreased MMP as a result of reduced MOT-2 activity (Yang et al., 2011). MOT-2 knockdown, however, did not stop Parkin from being translocated to the mitochondria (Yang et al., 2011). This group also tested the effects of WT Parkin overexpression in HeLa cells with the previously studied MOT-2 knockdown. Results showed that overexpression of Parkin prevented ROS accumulation and prevents loss of MMP (Yang et al., 2011). These results suggest that impaired Parkin function due to decreased interaction with MOT-2 may be responsible for mitochondrial dysfunction in PD.

Van Laar and colleagues (2007) conducted a proteomic analysis of rat brain mitochondria after exposing the tissues to DA quinones as a model of PD. A significant loss of a specific set of proteins, including MOT-2, was found.

Similarly, Weiss and colleagues (2006) found that an injection of human umbilical cord matrix (UCM) stem cells into the striatum of a 6-OHDA lesioned PD model rat completely alleviates the rotational symptoms induced by apomorphine injection. Upon proteomic analysis, the authors collected the 50 most highly expressed proteins from the UCM stem cells. MOT-2 was among these highly expressed proteins, leading to further support the hypothesis that MOT-2 has strong implications in PD pathogenesis, and perhaps possible PD therapeutics (Weiss et al., 2006).

α-synuclein and DJ-1 proteins have been linked, previously, to both sporadic and familial PD. Both proteins are found aggregated in Lewy Bodies. Although known to co-localize, α-synuclein and DJ-1 do not interact directly (Jin et al., 2007). Jin and colleagues (2007) hypothesized that there must be a docking protein that implicates the two proteins, and discovered that MOT-2 can be found in complexes with both α-synuclein and DJ-1. The authors also confirmed that neither α-synuclein nor DJ-1 could be found in complex with one another. As MOT-2 was previously implicated in PD, this study suggests that it may modulate PD pathology by interactions with α-synuclein and DJ-1 (Jin et al., 2007; Burbulla et al.,

2010). Interestingly, MOT-2 has also recently been found to interact with Parkin (Londono et al., 2012).

Multiple groups have found previously unidentified missense mutations of MOT-2 in patients with PD that were not present in any healthy control (De Mena et al., 2009; Burbulla et al., 2010). It is possible that these mutations could be involved in the pathogenesis of PD via detrimental effects on MOT-2 chaperone function and its interactions with other proteins, such as α-synuclein and DJ-1 (De Mena et al., 2009). Further, these mutants have been implicated in mitochondrial dysfunction *in vitro* (Burbulla et al., 2010). Interestingly, of the MOT-2 variants, two separate point mutations are located at the C-terminal end of MOT-2, from which CRP40 is derived (Burbulla et al., 2010).

Recent studies using post-mortem brain tissue of patients with PD found a marked decrease in concentrations of MOT-2 in the frontal cortex and in mitochondrial samples from the SN (Shi et al., 2008). Specifically, the trend is quantitative; more severe MOT-2 loss is strongly associated with disease progression (Shi et al., 2008; Jin et al., 2006; Jin et al., 2007; Van Laar et al., 2008). MOT-2/CRP40 depletion was also observed in cellular and preclinical animal models of PD (Jin et al., 2006; Jin et al., 2007; Chiasserini et al., 2011). This includes the 6-OHDA rat model; striatal samples exhibit significant reduction of CRP40 protein (Modi et al., 1996). The 6-OHDA model will be discussed further in section 4.1.

Most recently, work done by Dr. Gabriele (McMaster University) in collaboration with Dr. DiPaolo at the University of Laval suggests that concentrations of CRP40 mRNA are in deficit in blood platelet samples from a primate model of PD compared to controls (data unpublished)– an important finding to the studies presented here.

CHAPTER 4

CRP40 PROTEIN ALLEVIATES BEHAVIOURAL SYMPTOMS IN A RAT MODEL OF PARKINSON'S DISEASE

4.0 Objectives

Based on earlier findings, which show that CRP40 has significant dopaminergic and chaperone-like functions, and may be dysregulated in PD, the study presented here was designed to demonstrate the potential functional role of CRP40 in a rat model of PD.

The current objective was to test whether intra-striatal injection of 100µg of CRP40 protein has an effect on behavioural symptoms in the 6-OHDA hemi-Parkinson's rat model. This model, discussed in further detail in section 4.1, exhibits locomotor dysfunction caused by unilateral degeneration of the nigrostriatal tract. The animals show measurable hyper-locomotion, impairments in reaching, increased grip strength, and full body rotations under the influence of DA receptor agonists (Ungerstedt, 1970; Jeyasingham et al., 2001; Schober, 2004). For the current project, tests of locomotor activity and full body rotations, as well as a test for sensorimotor gating, were employed.

Since early studies of CRP40 suggest that its increased expression caused increased concentrations of DA *in vitro* (Gabriele et al., 2010a), High Performance Liquid Chromatography (HPLC) was used to measure concentrations of DA in various brain regions post-treatment in order to elucidate whether a change in DA activity after treatment with CRP40 may be responsible for its effects on behaviour.

4.1 6-hydroxydopamine model of PD

6-OHDA has been found to deplete the DA content of dopaminergic neurons. Specifically, depletion occurs at the nerve terminal when the toxin is injected into the striatum (Ungerstedt, 1968). Only the area directly adjacent to the injection is affected by the toxin because only the neurons that come in direct contact with 6-OHDA are depleted of DA (Ungerstedt, 1968). 6-OHDA is accumulated by catecholamine-containing neurons via active transport, and destroys them by auto-oxidation and formation of quinones (Siegel et al., 1994). This anterograde degeneration of the entire nigrostriatal tract can be used to create reliable lesions in mice, rats, and primates as animal models of PD.

A lesion using 6-OHDA must deplete 90% of nigral neurons to effectively decrease extracellular concentrations of DA (Castaneda et al., 1990; Schwarting and Huston, 1996; Betarbet el al., 2002). At that point, the animals exhibit hyper-locomotion and, since lesioning causes imbalance in dopaminergic activity between the left and right striatum, rats with unilateral 6-OHDA lesions show a marked preference for movement of the head and neck in the direction ipsilateral to their lesion. Amphetamine injection induces a compulsive full body ipsilateral rotation caused by increased DA release and decreased DA degradation (Ungerstedt et al., 1970; Schwarting and Huston, 1996). Any nigral dopaminergic neurons that remain intact show a response sufficient to maintain a relatively

normal concentration of DA when activated by amphetamine (pre-synaptic DA receptor agonist) (Castaneda et al., 1990). Apomorphine (post-synaptic DA receptor agonist) injection causes a similar compulsive rotational behaviour, but in the direction contralateral to the lesion by direct dopamine receptor binding and activation (Ungerstedt et al., 1970; Schwarting and Huston, 1996). The intensity of the rotations depends strongly on the extent of the lesion and dopaminergic deficit. As such, rotational behaviour is considered a symptom of PD in this animal model. The total number of rotations per fixed time period is used as a measure of better or worsening symptomology. A holding chamber in which the animal is confined to a circular shaped floor is used to count rotations, as it has been confirmed that this constitutes a better arrangement for measurement than an open field box (Ungerstedt et al., 1970).

Lesions affecting more than 90% of nigral neurons have been found to cause a 43% increase in post-synaptic binding of apomorphine compared to non-lesioned controls. This phenomenon is due to super-sensitivity caused by an increased number of D2 receptors expressed by post-synaptic striatal neurons (Creese et al., 1977; Siegel et al., 1994; Schober, 2004). This finding explains why unilateral lesions cause unidirectional rotating behaviour. D1 receptors also become super-sensitized, but in this case, it is due to a change in affinity state of the receptor, and not a change in density (Pifl et al., 1992).

4.2 Methods and materials

4.2.1 Preparation of HDAT-human CRP40-pEGFP1 Plasmid

A CRP40 GFP plasmid was constructed from the GST-CRP40 plasmid deoxyribonucleic acid (DNA) as used by Gabriele and colleagues (2009). Forward primer with Kpn2I restriction site TAG TCC GGA ATG GAT TCT TCT GGA CCC AAG CAT, and reverse primer with Bam H1 site CTA GGA TCC TTA CTG TTT TTC CTC CTT TTG ATC TTC were used. The amplification was performed as follows: denaturation was done at 94°C first for 4 minutes, then 40 cycles of 30 seconds. Annealing was then done at 57°C for 1.2 minutes and extension at 72°C for 2 minutes. Final extension was done at 72°C for 7 minutes. The purified fragment and pEGFP-C1 vectors were cut with Kpn2I and Bam H1 and ligated at 37°C for 1 hour at a ratio of 3:1 (vector:amplicon). The ligated mix was transformed into One Shot Top 10 competent cells (Invitrogen). The obtained positive clone was sequenced to confirm correct cloning. The resulting plasmid was labelled as GFP-CRP40 plasmid DNA.

An amplicon of size 1.5kb was amplified using the forward primer TAG GGA TCC CGC CAC CAT GGT GAG CAA G and the reverse primer CTA GGG CCC TTA CTG TTT TTC CTC CTT TTG AT. The amplification was performed as follows: denaturation at 94°C for 4 minutes, then 40 cycles of 30 seconds, annealing at 55°C for 45 seconds, and extension at 72°C for 1.15 minutes. Final extension was at 72°C for 7 minutes. The amplicon

and PCDNA3.1 were cut with Apa1 and BamH1 (Fermentas Fast Digest) according to manufacturer instructions and ligated by T4DNA ligase enzyme at a ratio of 1:3 at 25°C overnight. The obtained positive clone (sequenced to confirm correct cloning) had a Kozaak sequence, GFP tag, CRP40 plasmid DNA and a BGH pA termination sequence and was labeled as GFP-CRP –PCDNA3.1/His/C plasmid DNA.

An amplicon of size 2kb was amplified from GFP-CRP40 – PCDNA3.1/His/C using the forward primer TAG GGT ACC CGC CAC CAT GGT GAG CAA G and reverse primer CTA CTT AAG CCA TAG AGC CCA CCG CAT C. The amplification was performed as follows: denaturation at 94°C for 3 minutes, then 35 cycles of 15 seconds at 93°C, annealing at 56°C for 30 seconds, and extension at 68°C for 2 minutes. Final extension was at 72°C for 7 minutes using the LongRange PCR kit (Qiagen). The amplicon and hDAt-PEGFP-C1 vector (as provided by Dr. Bannon`s Lab, McMaster University) were cut with KpnI and AflII (Fermentas Fast Digest), then purified and ligated using t4DNA ligase at 25°C overnight. DNA was then transformed in One Shot Top 10 competent cells (Invitrogen). The obtained positive clone was sequenced to confirm correct cloning. The final plasmid was labeled as HDAT CRP40 PEGFP1 plasmid DNA.

4.2.2 Preparation of HDAT-human MOT-2 pEGFP1

RNA was extracted from lymphocytes of a human cancer patient and the full-length cDNA was synthesized using the LongRange cDNA synthesis kit (Qiagen), according to manufacturer's instructions. The MOT-2 full-length cDNA was obtained using the LongRange cDNA synthesis kit (Qiagen) and the primers: TAG TCC GGA ATG ATA AGT GCC AGC CGA GCT G which included a Kpn2I restriction site; and CTA GGA TCC TTA CTG TTT TTC CTC CTT TTG ATC TTC which included a BamHI restriction site. The resulting amplicon was 2kb in length with Kpn2I and BamH1 restriction sites. The amplicon was ligated to pEGFP-C1 using T4DNA ligase after cutting with kpn2I and Bam H1 (Fermentas Fast Digest) for 30 minutes and purification by gel electrophoresis. The ligation was done overnight at 25°C. DNA was then transformed in One Shot Top 10 competent cells (Invitrogen). The obtained positive clone was sequenced to confirm correct cloning (98% homology to MOT-2). This plasmid was labelled as MOT2-GFP-PEGFP1 plasmid DNA.

To sub-clone the MOT-2 DNA into pCDNA3.1/His/c, the cDNA was amplified using forward primer TAG GGA TCC CGC CAC CAT GGT CAG CAA G containing Bam H1; and reverse primer CTA CTC GAG TTA CTG TTT TTA TCC TTT TGA TC containing xho1 using the LongRange PCR kit (Qiagen) with an annealing temp of 53°C. The amplicon and PCDNA3.1/His/C were cut with BamH1 and xho1 (Fermentas Fast

Digest), then purified and ligated overnight at 14°C. DNA was then transformed into One Shot Top 10 competent cells (Invitrogen). The obtained positive clone was sequenced to confirm correct cloning (99% homology to MOT-2). This plasmid is labeled as MOT2-PCDNA3.1 plasmid DNA.

To clone the MOT-2 cDNA into an HDAT-pEGFP vector, a full-length fragment was amplified with forward primer TAG GGT ACC CGC CAC CAT GGT GAG CAA G and reverse primer CTA CTT AAG CCA TAG AGC CCA CCG CAT C using the LongRange PCR kit (Qiagen) at an annealing temp of 56°C. The amplicon and HDAT-PEGFP were cut with KpnI and AflII (Fermentas Fast Digest), then ligated for 1 hour at 25°C. The ligated mix was transformed into One Shot Top 10 competent cells (Invitrogen). The obtained positive clone was sequenced to confirm correct cloning (99% homology to MOT-2). This plasmid is labelled as HDAT-human MOT2-PEGFP1 plasmid DNA.

4.2.3 Large scale preparation of HDAT-Crp40-GFP

3ml of Lysogeny broth (LB) Kanamycin (50ug/ml) was inoculated by 100µl of glycerol stock of HDAT Crp40-GFP in E. Coli and shaken overnight at 37°C. 100ml of the LB Kanamycin was then inoculated with 1ml of overnight culture. The next day, 4 x 1L was inoculated with 10ml overnight culture and incubated overnight at 37°C while shaking at 225rpm. Next, the cells were centrifuged down at 4000rpm for 15 minutes and plasmid DNA was extracted using the HiSpeed Maxi Kit (Qiagen; 12662) according to manufacturer's instructions. The DNA was then eluted and the plasmid DNA was quantified. The average yield was 10mg/4L of culture.

4.2.4 Large scale preparation of CRP40 pcdna3.1/His -GFP

3ml of LB Kanamycin (50ug/ml) was inoculated by 100µl of glycerol stock of HDAT CRP40fl-GFP in E. Coli and shaken overnight at 37°C. 100ml of the LB Kanamycin was then inoculated with 1ml of overnight culture. The next day, 4 x 1L was inoculated with 10ml overnight culture and incubated overnight at 37°C while shaking at 225rpm. Next, the cells were centrifuged down at 4000rpm for 15 minutes and plasmid DNA was extracted using the HiSpeed Maxi Kit (Qiagen; 12662) according to manufacturer's instructions. The DNA was then eluted and the plasmid DNA was quantified. The average yield was 10mg/4L of culture.

4.2.5 Large scale preparation of HDAT-MOT-2-GFP

3ml of LB Kanamycin (50ug/ml) was inoculated by 100µl of glycerol stock of HDAT MOT-2-GFP in E. Coli and shaken overnight at 37°C. 100ml of the LB Kanamycin was then inoculated with 1ml of overnight culture. The next day, 4 x 1L was inoculated with 10ml overnight culture and incubated overnight at 37°C while shaking at 225rpm. Next, the cells were centrifuged down at 4000rpm for 15 minutes and plasmid DNA was extracted using the HiSpeed Maxi Kit (Qiagen; 12662) according to manufacturer's instructions. The DNA was then eluted and the plasmid DNA was quantified. The average yield was 10mg/4L of culture.

4.2.6 Preparation of CRP40 full-length protein

Expression:

Solutions for this protocol were prepared as follows:

1. One mini C tablet (Roche; 04693116001) in 300ml PBS,
2. Wash buffer: 0.1% TX-100, 0.5M NaCl in PBS with mini C,
3. Elution Buffer: 0.1% Tx-100, 1M NaCl in PBS with mini C.

100µl of glycerol stock CRP40fl-GST plasmid DNA in E.Coli was transferred to 3ml LB ampicillin (100mg/ml) and incubated overnight at 37°C while shaking at 225rpm. 1ml of overnight culture was then transferred to 100ml LB ampicillin and grown overnight. 8 x 1L of LB ampicillin was inoculated with 10ml of overnight culture, and OD was monitored at 600nm until it reached 0.6. The culture was then induced with IPTG (100µl of 100mM stock) and incubated at 12°C overnight while shaking at 225rpm. The cultures were then centrifuged down at 4000rpm for 15 minutes. The pellet was washed in 100ml PBS and centrifuged down again at 8000rpm for 10 minutes using a JA20 rotor. The supernatant was removed and the wet weight of the pellet was calculated. The pellet was then resuspended in PBS mini C without EDTA so that the suspension was 250g/L.

Cell disruption:

The cell disruptor used was Model: TS2/40/AA/AA by Constant Systems Ltd. The protocol used was for 15,000psi for cytoplasmic proteins according to manufacturer's instructions.

Glutathione sepharose binding:

Lysate from cell disruption was centrifuged down at 12,000rpm for 20 minutes using a JA20 rotor, and then clear lysate was collected for binding. 4 x 1.25ml of sepharose 4FF beads was added to lysate and centrifuged at 500g for 5 minutes. The supernatant was removed and 5ml of PBS was added. The mixture was centrifuged down again at 500g for 5 minutes, and the supernatant was removed. The clear lysate was transferred equally to 4 falcon tubes, closed tightly and covered with parafilm. The tubes were rocked end to end at 4°C overnight. The bound lysate was transferred into 4 columns, and the unbound lysate was allowed to flow through. Each column was then washed with 20ml wash buffer and with 5ml of PBS *without* mini C (the serine protease inhibitor will reduce the efficiency of the cleavage).

On-Column cleavage by thrombin protease:

Enzyme was prepared by mixing 4 x 75µl thrombin enzyme with 4 x 1.425ml PBS. Beads on the column were then mixed with 1.5ml of the

thrombin buffer using a glass rod and left overnight for the completion of cleavage. The flow-through (F/T) was then collected in 1.5ml eppendorf tubes from each column. The protein content of the pooled fractions was checked, and all fractions containing significant amounts of protein were pooled. Average total volume was 17.5ml. 52.5µl of 100mM PMSF (in ethanol) was added to the protein and incubated at 37°C for 15 minutes. The protein was divided into 2 dialysis bags (10,000 MWCo) and dialysed against 2L PBS, changing the buffer every 12 hours, for 2 days (5 changes in total). Dialysed protein was transferred to 15ml falcon tubes. The protein was then lyophilized to a powder. The final powder was resuspended in 0.5ml (x 2) sterile water to get CRP40 protein and was checked 25µl on a 10% polyacrylamide and stained for purity of the protein.

4.2.7 Animals

79 Sprague Dawley lab rats were ordered from Charles River (Boston, MA); 6 of the animals were non-lesioned controls, and 73 were lesioned with 6-OHDA at the SN.

After delivery to the Central Animal Facility at McMaster University (Hamilton, Ontario), all rats were handled by experimenters for 7 days. Animals were then subjected to a series of behavioural tests for baseline measures. The test battery included: apomorphine-induced rotation, locomotor activity (open field), and prepulse inhibition (PPI). Protocols for these behavioural tests will be described in sections 4.2.8, 4.2.9, and 4.2.10, respectively.

Once all baseline data were collected, the rats were placed under gaseous anaesthesia and injected with one of the seven treatments at either the SN or striatum as described in Table 2. Treatments used include: saline sham (20µl); CRP40 protein (100µg), MOT-2 protein (100µg), CRP40 plasmid DNA (20µg), MOT-2 plasmid DNA, (20µg), Heat Shock Protein 47 (HSP47) protein (negative control; 100µg), RNA Polymerase β' Subunit (RpoC) protein (negative control; 100µg).

Animals were monitored daily for one week following surgery, and weighed daily to ensure healthy recovery and weight gain. If a 30% reduction in body weight was observed, animals were immediately euthanized as endpoints had been reached.

All animals were again tested using the same behavioural methods for apomorphine-induced rotations at days 4, 7, and 10 post-injection. Animals treated with plasmid DNA were only tested for behaviour on days 7 and 10 post-injection to allow one week for protein synthesis to occur after injection. Locomotor activity and PPI were not repeated since the baseline measures were not different between lesioned and non-lesioned animals. On day 15 post-injection, all rats were sacrificed by isoflurane overdose and decapitation. Fresh brain tissue was sliced using razor blades and a brain mould, then micro-punched for specific brain area samples, and flash frozen on dry ice.

Animals were housed and tested in compliance with the guidelines described in the Guide to the Care and Use of Experimental Animals (Canadian Council on Animal Care, 1984; 1993). The McMaster University Committee for Animal Welfare approved all protocols.

4.2.8 Behavioural testing: Apomorphine-induced Rotations

The weight of each rat was recorded in grams. Apomorphine diluted in ascorbate-saline (0.05 mg/kg) was injected subcutaneously at the hind leg according to weight as follows: weight (g)/1000 = injection volume (ml). So, for a 254g rat, 0.254ml of Apomorphine was given.

Once injected, the animal was placed in a clear plastic cylinder and allowed 5 minutes for habituation. After habituation, a timer was started for 10 minutes and a cell counter was used to manually count the number of full rotations the animal made until the timer was done. “Total number of rotations” was recorded. The rat was then placed back in its home cage and the cylinder was cleaned with 70% ethanol. This protocol was repeated for all animals.

4.2.9 Behavioural testing: Locomotor activity

All locomotor tests were performed as close as possible to or during the dark period of the animals' light cycle, since rats show maximum activity during these hours. Locomotor activity was measured in computerized cages, with multidirectional movements recorded by a computerized system. Six infrared light beams captured movements via beam interruption and translate them into a variety of parameters, such as total distance traveled (cm), and total stereotyped behaviours (repetitive head movements, hind leg rearing, etc.). Locomotion was recorded for a total of 180 minutes; the first 30 minutes were considered habituation and the last 120 minutes were recorded as actual activity. In the current testing paradigm, distance traveled every 10 minutes (18 segment log for each rat) was sampled.

4.2.10 Behavioural testing: Prepulse inhibition (PPI)

Startle responses were measured using the SR-LAB system (San Diego Instruments). A speaker, mounted 24cm above the Plexiglas cylinder containing the animal, provided background noise, prepulse stimuli, and startle stimuli, controlled by the SR-LAB software. Prepulse stimuli were 3, 6, and 12 decibels (dB) above a 65 dB background white noise. Time lag from prepulse stimulus and startle stimulus was 100 ms for maximum inhibition of startle response. Each testing session lasted 25 minutes, beginning with a 5-minute acclimatization period during which the 65dB white noise was presented in the background. Next, a series of 5 startle-pulse alone (120dB, 40ms) trials were presented for use in analyzing habituation. This series of stimuli was followed by 65 randomized trials consisting of no pulse (0dB, no additional stimuli other than 65dB background white noise present), a startle pulse (120dB, 40ms), one of three prepulse intensities (68dB, 71dB, or 77dB; 20ms) presenting 100ms preceding the startle pulse, or one of three prepulse intensities alone (for a total of 7 different trial types). Lastly, another series of five startle-pulse alone trials was presented. The time between each trial ranges from 10 to 20 seconds to average 15 seconds, with startle responses measured every 1ms for a 100 ms period after the onset of the startle stimulus.

4.2.11 Stereotaxic injection surgery: Rat

Prior to beginning surgery, all instruments were thoroughly soaked in liquid disinfectant (Coldspore; available from the McMaster Central Animal Facility (CAF)) for 20 minutes and rinsed with sterile double distilled water (Baxter). All surfaces, towels, and gauze pads used were also sterile.

All animals were weighed, and weight was recorded in grams. The first animal was placed in the gaseous anaesthetic chamber (oxygen flow: 2.5, isoflurane flow: 4), and allowed to reach full sedation. The animal was then shaved from between the ears to between the eyes. The sedated animal was then mounted on the stereotax using the ear bars and nose cone. The primary surgeon prepared the injectable drugs as follows: Anaphen: subcutaneous (0.2ml prevents fluid build-up in lungs), saline: subcutaneous (5ml for hydration), and Baytril: intramuscular (0.05ml antibiotic; injected post-surgery). The primary surgeon then scrubbed-in according to the McMaster CAF survival surgery guidelines.

The primary surgeon cleaned the shaved area on the animal's head using 3 step prep solutions; available from the McMaster CAF). Someone other than the primary surgeon applied a generous amount of Lacri-Lube (eye ointment; available from the McMaster CAF– to ensure the eyes do not dry out during the procedure), then injected saline and Anaphen.

Anaesthetic maintenance levels are suggested around 2.0; but our lab used an approximate maintenance level of 3.0 due to the invasive nature

of this procedure. The primary surgeon made a midline incision in the scalp from behind the eyes to the area between the ears. The periosteum was removed using a bone curette. The skin was then retracted using four haemostats and the incision area was thoroughly cleaned and dried using sterile gauze or sterile cotton swabs.

Someone other than the primary surgeon located the desired reference point (Bregma) using the stereotaxic equipment, and recorded the coordinates, then calculated the desired coordinates for drilling from these references. Coordinates used for the striatum were: 0.7mm anterior to Bregma, 3.0mm lateral to midline, and 5.0mm below the skull surface. Coordinates used for the SN were: 4.8mm anterior to Bregma, 1.8mm lateral to midline, and 8.2mm below the skull surface. The primary surgeon then drilled the desired holes with the automatic drill using the foot pedal.

Someone other than the primary surgeon inserted the Hamilton syringe (25µl capacity; mounted to the stereotax) to the desired depth. Infusion rate was set to 1µl/minute. Five minutes was allowed for infused solution to diffuse into the skull before retracting the syringe.

Once the Hamilton syringe was retracted, the incision was closed: the primary surgeon closed the skin using staples while pinching the skin together using forceps. The animal was then injected with antibiotic Baytril into the thigh muscle, and removed from the stereotax. The animal was

placed under a heating lamp for recovery in a clean cage lined with paper towels.

4.2.12 Animal sacrifice and tissue collection

Decapitation:

All animals to be sacrificed were taken to the post-mortem room of the McMaster CAF. While one animal was being sacrificed, the other cages were left covered in a separate room. Overdose with isoflurane was done by setting the oxygen flow to 2.5 and anaesthetic flow to 5. The rat was then placed into the guillotine. The guillotine arm was pushed down in one swift motion, cutting straight through the animal's neck and separating the head from the body.

Tissue collection:

Using scissors and a bone rongeur, the skull was opened from the back and the brain was cleared of any surrounding bone. Once the entire brain was exposed, the head was flipped over and the optic nerve was detached. The brain was then placed in the brain mould and sliced with razor blades. Slices of interest were chosen according to a rat brain atlas as follows: SN, NA, VTA, striatum, and mPFC; all others were disposed of. Using a micro-punch, the areas of interest were removed and placed into labelled eppendorf tubes, then flash frozen on dry ice. Tissues were kept frozen at -80°C until needed for analysis.

4.2.13 High performance liquid chromatography

HPLC for DA analysis was performed as in Culver et al., 2002.

Mobile phase:

Mobile phase was prepared specifically for the detection of DA. The following ingredients were first combined with 950ml of double distilled water: 6.8g sodium acetate (50mM), 4.2g citric acid (20mM), 215mg sodium octyl sulphate (2mM), 170µl Di-N-Butylamine (1mM), 40mg EDTA (100µM), 151.1mg potassium chloride, and 40ml HPLC Grade Methanol. The pH of the solution was measured and adjusted to 3.5. Finally, the solution was filtered through a 0.5µm glass fibre filter.

DA standards:

0.1M PCA was first prepared by diluting 428µl PCA with 50ml of double distilled water. 0.25mg/ml stock DA was then prepared by dissolving 5mg DA in 20ml 0.1M PCA. Stock was then diluted to 0.000125mg/ml by adding 10µl of the 0.25mg/ml stock DA to 19,990µl 0.1M PCA. 0.25mg/ml stock DHBA was prepared by dissolving 5mg dry DHBA in 20ml 0.1M PCA. Stock was then diluted to 0.0025mg/ml by adding 10µl of the 0.25mg/ml stock DHBA to 1000µl 0.1M PCA. Five DA standards of equal volume were prepared with equal concentrations of DHBA (internal control) according to the following table:

	Mass of DA in 20 µl	Concentration of DA in 20 µl	0.1M PCA	0.000125 mg/ml DA	0.0025mg/ml DHBA	Total
1	0.5 $x10^{-4}$ µg	0.25$x10^{-5}$µg/ µl	970µl	20 µl	10µl	1000µl
2	1.0 $x10^{-4}$ µg	0.50$x10^{-5}$µg/ µl	950µl	40 µl	10µl	1000µl
3	1.5 $x10^{-4}$ µg	0.75$x10^{-5}$µg/ µl	930µl	60 µl	10µl	1000µl
4	2.0 $x10^{-4}$ µg	1.00$x10^{-5}$µg/ µl	910µl	80 µl	10µl	1000µl
5	2.5 $x10^{-4}$ µg	1.25$x10^{-5}$µg/ µl	890µl	100 µl	10µl	1000µl

Each standard sample was vortexed and then filtered into a clean HPLC vial. Samples were run with 3 x 20µl PCA blanks through the HPLC to generate a standard curve of DA concentration.

Rat brain tissue (single punch sample) preparation:

PCA+DHBA stock was prepared by adding 10µl of 0.0025mg/ml DHBA stock to 990µl of 0.1M PCA stock. Tissue samples to be analyzed were weighed in an eppendorf tube. 100µl of the PCA+DHBA stock was added to each sample. Samples were homogenized by hand using a sterile pestle (15-20 strokes), then centrifuged down for 10 seconds. Tissue samples were then homogenized on ice using dismembrator for 3 x 1 second. Samples were centrifuged down again for 20 minutes at 13,000rpm. At this point, supernatant was collected from each sample and filtered (13mm, 0.2um syringe filter) into a clean HPLC vial. Filtered

samples were run through HPLC and concentrations of DA were calculated by comparing tissue sample concentrations to the standard curve.

4.2.14 Data analysis

Apomorphine-induced rotations:

Change in rotations over time across treatment groups was analyzed using repeated measures ANOVA. *Post hoc* pairwise contrasts among treatment groups were examined using the Tukey test. Twenty observations (9.6%) were coded as missing for the rotation data. Since the data were assumed to be missing at random, multiple imputation was implemented in the analysis to maximize statistical power.

Locomotor activity:

Total distance traveled (cm) was compared between groups and across all time points using multiple one-way ANOVAs performed with Tukey's post-hoc test.

PPI:

Percent PPI (%PPI) is calculated for each prepulse intensity. The equation used to calculate prepulse inhibition is as follows:

> %PPI = [(average response magnitude to startle-pulse only trials – average startle response magnitude to prepulse + startle pulse trials)/average response magnitude to startle-pulse only trials]*100

%PPI was compared between groups, at each prepulse intensity, and across all time points using multiple one-way ANOVAs performed with Tukey's post-hoc test.

HPLC:

Analysis of HPLC data was performed as in Culver et al., 2002 using one-way ANOVAs, and paired t-tests ($p<0.05$).

4.3 Results

In the PPI and locomotor activity behavioural tests, 6-OHDA lesioned rats showed no significant difference from controls at baseline (Figure 8; 9). For this reason, neither test was used to collect post-treatment data.

None of the treatment or control injections into the SN had any effect on apomorphine-induce rotational symptoms (Figure 10a-e). Injection of CRP40 protein into the striatum, however, alleviated the apomorphine-induced rotational symptoms 4 days after treatment (Figure 11d). Analysis of rotational behaviour data demonstrated a significant effect across treatment groups over time ($p<0.0001$). Pairwise contrasts showed that the CRP40 protein treatment group displayed significantly decreased rotations from baseline compared to all other groups and controls on day four ($p<0.0001$ for both). CRP40 plasmid, MOT-2 plasmid, and MOT-2 protein injection exhibited a similar alleviatory trend as CRP40 protein, but results were not significant (Figure 11b; 11c; 11e). None of the control injections into the striatum had any effect on apomorphine-induced rotational symptoms (Figure 11a; 11f; 11g; 11h).

HPLC analysis showed no discernable trend in the concentrations of DA in the SN & striatum of the striatal-injected, or SN injected rats in the lesioned hemisphere in comparison to concentrations from the same rat in the non-lesioned hemisphere (data not shown). Due to low group size ($n=2$), this study must be repeated in order to validate results.

4.4 Discussion

This study examined the effect of CRP40 protein and CRP40 plasmid injection on the behavioural phenotypes seen in the 6-OHDA rat model of PD to explore the possible future use of CRP40 as a therapeutic for PD. From past studies, we know that DA can modulate CRP40 expression (Gabriele et al., 2007; Gabriele et al., 2009). Further, we know that knockdown of CRP40 in the medial mPFC causes deficits in DA-dependant behaviours (Gabriele et al., 2010a). This lead us to believe that CRP40 can also modulate DA– a functional property that could possibly be exploited as a potent treatment option for diseases involving dysfunctional DA regulation.

The results suggest that intra-striatal injection of CRP40 protein transiently alleviated the rotational symptomology in 6-OHDA hemi-lesioned rats. Results also indicate that injection of CRP40 protein into the SN did not have any measurable effect on rotational behaviour. Taken together, the findings of this study suggest that CRP40 acts either at the presynaptic terminal (axon terminal) of neurons originating in the SN, or at the postsynaptic terminal (soma) of neurons originating in the striatum. These findings are preliminary, and will require further investigation to demonstrate the mechanisms of CRP40, possible contributions to neuroprotection and mitochondrial homeostasis, and importance to PD pathophysiology. Results will need to be validated and extended by

following up with dose-response and other studies in order to determine the most effective therapeutic dose of the protein in the rats.

After day four in the CRP40 protein treated group, rotational symptoms began to return to baseline. CRP40 may be degraded, depleted, or washed-out over time, therefore, administering a dose of CRP40 on a weekly basis may be the best approach when conducting long-term studies of CRP40 as a potential treatment for 6-OHDA hemi-lesioned rats.

As this was a novel pilot study, it was important that appropriate negative controls were established and validated for use in future studies. HSP47, a collagen-specific chaperone, was chosen for it similarities in heat shock-like functions to CRP40 and MOT-2, as well as for its closeness in size (47kDa) to CRP40 (Nagata et al., 1998). RpoC was chosen because it shares homologous sequence lengths with CRP40 (Gupta and Smeath, 2007). Neither HSP47 nor RpoC treatment had any effect on rotational behaviour. These results confirm that HSP47 protein and RpoC protein are appropriate negative controls for CRP40 treatment in 6-OHDA hemi-lesioned rats.

HPLC analysis showed no discernable difference in concentrations of DA in the SN & striatum of any rats. Concentrations in the lesioned hemisphere were compared to concentrations from the same rat in the non-lesioned hemisphere for accuracy of internal control. Since the

experiment yielded unexpected results, studies will be repeated with larger groups in an attempt to either reproduce or disprove these results.

In summary, these interesting and novel results suggest that CRP40 may modulate dopaminergic behaviours in the 6-OHDA rat model of PD. Future experiments will incorporate behavioural tests of gait, grip, and locomotor activity in a larger group of animals to validate the current results. Future studies are also in place to explore the therapeutic effects of CRP40 on the Parkinsonian symptoms of the 1-Methyl-4-phenyl-1,2,3,6-tetrahydropyridine (MPTP) mouse model of PD, and to identify the mechanisms by which CRP40 dysfunction may contribute to PD pathogenesis.

	Striatal Injection	SN Injection	No Injection
Saline	10	2	-
CRP40 Plasmid	4	3	-
CRP40 Protein	11	3	-
MOT-2 Plasmid	3	3	-
MOT-2 Protein	2	3	-
RpoC Protein	10	-	-
HSP47 Protein	10	-	-
No Treatment	-	-	3
No Lesion	-	-	6

Table 2: Description of treatment groups and group numbers (n). A total of 56 rats received striatal injections, and 14 rats received SN injections.

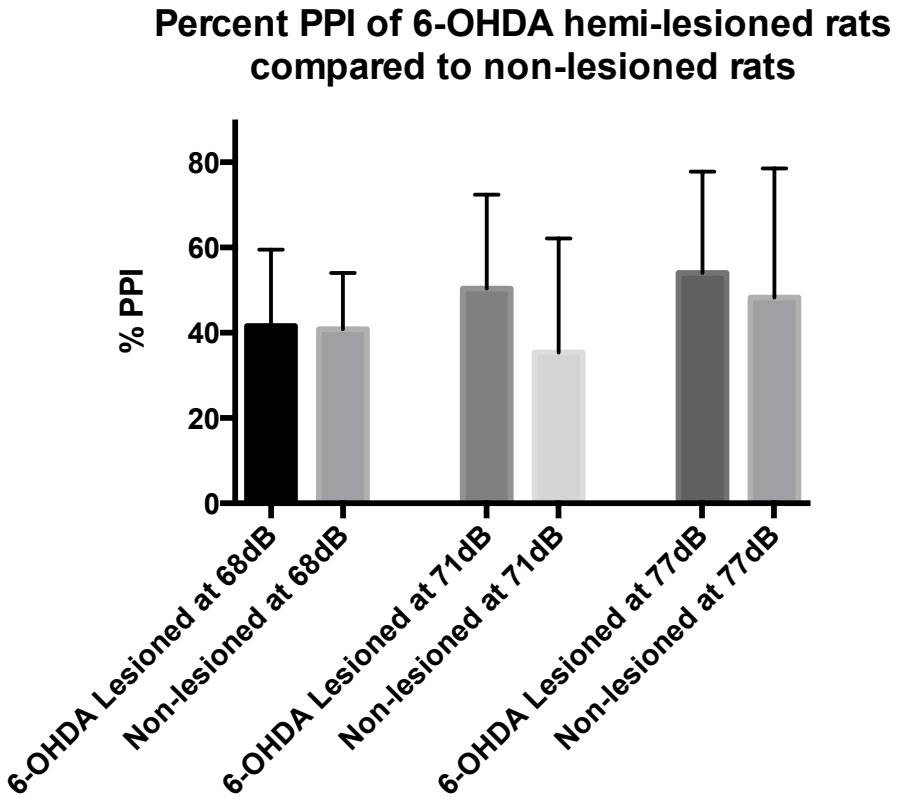

Figure 8: %PPI was not significantly different between 6-OHDA lesioned rats (n=24) and non-lesioned (n=6) control rats at baseline.

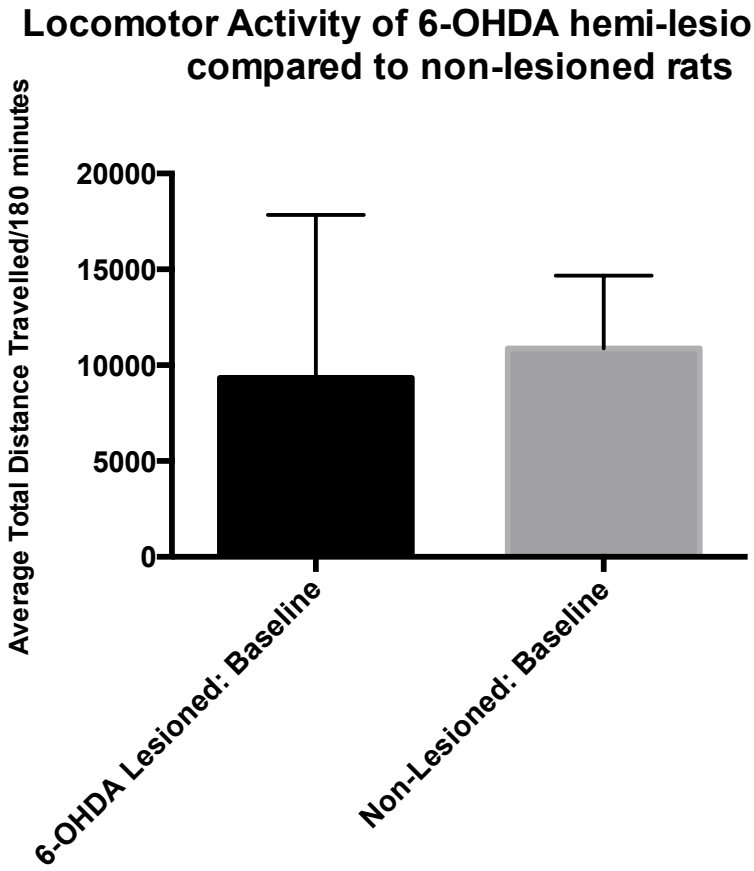

Figure 9: Total distance travelled was not significantly different between 6-OHDA lesioned rats (n=24) and non-lesioned (n=6) control rats at baseline.

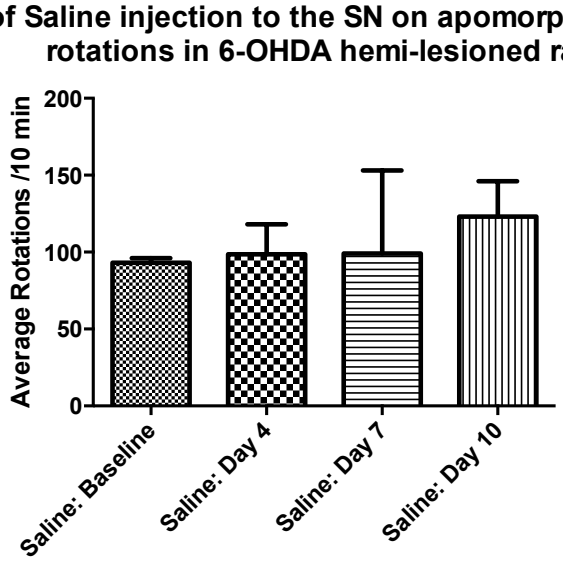

Figure 10a: Saline (sham) treated (SN injection) animals (n=2) showed no difference in number of rotations after treatment from baseline.

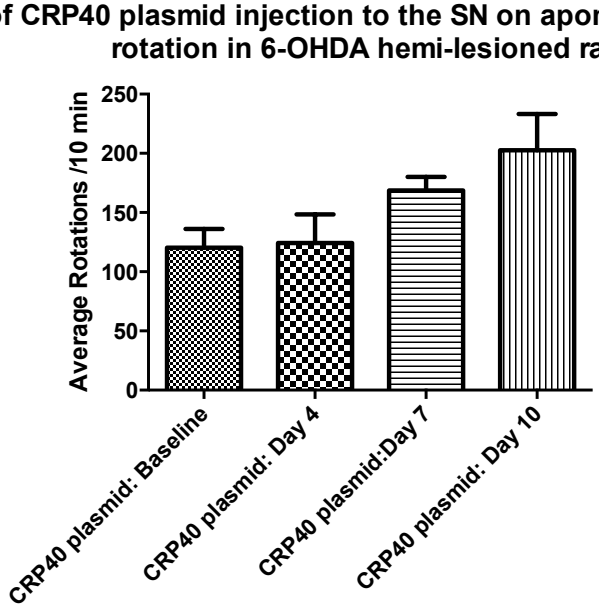

Figure 10b: CRP40 plasmid treated (SN injection) animals (n=3) showed no difference in number of rotations after treatment from baseline.

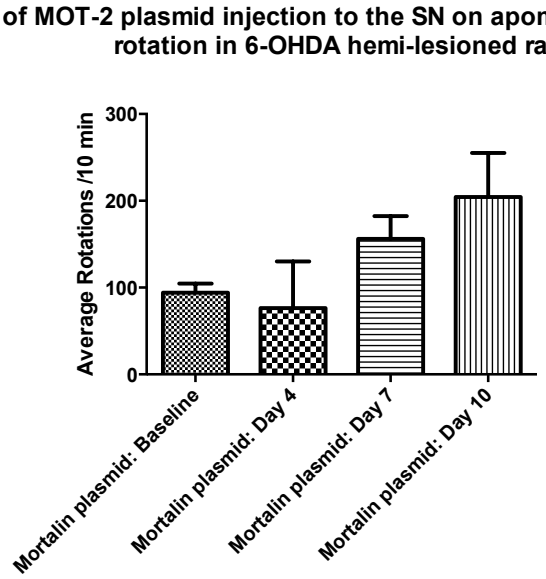

Figure 10c: MOT-2 plasmid treated (SN injection) animals (n=3) showed no difference in number of rotations after treatment from baseline.

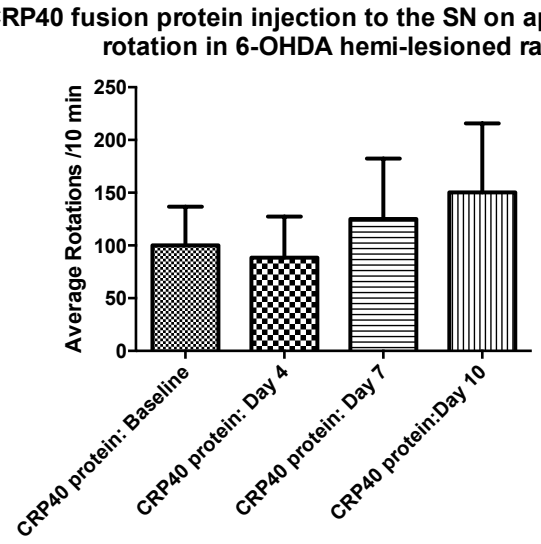

Figure 10d: CRP40 protein (SN injection) treated animals (n=3) showed no difference in number of rotations after treatment from baseline.

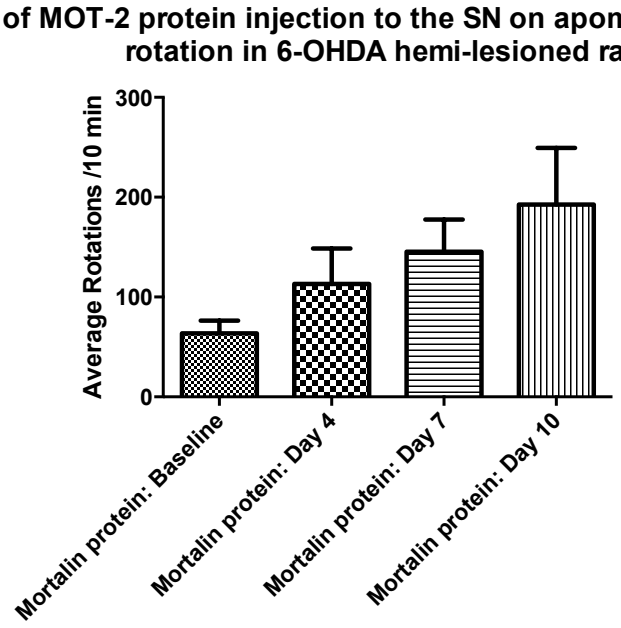

Figure 10e: MOT-2 protein (SN injection) treated animals (n=3) showed no difference in number of rotations after treatment from baseline.

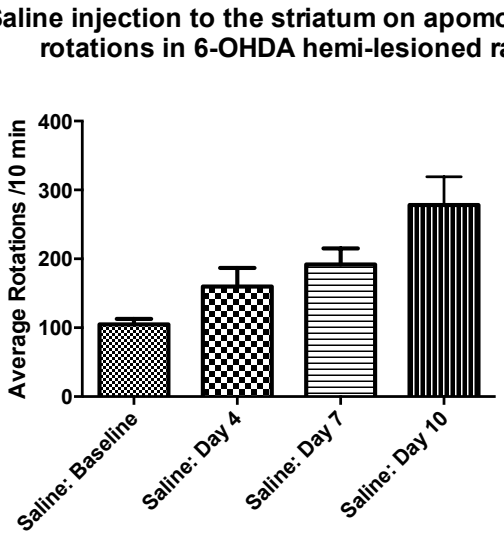

Figure 11a: Saline (sham) treated (striatum injection) animals (n=10) showed no difference in number of rotations after treatment from baseline.

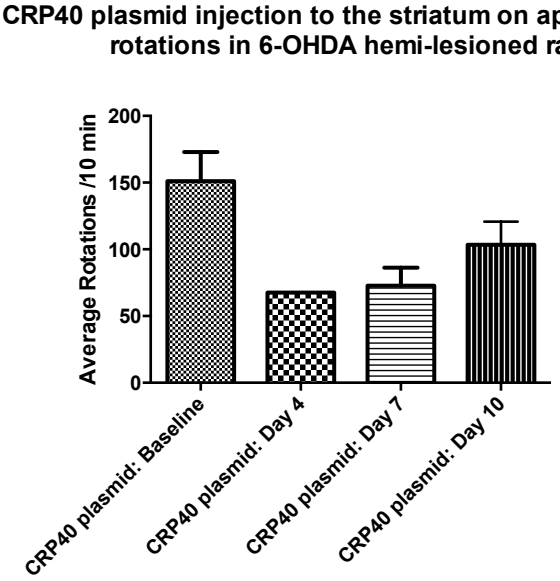

Figure 11b: CRP40 plasmid treated (striatum injection) animals (n=4) showed some difference (no significance) in number of rotations after treatment from baseline.

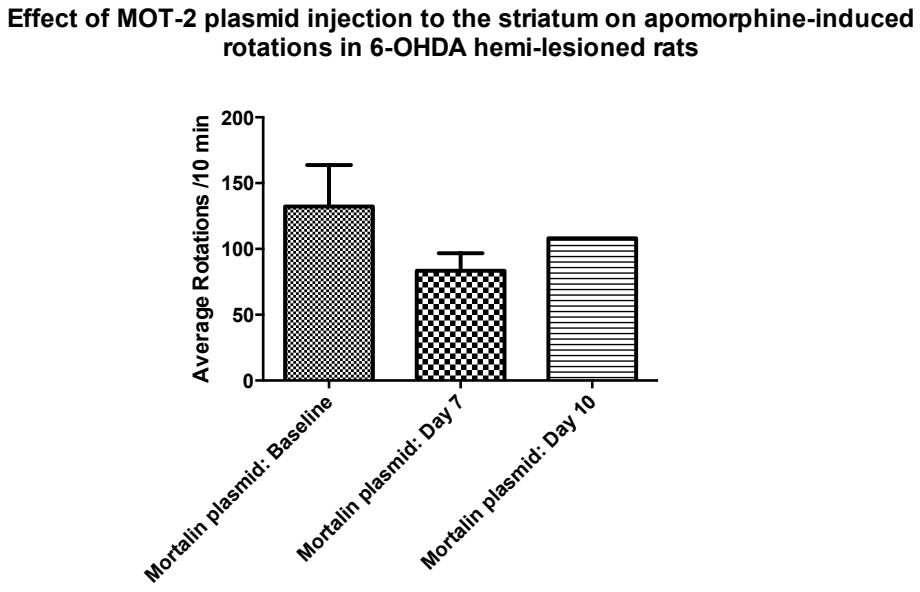

Figure 11c: MOT-2 plasmid treated animals (striatum injection) (n=3) showed some difference (no significance) in number of rotations after treatment from baseline.

Figure 11d: CRP40 protein treated (striatum injection) animals (n=11) showed significantly decreased number of rotations at day four after treatment from baseline ($p<0.0001$***).

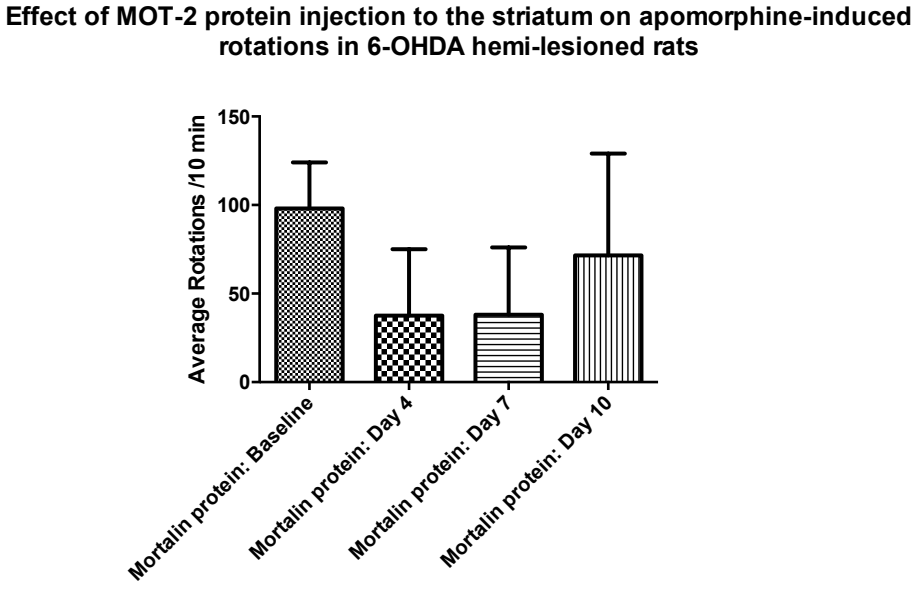

Figure 11e: MOT-2 protein treated (striatum injection) animals (n=2) showed some difference (no significance) in number of rotations after treatment from baseline.

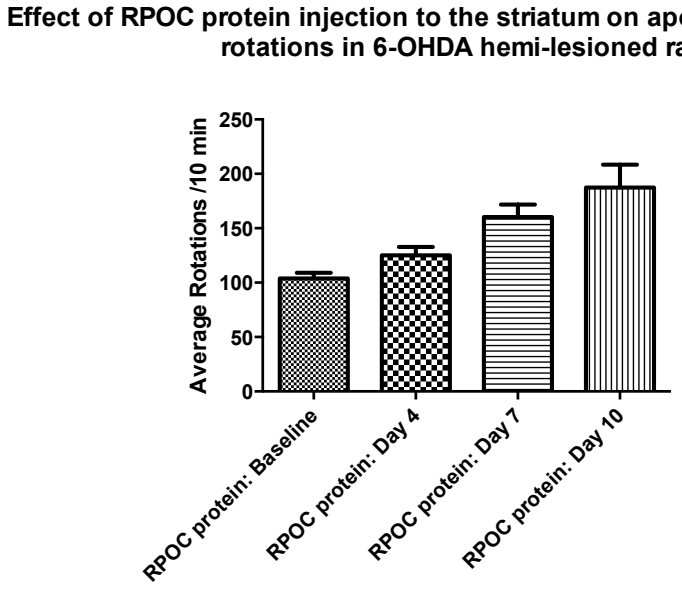

Figure 11f: RpoC protein treated (striatum injection) animals (n=10) showed no difference in number of rotations after treatment from baseline.

Effect of HSP47 protein injection to the striatum on apomorphine-induced rotations in 6-OHDA hemi-lesioned rats

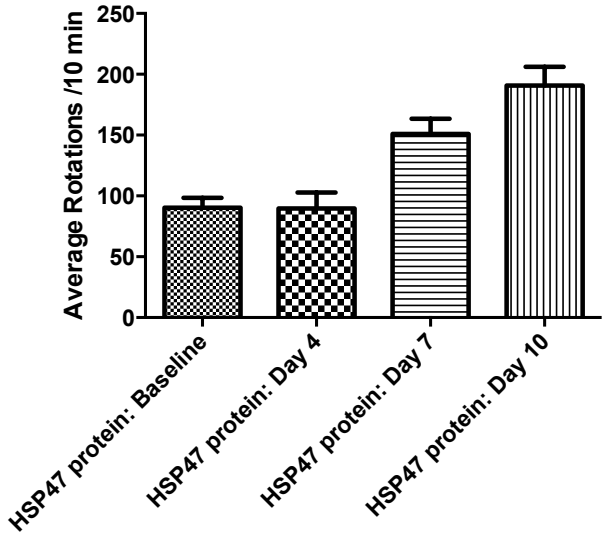

Figure 11g: HSP47 protein treated (striatum injection) animals (n=10) showed no difference in number of rotations after treatment from baseline.

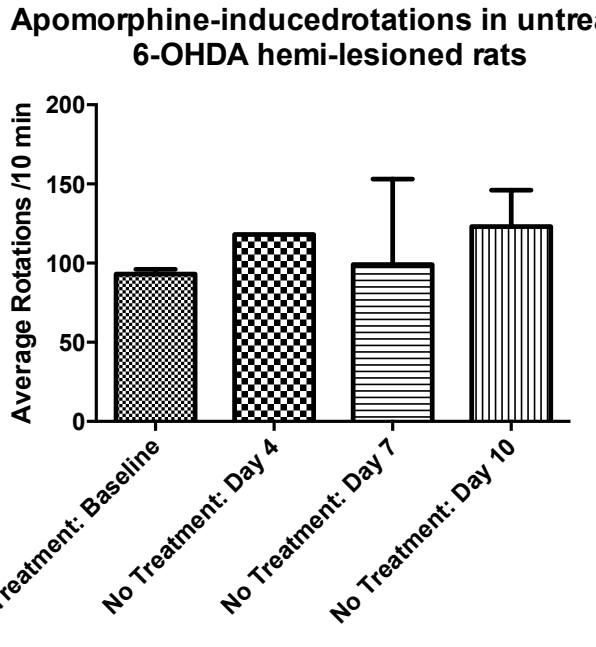

Figure 11h: Non-treated animals (n=3) showed no difference in number of rotations on any day from baseline.

CHAPTER 5

CLONED FRAGMENTS OF CRP40 ALLEVIATE BEHAVIOURAL SYMPTOMS IN A RAT MODEL OF PARKINSON'S DISEASE (A PILOT STUDY)

5.0 Objectives

Based on earlier findings, which have demonstrated that intra-striatal injection of 100µg of CRP40 protein transiently alleviated rotation symptoms in the 6-OHDA hemi-lesioned rat model of PD (Figure 11d), the study presented here was designed to test whether a smaller fragment of this protein may have a similar behavioural effect. In order to elucidate the active segment of CRP40, fragments of various sizes were cloned, expressed and purified by Jovana Lubarda (PhD candidate, McMaster University) for injection into the striatum of PD rats. The apomorphine-induced rotations test was used for baseline and post-treatment measures of behaviour.

Further, since CRP40 binds catecholamines (Figure 7) (Gabriele et al., 2009), the project was also designed to test whether the most behaviourally effective fragment of CRP40 also possesses the ability to bind DA to elucidate whether DA or apomorphine binding is correlated to the observed changes in behaviour. Receptor binding studies using tritiated DA were employed to explore this question in detail.

5.1 Methods and materials

5.1.1 Preparation of CRP40 fragment peptides

Peptide fragments of the full-length CRP40 protein were cloned, expressed, and purified by Jovana Lubarda. Protocols for these procedures can be found in detail in her PhD thesis (currently in preparation; McMaster University, 2013). Peptide fragments tested for therapeutic efficacy in this study included: 27kDa fragment of CRP40 (named 1,5); 17kDa fragment of CRP40 (named 1,4); and 7kDa fragment of CRP40 (named 2,4).

5.1.2 Animals

6 Sprague Dawley lab rats were ordered from Charles River (Boston, MA) lesioned with 6-OHDA at the SN.

After delivery to the Central Animal Facility at McMaster University (Hamilton, Ontario) all rats were handled by experimenters for 7 days. Animals were then subjected to the apomorphine-induced rotations test.

Once all baseline data were collected, the rats were placed under gaseous anaesthesia and injected with one of three treatments into the striatum as described in Table 3. Treatments used include: 27kDa fragment of CRP40 (1,5) (65µg); 17kDa fragment of CRP40 (1,4) (41µg); 7kDa fragment of CRP40 (2,4) (15µg).

Animals were monitored daily for one week following surgery, and weighed daily to ensure healthy recovery and weight gain. If a 30% reduction in body weight was observed, animals were immediately euthanized as endpoints had been reached.

All animals were again tested using the same behavioural methods for apomorphine-induced rotations at days 4, 7, and 10 post-injection. On day 15 post-injection, all rats were sacrificed by isoflurane overdose and decapitation. Fresh brain tissue was sliced using razor blades and a brain mould, then micro-punched for specific brain area samples, and flash frozen on dry ice.

Animals were housed and tested in compliance with the guidelines described in the Guide to the Care and Use of Experimental Animals (Canadian Council on Animal Care, 1984; 1993). The McMaster University Committee for Animal Welfare approved all protocols.

5.1.3 Behavioural testing: Apomorphine-induced rotations

Performed as described in section 4.2.8.

5.1.4 Stereotaxic injection surgery: Rat

Performed as described in section 4.211.

5.1.5 Animal sacrifice and tissue collection

Performed as described in section 4.2.12.

5.1.6 Competitive binding with tritiated dopamine and cold dopamine

The ability of cold DA to displace bound tritiated dopamine ([^{3}H]-DA) in CRP40 protein, 7kDa (2,4) fragment, or HSP47 was assessed by competitively binding [^{3}H]-DA in the presence of different concentrations of unlabeled DA (in 0.1% ascorbic acid) using the same methodology as in (Gabriele et al., 2009). Briefly, the binding of [^{3}H]-DA was carried out in triplicate in 1.0ml of assay buffer containing 1nM of radioligand, the indicated concentrations of unlabeled DA (0.0 M, 10^{-13} M, 10^{-9} M, 10^{-5} M) and 10µg of one of CRP40 protein, 7kDa (2,4) fragment, or HSP47. At the end of incubation, the bound and free ligands were separated by vacuum filtration through Whatman GF/B filters. The filters were washed with 3 x 5ml of Tris–EDTA buffer and the radioactive counts were determined on a Beckman scintillation counter.

Assay Buffer was prepared by adding the following components to 500ml of double distilled water: 25ml 1M Tris-HCl (pH 8; 50 mM), 0.5ml 500mM EDTA (1mM), 100mM PMSF in ethanol (0.1mM), 0.508g $MgCl_2 \cdot 6H_2O$ (5mM), 0.0077g DTT (0.1mM), 0.050g Bacitracin (100 µg/ml), and 0.0025g Soybean Trypsin (5 µg/ml). The final pH was adjusted to 7.4.

Filtration Buffer was prepared by adding the following components to 2L of double distilled water: 100ml 1M Tris-HCl (pH 8; 50 mM), and 4ml 500mM EDTA (1mM). The final pH was adjusted to 7.4.

5.1.7 Competitive binding with tritiated dopamine and cold apomorphine

The ability of cold apomorphine to displace bound tritiated dopamine ([^{3}H]-DA) in CRP40 protein, 7kDa (2,4) fragment, or HSP47 was assessed by competitively binding [^{3}H]-DA in the presence of different concentrations of unlabeled apomorphine (in 0.1% ascorbic acid) using the same methodology as in (Gabriele et al., 2009). Briefly, the binding of [^{3}H]-DA was carried out in triplicate in 1.0ml of assay buffer containing 1nM of radioligand, the indicated concentrations of unlabeled apomorphine (0.0 M, 10^{-13} M, 10^{-9} M, 10^{-5} M) and 10µg of one of CRP40 protein, 7kDa (2,4) fragment, or HSP47. At the end of incubation, the bound and free ligands were separated by vacuum filtration through Whatman GF/B filters. The filters were washed with 3 x 5ml of Tris–EDTA buffer and the radioactive counts were determined on a Beckman scintillation counter.

Assay Buffer was prepared by adding the following components to 500ml of double distilled water: 25ml 1M Tris-HCl (pH 8; 50 mM), 0.5ml 500mM EDTA (1mM), 100mM PMSF in ethanol (0.1mM), 0.508g MgCl2 · 6H2O (5mM), 0.0077g DTT (0.1mM), 0.050g Bacitracin (100 µg/ml), and 0.0025g Soybean Trypsin (5 µg/ml). The final pH was adjusted to 7.4.

Filtration Buffer was prepared by adding the following components to 2L of double distilled water: 100ml 1M Tris-HCl (pH 8; 50 mM), and 4ml 500mM EDTA (1mM). The final pH was adjusted to 7.4.

5.1.8 Data analysis

Apomorphine-induced rotations:

Performed as in section 4.2.14.

Competitive binding:

Competitive binding was compared between CRP40 protein and 7kDa (2,4) fragment using an un-paired t-test ($p<0.05$) for each of apomorphine, and DA competition.

5.2 Results

Injection of the 7kDa (2,4) protein fragment into the striatum of 6-OHDA hemi-lesioned rats alleviated the apomorphine-induced rotational symptoms four days after treatment (Figure 12a). Both the 27kDa (1,5) fragment and the 17kDa (1,4) fragment treatments showed a similar trend, however, group size was too small to validate this result (Figure 12b; 12c). Analysis of rotations data demonstrated a significant effect across treatment groups over time ($p<0.0001$). Pairwise contrasts showed that the 7kDa (2,4) protein fragment treated group displayed significantly decreased rotations from baseline compared to all other groups on day four ($p<0.0001$).

Comparison of specific binding of [^{3}H]-DA by CRP40 protein in competition with cold DA to specific binding of [^{3}H]-DA by 7kDa (2,4) fragment in competition with cold DA revealed a significant difference ($p<0.05$) (Figure 13a). Comparison of specific binding of [^{3}H]-DA by CRP40 protein in competition with cold apomorphine to specific binding of [^{3}H]-DA by 7kDa (2,4) fragment in competition with cold apomorphine also revealed a significant difference ($p<0.05$) (Figure 13c). The CRP40 protein binds DA, as previously reported (Figure 7; Figure 13a) (Gabriele et al., 2009), and also binds apomorphine (Figure 13c). The 7kDa (2,4) fragment does not bind either of DA (Figure 13a) or apomorphine (Figure 13c). The HSP47

protein (negative control) does not bind either of DA (Figure 13b) or apomorphine (Figure 13d).

5.3 Discussion

This study examined the effect of CRP40 fragment injection on the behavioural phenotypes of the 6-OHDA model of PD to identify the segment of the CRP40 full-length protein responsible for behavioural effects.

Injection of the 7kDa (2,4) protein fragment (60 amino acids) into the striatum transiently alleviated the apomorphine-induced rotational symptoms in 6-OHDA hemi-lesioned rats in a similar trend seen after treatment with the CRP40 full-length protein. These findings suggest that the region of CRP40 that confers behavioural effects is located within the 7kDa sequence of the (2,4) fragment. These results require extension by following up with dose-response and mechanism studies.

After day seven, rotational symptoms began to return to baseline. As such, the 7kDa (2,4) protein fragment shows a longer therapeutic effect than the full-length protein. It is possible that protein treatments may become degraded, depleted or, washed-out over time, and administration of a dose on a weekly basis may be the best approach when conducting long-term studies of CRP40 as a potential treatment for 6-OHDA hemi-lesioned rats.

Similar to previous reports by Gabriele and colleagues (2009), the current binding studies show that the CRP40 full-length protein binds DA (Figure 7; Figure 13a). These novel binding studies also revealed that the CRP40 full-length protein binds apomorphine (Figure 13c), and that the 7kDa (2,4)

fragment does not bind either of DA (Figure 13a) or apomorphine (Figure 13c). Finally, these studies demonstrate that the HSP47 protein does not bind either of DA (Figure 13b) or apomorphine (Figure 13d), reinforcing its use as a valid and appropriate negative control for studies involving CRP40 and fragments thereof.

In summary, both proteins (the CRP40 protein and the 7kDa (2,4) fragment) alleviated behavioural symptoms in the 6-OHDA hemi-lesioned rat model of PD. Since the full-length CRP40 protein was found previously to bind DA and the 7kDa (2,4) has now been found not to bind DA, these findings suggest that CRP40 has a dual biological function in PD: binding and modulation of DA, as well as a behavioural effect (the mechanism of which is still unknown).

It is possible that behavioural effects are conferred by some indirect dopaminergic function of CRP40. For example, since rotations in the 6-OHDA model are due to D2 receptor sensitization, perhaps the 7kDa (2,4) fragment activates the desensitization of these receptors via internalization. On the other hand, behavioural changes reported here may be caused by some other function of this segment of CRP40 altogether. Future mechanistic studies will focus on elucidating the functional properties of both the full-length CRP40 and the 7kDa (2,4) fragment.

	Striatal Injection
27kDa (1,5) fragment	1
17kDa (1,4) fragment	1
7kDa (2,4) fragment	4

Table 3: Description of treatment groups and group numbers (n). A total of 6 rats received striatal treatment injections.

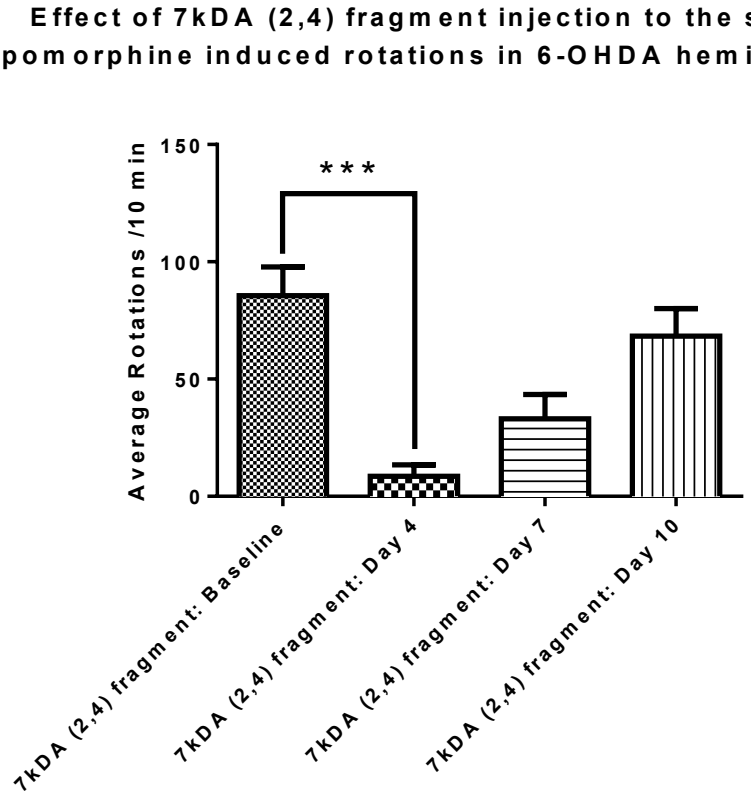

Figure 12a: 7kDa (2,4) protein fragment treated animals (striatum injection; n=4) showed significantly decreased number of rotations at day four after treatment from baseline ($p<0.0001$***).

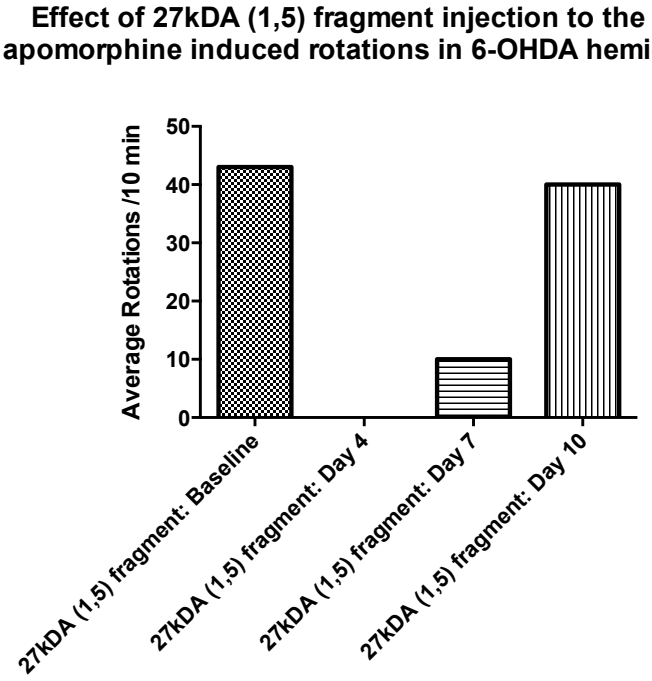

Figure 12b: 27kDa (1,5) protein fragment treated animal (striatum injection; n=1) showed decreased number of rotations at day 4 after treatment from baseline.

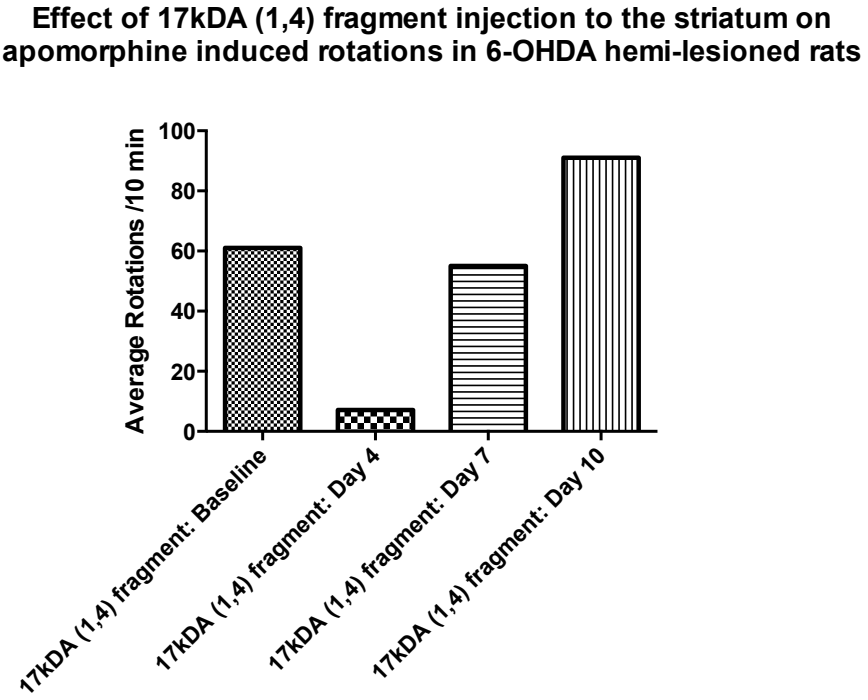

Figure 12c: 17kDa (1,4) protein fragment treated animal (striatum injection; n=1) showed significantly decreased number of rotations at day four after treatment from baseline.

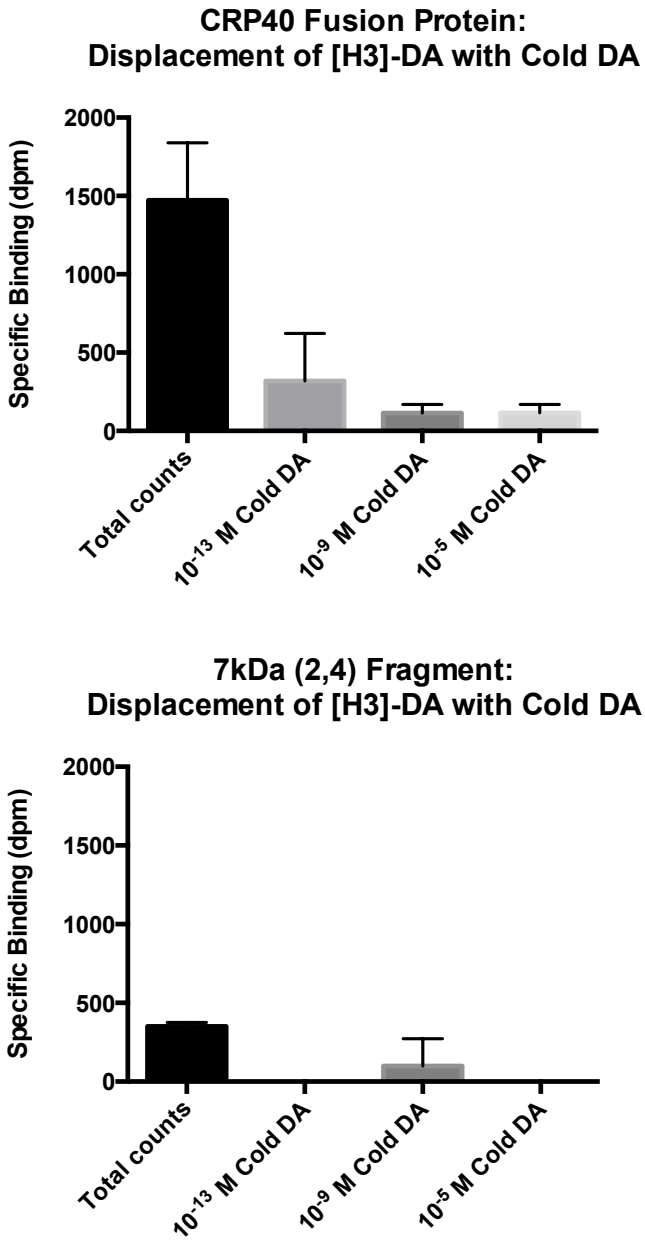

Figure 13a: Comparison of specific binding of [^{3}H]-DA by CRP40 protein in competition with cold DA to specific binding of [^{3}H]-DA by 7kDa (2,4) fragment in competition with cold DA.

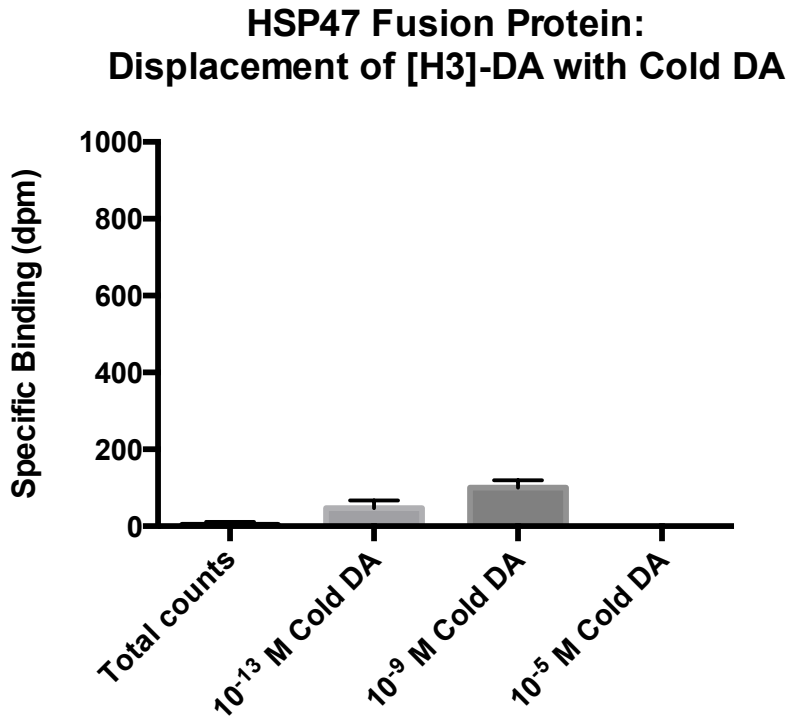

Figure 13b: Specific binding of [^{3}H]-DA by HSP47 protein in competition with cold DA.

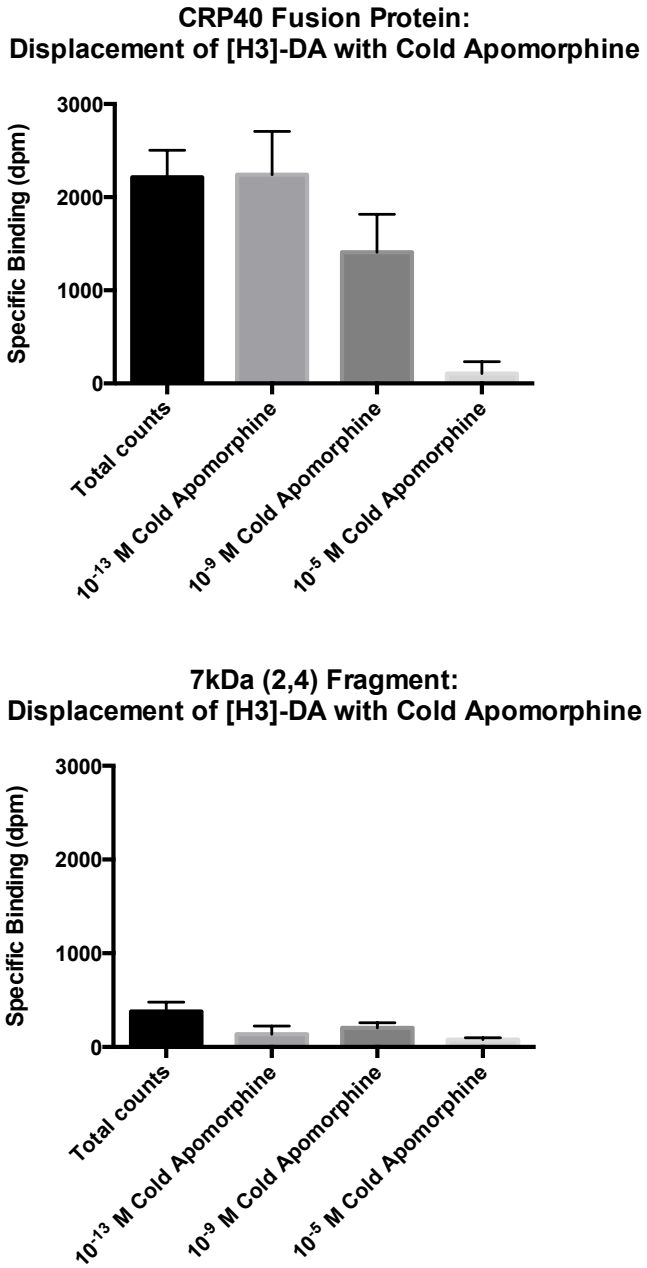

Figure 13c: Comparison of specific binding of [^{3}H]-DA by CRP40 protein in competition with cold apomorphine to specific binding of [^{3}H]-DA by 7kDa (2,4) fragment in competition with cold apomorphine.

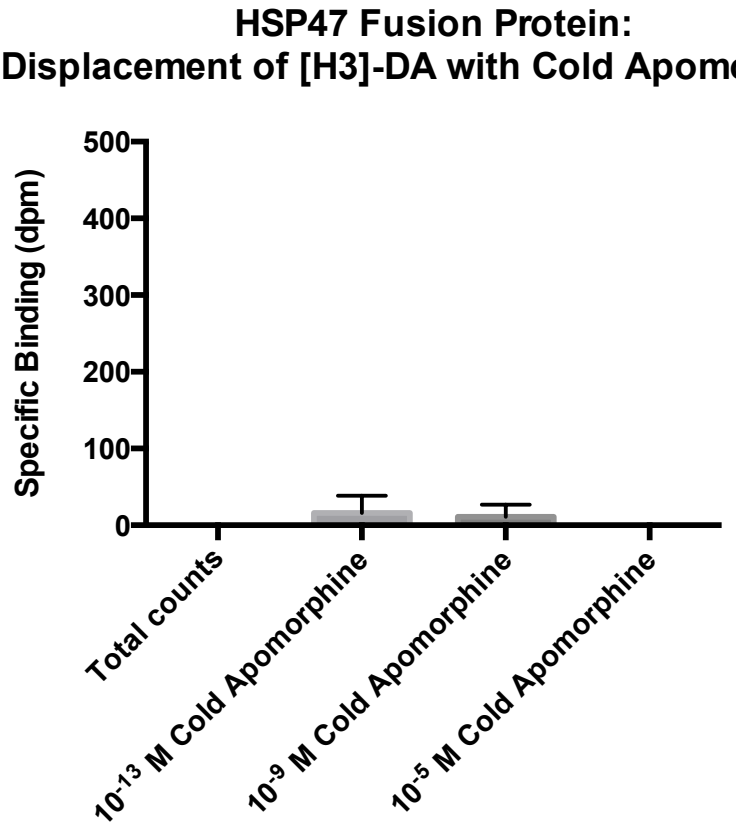

Figure 13d: Specific binding of [^{3}H]-DA by HSP47 protein in competition with cold apomorphine.

CHAPTER 6

EFFECTS OF CRP40 ON MEMORY AND COGNITION IN A TRANSGENIC MOUSE MODEL OF ALZHEIMER'S DISEASE (A PRELIMINARY STUDY)

6.0 Alzheimer's disease

Dementia affects 1% of people 60 to 69 years old, and 39% of people 90 to 95 years old worldwide (Jorm et al., 1987; Ritchie et al., 1992).

Early symptoms of AD include impairment of learning and memory (Forstl and Kurz, 1999; Mohs et al., 2000). Late-stage symptoms relate to cognitive dysfunction including disturbances of thought, perception, affect, and behaviour (Forstl and Kurz, 1999; Mohs et al., 2000). Morphologically, brain samples from patients with AD exhibit significant atrophy, as well as neuritic plaques and neurofibrillary tangles (Yaari and Corey-Bloom, 2007).

Diagnosis of AD is by clinical interview, such as the mini-mental state examination (MMSE), and behavioural observation. Standardized examination of patients' mental state is part of the Diagnostic and Statistical Manual of Mental Disorders-IV (DSM-IV), which covers memory, language, perceptual skills, attention, constructive abilities, orientation, problem solving and functional abilities (American Psychiatric Association). Recently, a CSF test was introduced for the diagnosis of AD where β-amyloid, tau, and phospho-tau-181 are measured as biomarkers (Marksteiner et al., 2007).

Research based on the pathophysiology of AD has been, and continues to be, approached from a range of causal hypotheses. For example, there are theories that relate to amyloid protein pathology, tau protein pathology,

and dysfunction of the acetylcholine neurotransmitter system.

β-amyloid is abnormally processed in AD neurons, causing fragmentation of the protein into insoluble peptides that coagulate and form plaques in the brain (Bayer et al., 2001; Hardy and Selkoe, 2002; Cummings et al., 1998). It is possible that this protein aggregation causes neuronal dysfunction, initiates cell death and causes degeneration.

Tau is found hyper-phosphorylated and clustered into inclusion bodies in the AD brain (Yaari and Corey-Bloom, 2007). These neurofibrillary tangles are located inside neurons and cause disruption of normal cytoskeletal architecture, which may cause neuronal cell death leading to neurodegeneration.

Finally, decreased concentrations of acetylcholine are a cardinal characteristic of AD, and strongly correlate with the degree of cognitive impairment in patients (Francis et al., 1993; Perry et al., 1972; Wilcock et al., 1982; Sims et al., 1983; Francis et al., 1999). Studies show that dysfunctions exist in the synthesis, release, and re-uptake of acetylcholine in AD– confirming theories of an underlying broad cholinergic system failure (Bowen et al., 1976; Davies and Maloney, 1976; Perry et al., 1977; Rylett, et al., 1983; Francis et al., 1999).

Current options for AD treatment include pharmaceutical therapy and psychosocial intervention. Patients are prescribed acetylcholinesterase inhibitors, and may also be prescribed memantine (an NMDA receptor

antagonist) (Kelly et al., 1997; Farlow et al., 2008). Patients may or may not undergo intervention as a complimentary management strategy (WHO, 2000).

6.1 Implications of MOT-2 and CRP40 in Alzheimer's disease

Chaperone proteins have been examined extensively in the realm of AD. MOT-2/CRP40 have been found, in a few studies to show some relation to the pathology of this disease.

Studies show that MOT-2 is regulated by Apo-E in the hippocampus of patients with AD (Osorio et al., 2007). Apo-E knockout mice, an experimental model of AD, exhibit exacerbated protein oxidation in the brain. MOT-2 was found to be among the six most heavily oxidized proteins found in these mice, suggesting its dysfunction as a contributing factor to the degeneration seen in patients with AD (Choi et al., 2004).

Cell studies of AD and neurotoxicity display evidence that mitochondrial import of MOT-2 is significantly declined after treatment with sub-lethal β-amyloid causing mitochondrial dysfunction and cell death not unlike the human disease state (Sirk et al., 2007). Another study using SH-SY5Y cells found that MOT-2 overexpression actually mitigates β-amyloid-induced damage and cell death, suggesting protective effects of MOT-2/CRP40 in AD (Qu et al., 2011).

Since MOT-2/CRP40 show evidence of neuroprotective characteristics, and MOT-2 exhibits multiple mitochondria-related functions, this protein could be involved in AD pathophysiology.

6.2 3xTg-AD triple knockout model of Alzheimer's disease

The 3xTg-AD triple knockout mouse model of AD has been commonly used in many recent animal studies of dementia. These mice are homozygous for three mutant alleles: *Psen1* mutation, and co-injected APPSwe and tauP301L transgenes. The animals are viable, fertile, and display no initial gross physical or behavioural abnormalities. The 3xTg-AD mice progressively develop plaques and tangles via β-amyloid peptide deposition (Oddo et al., 2003). Synaptic transmission and long-term potentiation are impaired in mice six months of age (Gimenez-Llort et al., 2007; Sterniczuk et al., 2010). Behaviourally, the 3xTg-AD mice exhibit reduced exploratory behavior, as well as learning and memory deficits as tested using the Morris Water Maze (MWM) paradigm (Gimenez-Llort et al., 2007; Sterniczuk et al., 2010).

6.3 Objectives

Based on earlier findings, which show that MOT-2 protects against β-amyloid-induced cell death and may be dysregulated in AD (Sirk et al., 2007), and since CRP40 shows similar neuroprotective chaperone functions to MOT-2, the study presented here was designed to explore whether CRP40 demonstrates a potential therapeutic role in a mouse model of AD.

The current objective was to test whether injection of 10µg of CRP40 full-length protein into the entorhinal cortex has an effect on cognitive symptoms in the 3xTg-AD mouse model of AD. This model, discussed in detail in section 6.2, exhibits reduced exploratory behavior, and deficits in learning and memory. For the current project, the MWM test of learning and memory was employed.

6.4 Materials and methods

6.4.1 Preparation of CRP40 full-length protein

Performed as described in section 4.2.6.

6.4.2 Animals

3xTg-AD mice homozygous for all three mutant alleles (*Psen1* mutation and APPSwe/tauP301L transgenes (Tg(APPSwe,tauP301L)1Lfa)) were used in this study. Both 3xTg-AD (10) and B6129SF1-J WT control (11) mice (approximately 50g in weight) were originally from the Jackson Laboratory (Bar Harbor, ME).

After delivery to the animal housing facility at the Henderson General Hospital (Hamilton, Ontario), all mice were handled by experimenters for 7 days. Animals were then subjected to the eight-day protocol for the MWM for baseline measures. Protocols for the MWM tests will be described in section 6.2.3.

Once all baseline data were collected, mice were placed under gaseous anaesthesia and injected with one of the two treatments at either the entorhinal cortex as described in Table 4. Treatments used include: CRP40 protein (10µg), and HSP47 protein (negative control; 10µg).

Animals were monitored daily for one week following surgery, and weighed daily to ensure healthy recovery and weight gain. If a 30% reduction in body weight was observed, animals were immediately euthanized as endpoints had been reached.

All animals were again tested using the same behavioural methods for the eight-day MWM. All mice were sacrificed by carbon monoxide asphyxiation.

Animals were housed and tested in compliance with the guidelines described in the Guide to the Care and Use of Experimental Animals (Canadian Council on Animal Care, 1984; 1993). The McMaster University Committee for Animal Welfare approved all protocols.

6.4.3 Behavioural testing: Morris water maze

The pool used for the MWM task was a circular tank (1.5 m diameter) painted white and filled with water maintained at 26–29 °C. The maze was located in a room containing several simple visual, extra-maze cues. Memory and cognition were measured using Noldus EthoVision software (Leesburg, VA). The protocol used in this study was adapted from Clinton et al., 2007 and Sakic et al., 1993.

The eight days of this protocol were carried out as follows: day one– cue trials, day two– 1st acquisition trial, day three– 2nd acquisition trial, day four– 3rd acquisition trial, day five– 4th acquisition trial, day six– probe and extinction trials, day seven– cue reversal trial, day eight–acquisition reversal trial.

6.4.4 Stereotaxic injection surgery: Mouse

Prior to beginning surgery, all instruments were thoroughly soaked in liquid disinfectant (Coldspore; available from the McMaster Central Animal Facility (CAF)) for 20 minutes and rinsed with sterile double distilled water (Baxter). All surfaces, towels, and gauze pads used were also sterile.

All animals were weighed, and weight was recorded in grams. Animals were injected with Ketamine (anaesthetic; intraperitoneal) according to the guidelines from McMaster CAF for dosage. The animal was then shaved from between the ears to between the eyes. The sedated animal was then mounted on the stereotax using the ear bars and incisor bar. The primary surgeon prepared the injectable drugs as follows: Anaphen: subcutaneous (0.05ml prevents fluid build-up in lungs), saline: subcutaneous (1ml for hydration), and Baytril: intramuscular (0.01ml antibiotic; injected post-surgery). The primary surgeon then scrubbed-in according to the McMaster CAF survival surgery guidelines.

The primary surgeon cleaned the shaved area on the animal's head using 3 step prep solutions (available from the McMaster CAF). Someone other than the primary surgeon applied a generous amount of Lacri-Lube (eye ointment; available from the McMaster CAF (to ensure the eyes do not dry out during the procedure), then injected saline and Anaphen.

The primary surgeon made a midline incision in the scalp from behind the eyes to the area between the ears. The periosteum was removed using a

bone curette. The skin was then retracted using four haemostats and the incision area was thoroughly cleaned and dried using sterile gauze or sterile cotton swabs.

Someone other than the primary surgeon located the desired reference point (Lambda) and recorded the coordinates. Calculate the desired coordinates for drilling from these references. Coordinates used for the entorhinal cortex were: 0.3mm posterior to Lambda, 2.3mm lateral to midline, and 3.0mm below the skull surface. The desired hole was drilled with a large gauge needle.

Someone other than the primary surgeon inserted the Hamilton syringe (10µl capacity; mounted to the stereotax) to the desired depth. Infusion rate was set to 0.1µl/minute. Five minutes was allowed for infused solution to diffuse into the skull before retracting the syringe.

Once the Hamilton syringe was retracted, the incision was closed: the primary surgeon closed the skin using VetBond (suture-replacing glue) pinching the skin together using forceps. The animal was then injected with antibiotic Baytril into the thigh muscle, and removed from the stereotax. The animal was placed under a heating lamp for recovery in a clean cage lined with paper towels.

6.4.5 Data analysis

Morris Water Maze:

The protocol used for data analysis was adapted from Clinton et al., 2007 and Sakic et al., 1993. Briefly, dependent measure was analyzed by analysis of variance (ANOVA) and included age, genotype, and MWM performance ($p<0.05$). The relationship between behavioural variables (acquisition latency, memory retention, and learning rate) and genotype was assessed by Multiple Regression.

6.5 Results

All mice were tested for baseline MWM performance and results showed a significant difference ($p<0.05$) between AD and controls. Specifically, AD animals performed significantly slower on the MWM paradigm.

Following either CRP40 or HSP47 protein injection, none of the animals showed any significant difference compared to baseline (data not shown).

6.6 Discussion

Following either CRP40 or HSP47 protein injection, none of the AD animals in this study showed any significant difference on MWM performance from baseline. Specifically, AD animals performed significantly slower on the MWM paradigm both before and after treatment. Since all mice were tested for baseline MWM performance, and results showed a significant difference ($p<0.05$) between AD and controls as expected, it can be ruled out that the lack of performance change post-treatment was due to some issue with the model. As such, this result suggests that either the invasive nature of the surgeries themselves confounded any change in MWM performance, or CRP40 protein treatment was not effective in treating behaviour, cognition, and memory in this model.

It is possible that due to the confounding effects of invasive surgery, no conclusive results can be extrapolated from the data. Animals recovered well from the surgical procedure, however, and there were no significant indications that mice were injured in such a way that would hinder their behavioural performance in the MWM paradigm.

It is also possible, and perhaps more probable, that CRP40 does not confer any therapeutic effect on this animal model of AD. Since this disease has very little to do with the DA system, it is not likely that CRP40 would be involved directly in the disease process. Instead, it is be more

probable that previously reported MOT-2 implications in PD (Osorio et al., 2007; Choi et al., 2004; Sirk et al., 2007; Qu et al., 2011) are specific to the mitochondrial mother protein, and do not actually implicate CRP40 as a factor in the pathophysiology of AD.

	Entorhinal Injection
3xTg-AD: HSP47 protein	5
3xTg-AD: CRP40 protein	5
B6129SF1-J WT Control: HSP47 protein	4
B6129SF1-J WT Control: CRP40 protein	7

Table 4: Description of treatment groups and group numbers (n). A total of 21 rats received striatal treatment injections: 10 were 3xTg-AD, and 11 were B6129SF1-J WT Control.

CHAPTER 7

HUMAN BLOOD ANALYSIS REVEALS DIFFERENCES IN GENE EXPRESSION OF CRP40 IN PARKINSON'S DISEASE

7.0 Platelets: systemic markers for studying neurodegenerative disease

Blood is an ideal tissue for studies involving live human patients since it is so easy to harvest and can be separated into cell specific samples using straightforward protocols. Platelets, specifically, can be collected at high yield from small amounts of whole blood.

The use of platelets to study CNS disorders is not a new concept. Many have reported important findings by use of this peripheral tissue. For example, the effects of mitochondrial dysfunction in ALS can be observed by studying platelets (Pretorius, 2008; Shrivastava et al., 2011). Further, AD patients show similar concentrations of serotonin depletion in platelet samples compared to samples from affected neurons (Kumar et al., 1995; Dupuis et al., 2010). Most important to the current study is that DJ-1 is found dysregulated in the human PD blood samples, and the amount of platelet contamination in these samples can significantly change the concentration of DJ-1 (Shi et al., 2010). As well, platelets are known to exhibit concentrations of DA and L-DOPA that mirror catecholamines in the brains of patients with PD (Blandini et al., 2003).

Platelets are anucleated– they lack a nucleus and, therefore, lack contamination by nuclear DNA (Binder et al., 2006). Platelets are also rich in mitochondria (Binder et al., 2006). For this reason, platelets make excellent tissue samples for studies of mitochondrial dysfunction and oxidative stress.

7.1 Objectives

Based on earlier findings, which show that CRP40 is expressed in blood cells, may be dysregulated in PD (Jin et al., 2006), and is found in deficit in the platelets of a primate model of PD, the study presented here was designed to explore whether blood concentrations of CRP40 mirror concentrations of CRP40 in the brain of PD patients. Specifically, these studies tested whether PD subjects show differences in CRP40 mRNA concentrations in platelets compared to healthy controls.

7.2 Materials and methods

7.2.1 Study setting and participants

Ethical approval for this study was obtained from McMaster University/St. Joseph's Healthcare (Hamilton, Canada). A total of n=31 subjects were included in the current study (n=18 PD, n=13 controls) (Table 5). The mean age was 61.1 (±19.5) years and 71.4% of subjects were male. All subjects gave informed consent prior to enrolment in the study. Diagnosis of PD was confirmed by physical examination and a second opinion was attained from a movement disorder specialist. Controls were analyzed by the same method.

7.2.2 Preparation of blood samples

Blood (20–30ml) was collected from each subject. Platelets were prepared as per the following: 10ml of blood was collected in 1.42ml of acetate citrate dextrose BD vacutainers. The blood was centrifuged (980 g; 2 minutes), and 2/3 of the top layer (platelet-rich plasma region) were removed and centrifuged again (1200 g; 7 minutes). The pellet was washed twice in 7ml PBS-EDTA-Bovine Serum Albumin (PEB) solution, centrifuged (1200 g; 7 minutes), and then resuspended in 1ml of PEB wash solution. The final platelet pellet was then centrifuged (1200 g; 7 min) in an Eppendorf tube and the supernatant was removed. The pellet was collected and stored at -80°C.

RNA was extracted from platelet samples using the TRIzol method (Invitrogen Life Technologies, Canada) according to manufacturer's protocols. The TURBO DNA–free kit (Ambion, United States) was used to remove contaminating any DNA. RNA purity was quantified using a Beckman spectrophotometer DU-640. cDNA prepared with SuperScript III (Invitrogen Life Technologies, Canada) was used for analysis of CRP40/MOT-2 mRNA copy numbers. Since MOT-2 is highly homologous to CRP40, primers amplified both sequences.

7.2.3 Analysis of CRP40/ MOT-2 mRNA copy numbers

Absolute copy numbers of CRP40/MOT-2 mRNA were determined in triplicates (10ng cDNA) using real-time reverse-transcriptase polymerase chain reaction (RT-PCR), as previously optimized in (Gabriele et al., 2010b). No primer-dimers were detected and transcripts showed optimal efficiencies. Conditions were optimized to ensure amplifications were in the exponential phase and efficiencies remained constant throughout. Representative real-time RT-PCR products each showed 100% homology with the CRP40 gene regions. Data were normalized against cyclophilin (human housekeeping gene).

7.2.4 Data analysis

Student's t-test was used to compare CRP40/MOT-2 mRNA concentrations between PD subjects and healthy controls. Multiple regression analysis was used to examine the relationship between health status and CRP40/MOT-2 mRNA concentration, while controlling for the potential confounding effects of subject age and sex. Statistical tests were two-sided with $\alpha=0.05$.

7.3 Results

Mean CRP40/MOT-2 mRNA copy numbers were significantly lower among PD patients compared to controls ($p<0.001$) (Figure 14) (Lubarda et al., 2013). Given imbalances in the age and sex distribution, an adjusted analysis controlling for these factors was conducted using multiple regression. The association between PD and CRP40 concentrations remained after controlling for the effects of subject age and sex.

7.4 Discussion

The present study is the first to report significant reductions of CRP40/MOT-2 mRNA concentrations in the blood of live PD patients (Lubarda et al., 2013). Previous studies have indicated significant reductions in CRP40/MOT-2 concentrations in human post-mortem PD brain specimens; with progressive depletion in the later stages of the disorder as motor and cognitive symptoms worsen (Jin et al., 2006). Dysregulation of CRP40/MOT-2 in blood platelets mirrors previous observations in the brain. The findings of the current study concur with several studies that have implicated molecular chaperone proteins, including MOT-2, in oxidative stress and PD (Burbulla et al., 2010; Nair and Mishra, 2001; Shi et al., 2008).

PD pathogenesis is likely due to the combined effects of increased oxidative stress and impaired mitochondrial function (Schapira, 2009). MOT-2, the molecular chaperone from which CRP40 is expressed, performs various functions related to protein folding, oxidative stress response, and protection of mitochondria (Burbulla et al., 2010; Nair and Mishra, 2001; Shi et al., 2008). CRP40/MOT-2 have been linked to neurodegenerative diseases through interactions with PD-associated proteins (e.g., DJ-1), and expression from chromosome 5q31.1, a putative PD locus (Nair and Mishra, 2001; Sklar et al., 2004).

Recently, PD patients were found to show mutations in the *Mortalin-2* gene located within the C-terminal domain of the protein, from which CRP40 is expressed (Burbulla et al., 2010). Interestingly, the MOT-2 N-terminus is conserved among 70kDa heat shock proteins while the C-terminal substrate binding domain varies significantly, indicating the possibility of distinct roles for CRP40 (Luo et al., 2010). Based on these findings, the closely related protein, CRP40, requires further investigation for roles in mitochondrial homeostasis and disorders of oxidative stress such as PD.

The reduction of CRP40 in PD patient blood presents a compelling finding and suggests its possible role in the disease process. These findings are preliminary and require larger sample sizes for validation. Further, since PD patients in this study differed with regards to treatment (none, anti-PD medications, other medications), results showing decreased CRP40 cannot be attributed specifically to disease process. Future studies will analyze separate groups of PD patients as chronically treated or drug naïve. Investigation of CRP40 concentrations in newly diagnosed, drug naïve PD patients will further delineate roles of CRP40 in the PD pathology, as well as in mitochondrial homeostasis and oxidative stress in movement-related disease.

These preliminary findings are currently being validated by an on going blood collection initiative. Drs. Mishra and Gabriele (McMaster University)

are currently collaborating with the University of Laval, Le Centre Hospitalier Universitaire de Québec, University of Montreal (Le Centre Hospitalier de L'Universite to Montreal), and Toronto Western Hospital to procure blood samples from PD patients and healthy age-matched controls, as well as AD and stroke patients for use as negative controls.

In summary, these findings suggest that CRP40 is genetically dysregulated in PD, and can be observed and measured in blood samples from live patients. The molecular mechanism of CRP40 is incompletely understood, however, previous results suggest that this protein may be protective against oxidative damage (Volobоueva et al., 2008; Xu et al., 2009). These preliminary results provide insight about the implications of CRP40 in the pathogenesis of PD and present a significant opportunity for further investigation of molecular chaperone proteins as biomarkers.

	N=31
Health Status	
Control	13 (41.9%)
PD	18 (58%)
Age	61.1 (±19.5)
Sex[1]	
Male	20 (71.4%)
Female	8 (28.6%)
Reported as n (%), except for age (mean ± S.D.).	
[1]Frequencies may not sum to N=31 due to missing data.	

Table 5: Subject Descriptive Statistics (from Lubarda et al., 2013).

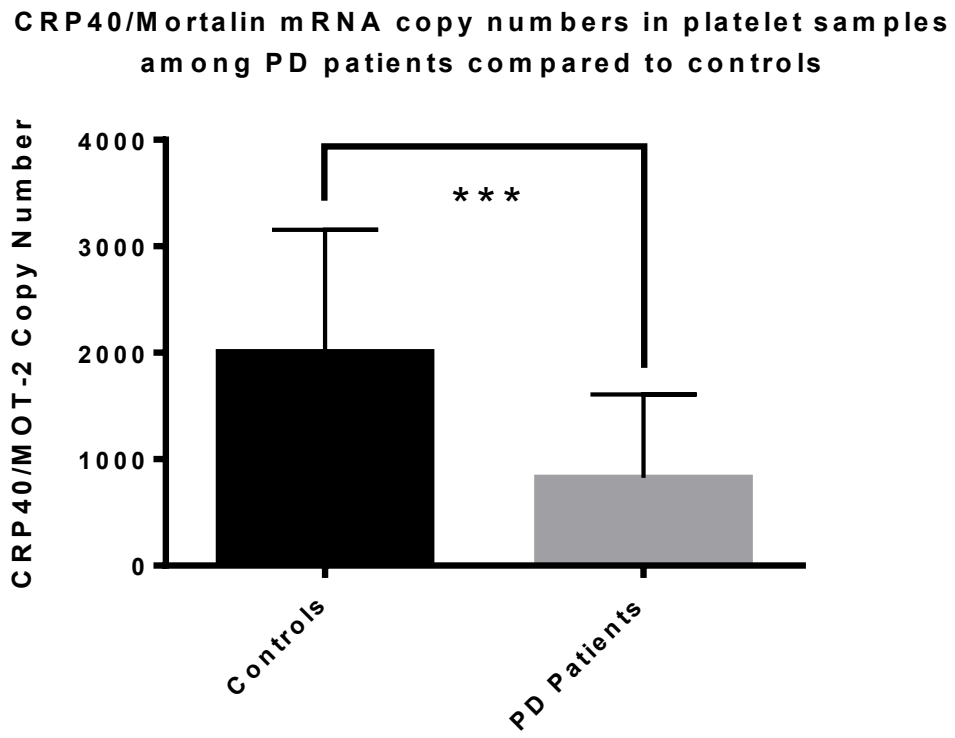

Figure 14: CRP40/MOT-2 mRNA expression in blood platelets is specifically reduced in PD subjects (n=18) ($p<0.001$***) compared to controls (n=13).

CHAPTER 8

APPLICATIONS FOR SCHIZOPHRENIA:

HUMAN BLOOD ANALYSIS REVEALS DIFFERENCES IN

GENE EXPRESSION OF CRP40

8.0 Schizophrenia

SCZ affects roughly 7 people per 1,000 adults (mostly within the age range of 15-35 years) worldwide (WHO, 2013). Major symptoms of this disease can be categorized as negative (the lack of some normal feature) and include flattened affect, social withdrawal, and attention impairment; or positive (the presence of some abnormal feature) and include hallucinations, delusions, unusual movements, and disorganized behaviour (Abi-Dargham et al., 2000; Lewis and Lieberman, 2000; Seeman and Kapur, 2000; Kasai et al., 2002; North et al., 2007).

There is also a prominent neurodegenerative characteristic of SCZ; imaging studies show loss of gray matter in the frontal and temporal lobes (Lim et al., 1996; Pe´rez-Neri et al., 2006; Pasternak et al., 2012). Morphologically, SCZ brain samples also show reductions in hippocampal volume, as well as enlargement of the lateral ventricles in comparison to healthy controls (Kempton et al., 2010; Adriano et al., 2012; Nelson et al., 1998).

Diagnosis of SCZ is by clinical interview and behavioural observation (WHO, 1998). Standardized examination of patients' mental state is part of the DSM-IV. There is no specific biomarker to confirm SCZ diagnosis.

The pathophysiology of SCZ is widely regarded as a dysfunction of synaptic connectivity (Martins-de-Souza et al., 2011), but various other theories for pathology have recently been considered. For example, many

studies implicate dysfunctional molecular chaperones in the pathogenesis of SCZ (Schwarz et al., 1999). Recent findings show that genetic variations of HSP70 are associated with SCZ (Kim et al., 2008; Pae et al., 2005; Pae et al., 2009). Further, dysregulation of HSPA12A has been found in patients with diagnoses of SCZ (Pongrac et al., 2004).

Other recent studies show that mitochondrial dysfunction and oxidative stress have considerable impact on the pathology of SCZ. Proteomic profiling results suggest that human brain tissue from patients with SCZ display exacerbated ROS production as a result of dysfunctional energy metabolism (Schwarz et al., 2008). Further, changes to mitochondrial morphology, and mutations in mitochondrial DNA are also common to patients with SCZ (Amar et al., 2007, Munakata et al., 2005, Clay et al., 2011). SCZ patients show higher than normal DA activity in the brain. The auto-oxidative nature of this neurotransmitter has long been thought to play a part in the oxidative stress and mitochondrial dysfunction contributing to the pathogenesis of SCZ (Ben-Shachar et al., 2004).

Current options for SCZ treatment include pharmaceutical therapy, behavioural therapy, and social rehabilitation. Patients are prescribed either a conventional or an atypical antipsychotic drug, which may or may not be complimented by therapy and social intervention (WHO, 1998).

8.1 Implications of MOT-2 and CRP40 in Schizophrenia

MOT-2/CRP40 have become an important clue towards understanding the pathophysiology of SCZ. Over several years, Gabriele and colleagues have made many discoveries along this line of research.

Post-mortem brain specimens from the Stanley Foundation Neuropathology Consortium show that SCZ patients have significantly decreased concentrations of CRP40 protein compared to healthy controls (Gabriele et al., 2005). Specifically, unmedicated SCZ patients exhibit the least CRP40, and anti-psychotic treated SCZ patients show CRP40 concentrations between that of untreated SCZ patients and healthy controls.

More recently, the same authors reported a positive correlation between lifetime antipsychotic use and CRP40 concentrations in the dorsolateral PFC of SCZ patients. Patients that had been taking higher doses for longer periods of time showed higher concentrations of CRP40 expression (Gabriele et al., 2010b). Antipsychotic drugs bind and block D2 receptors and dopaminergic firing, causing increased unbound DA at the synapse, and subsequent upregulation of CRP40 protein. Thus, a dysregulation of CRP40 may be one cause for the increased DA activity characteristic to the pathophysiology of SCZ (Gabriele et al., 2010b).

Findings from a rat study using CRP40/MOT2 knockdown in the mPFC show that underexpression of CRP40/MOT-2 causes DA-dependant

behavioural impairments (Gabriele et al., 2010a). Antisense knockdown technology caused sensorimotor gating deficits exhibited in the form of a significant deficit of startle habituation in the PPI paradigm (Gabriele et al., 2010a). The same PPI deficit can be seen in well-established animal models of SCZ, as well as in human SCZ patients. Startle habituation is a known DA-dependant behaviour, implicating MOT-2 and CRP40 in dopaminergic regulation and the pathogenesis of SCZ (Gabriele et al., 2010a).

8.2 Lymphocytes: systemic markers for studying schizophrenia

Lymphocytes are known to synthesize DA, express DA receptors, and express DAT (Buttarelli et al., 2011). These findings make them an ideal candidate for tissue samples used to study dopaminergic diseases of the CNS. For example, many groups report changes of the expression of DAT and DA receptors in lymphocytes of patients suffering from PD and SCZ (Buttarelli et al., 2011).

The use of lymphocytes to study SCZ is not a new concept. Certain cytokines have been identified as markers of SCZ and can be measured in lymphocytic samples (Busse et al., 2012). Lymphocytes have also been used to study apoptotic markers, such as caspase-3 activity, in SCZ (Djordjević et al., 2012). Most important to the current study, is that lymphocytic expression of various genes has been reported as a sensitive and specific way of discriminating between patients with SCZ and controls (Maschietto et al., 2012). For this reason, lymphocytes show potential as biological material for diagnosis of SCZ via biomarker studies.

8.3 Objectives

Based on earlier findings, which show that CRP40 is expressed in blood cells and may be dysregulated in SCZ (Gabriele et al., 2005; Gabriele et al., 2010b), the study presented here was designed to explore whether blood concentrations of CRP40 mirror concentrations of CRP40 in the brain of SCZ patients. Specifically, these studies tested whether newly diagnosed (drug naive) SCZ subjects show differences in CRP40 mRNA concentrations in lymphocytes compared to chronic, antipsychotic treated SCZ subjects, and to healthy controls.

8.4 Materials and methods

8.4.1 Study setting and participants

Ethical approval was obtained from McMaster University Health Sciences/St. Joseph's Healthcare (Hamilton, Ontario). A total of 58 subjects (38 males, 17 females) were recruited and gave informed consent. Chronic (n=28) and first episode (n=13) subjects met criteria of the DSM-IV for SCZ, and control participants were included based on lack of psychiatric illness and substance abuse (Table 6). Chronic SCZ subjects had undergone treatment with antipsychotic drugs, and first episode SCZ subjects did not previously undergo drug treatment.

8.4.2 Preparation of blood samples

Blood (20–30ml) was collected from each subject. White blood cells were prepared as follows: 10ml of blood was collected in 1.42ml of acetate citrate dextrose BD vacutainers with 10ml warm phosphate saline buffer (PBS) and layered over 15ml of Ficoll Paque (GE Healthcare Life Sciences, Quebec, Canada). The gradient was centrifuged (400 g; 30 minutes). The buffy coat (middle layer visible after spin) was collected, washed twice with 30ml PBS, and once with 1ml PBS (110 g; 10 minutes). The pellet was collected and stored at -80°C.

RNA was isolated using the TRIzol method (Invitrogen Life Technologies, Ontario, Canada) according to manufacturer's protocols. Contaminating DNA was removed using the TURBO DNA–free kit (Ambion, Texas, United States) and quantified using a Beckman spectrophotometer DU-640. cDNA prepared with SuperScript III (Invitrogen Life Technologies, Ontario, Canada) was used for analysis of CRP40/MOT-2 mRNA copy numbers. MOT-2 is highly homologous to CRP40; therefore, primers used in this study amplified both CRP40 and MOT-2.

8.4.3 Analysis of CRP40/ MOT-2 mRNA copy numbers

Absolute copy numbers of CRP40/MOT-2 mRNA were determined in triplicates (10ng of cDNA) using RT-PCR, as previously optimized in our laboratory (Gabriele et al, 2010a). No primer-dimers were detected and transcripts showed optimal efficiencies. Conditions were optimized to ensure amplifications were in the exponential phase and efficiencies remained constant throughout. Representative real-time RT-PCR products each showed 100% homology with the CRP40 gene regions. Data were normalized against the human housekeeping gene, cyclophilin.

8.4.4 Data analysis

One-way ANOVA was used to examine differences in concentrations of CRP40/MOT-2 mRNA across healthy controls, first episode, and chronic SCZ subjects. Post-hoc pairwise comparisons were conducted using the Scheffé procedure. Multiple regression analysis was used to examine the relationship between health status and CRP40/MOT-2 mRNA, controlling for age, sex, and prescribed treatment. Statistical tests were two-sided with $\alpha=0.05$.

Five subjects (8.6%) had missing values for sex and/or antipsychotic drug treatment. Multiple imputation (iterations=5) was implemented in the regression model to maximize statistical power (Rubin, 1987).

8.5 Results

Results showed significant differences in CRP40/MOT-2 mRNA concentrations across health states (Figure 15) (Groleau et al., 2013). Post-hoc comparisons suggested significant reductions in CRP40/MOT-2 mRNA expression among first episode and chronic SCZ subjects compared to healthy controls ($p<0.05$). A trend towards decreased CRP40/MOT-2 concentrations in first episode SCZ compared to chronic SCZ was observed ($p=0.09$) (Groleau et al., 2013).

The relationship between health status and CRP40/MOT-2 mRNA concentrations remained after controlling for sex, age, and antipsychotic drug treatment (Table 6). Both first episode ($p<0.0001$) and chronic SCZ ($p<0.0001$) subjects had significantly lower CRP40/MOT-2 mRNA concentrations compared to healthy controls. Potential sex differences in CRP40/MOT-2 mRNA concentrations are preliminary and require further study (Table 6).

8.6 Discussion

Findings presented here suggest that CRP40 is genetically dysregulated in SCZ, and provide insight about the relationship between CRP40, antipsychotic drug treatment, and oxidative stress in this disorder.

Previous findings indicate significant reductions in CRP40 expression in human post-mortem SCZ brain samples (Gabriele et al., 2005). The current study revealed significant reductions in white blood cell CRP40/MOT-2 mRNA concentrations across chronic and first episode SCZ subjects in comparison to healthy controls.

This study supports recent theories that molecular chaperones may play important roles in CNS disorders (Deocaris et al., 2008; Burbulla et al., 2010; Pae et al., 2005; Kim et al., 2008). These essential proteins are, therefore, important to consider in current neurological disease models.

Defects or direct knockdown of the *mortalin-2* gene (coding for both MOT-2 and CRP40) are known to cause mitochondrial impairments, increased oxidative stress, and increased susceptibility to apoptosis– common features of neurodegenerative disorders (Liu et al., 2005; Voloboueva et al., 2007; Xu et al., 2009; Burbulla et al., 2010). Pathological mechanisms involving impaired chaperone proteins and oxidative damage by mitochondrial dysfunction, epigenetic changes, and neuronal impairment can also be applied to SCZ (Yao et al., 2001; Schon and Manfredi, 2003; Bitanihirwe and Woo, 2011; Ciobica et al., 2011).

These results also suggest a trend towards lower CRP40 concentrations in first episode compared to chronic SCZ subjects, which may be related to antipsychotic drug treatment (Gabriele et al., 2010; Groleau et al., 2013). Similar findings of differential CRP40 expression in response to antipsychotic drugs have been reported previously (Gabriele et al., 2002, 2005, 2010a). Specifically, there is a positive correlation between CRP40/MOT-2 mRNA expression and the amount of antipsychotic drug treatment throughout total lifespan in post-mortem brains of SCZ patients (Gabriele et al., 2010b). Interestingly, recent *in vitro* studies using PC12 cells have shown that some atypical antipsychotic drugs reduce oxidative stress through upregulation of superoxide dismutase, a key enzyme in antioxidant defense (Bai et al., 2002; Wei et al., 2003a, 2003b; Park et al., 2011;). These findings are further supported by reports of increased oxidative stress in first-episode SCZ patients (Zhang et al., 2009). Taken together, and considering past evidence of neuroprotection, these studies suggest that if CRP40 concentrations are increased following antipsychotic drug use, this may explain reduced oxidative stress in SCZ patients using atypical antipsychotics. Observed differences in CRP40 in response to antipsychotic drugs are hypothesis-generating and require larger sample sizes for further investigation.

In summary, the results of this study present an opportunity for further investigation of CRP40 involvement in the pathophysiology of SCZ.

CRP40 shows potential for exploitation as a dynamic marker of SCZ in the future.

N=58	Mean ±S.D./n (%)
Health Status ***Control*** ***First Episode Schizophrenia*** ***Chronic Schizophrenia***	 17 (29.3%) 13 (22.4%) 28 (48.3%)
Age	40.7±14.7
Sex ***Male*** ***Female***	 38 (69.1%) 17 (30.9%)
Antipsychotic Drug Treatment[1] **Atypical** **Typical**	 26 (47.3%) 7 (12.7%)
[1]Chronic group only	

Table 6: Subject Descriptive Statistics (from Groleau et al., 2013).

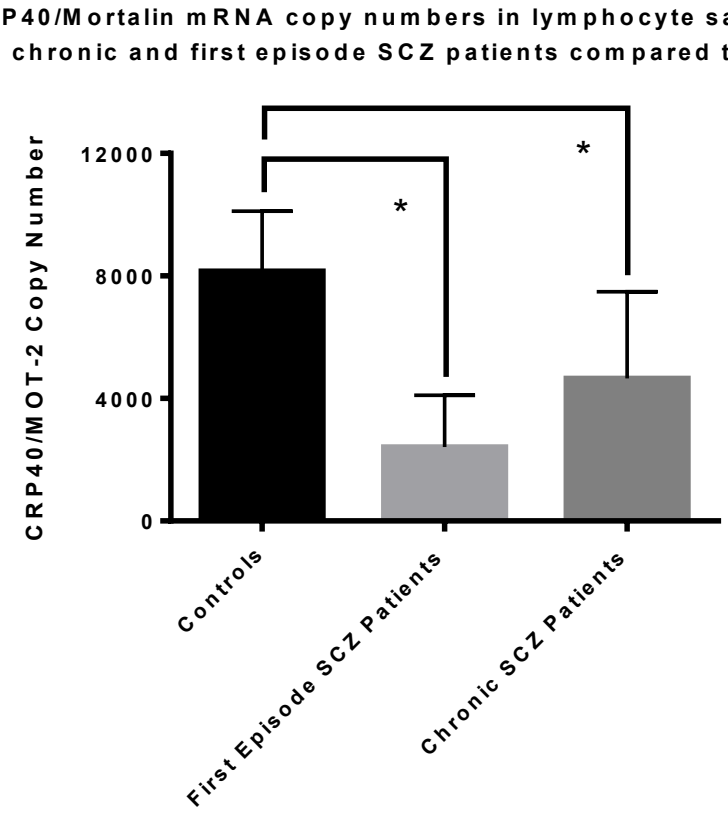

Figure 15: CRP40/MOT-2 mRNA expression in lymphocytes is specifically reduced in SCZ, both first episode (n=13) ($p<0.05$*) and chronic (n=28) ($p<0.05$*), compared to healthy controls (n=17).

CHAPTER 9

CONCLUSIONS

The experiments and results presented in this thesis suggest important findings to the field of PD research. The full-length CRP40 protein was found previously to bind DA and the 7kDa (2,4) has now been proven unable to bind DA. Both proteins, however, alleviate behavioural symptoms in the 6-OHDA hemi-lesioned rat model of PD. Taken together, these findings suggest that CRP40 has a dual biological function in PD: binding and modulation of DA, as well as a therapeutic effect (the mechanism of which is still unknown). It is possible that behavioural effects are conferred by some indirect dopaminergic function of CRP40. For example, since rotations in the 6-OHDA model are due to D2 receptor sensitization, perhaps the 7kDa (2,4) fragment activates the desensitization of these receptors via internalization. On the other hand, behavioural changes reported here may be caused by some other function of this segment of CRP40 altogether.

Not only has a protein now been identified with novel potential as a therapeutic agent for PD, but also that this behavioural effect is not due to a change in DA concentrations. Further, these experiments have elucidated the approximate region of the CRP40 protein responsible for therapeutic efficacy (2,4; within 60 amino acids).

A subsequent study presented in this thesis suggests that CRP40 is found dysregulated in platelets of PD patients. This evidence has revealed

CRP40 as a novel PD biomarker. On going studies are now in place to explore the potential of CRP40 as a diagnostic for PD.

The last study presented in this thesis indicates potential for CRP40 applications in SCZ. Since CRP40 was found dysregulated in lymphocytes of SCZ patients, it shows potential as a novel SCZ biomarker and should be explored further for use as a diagnostic for this disease.

CHAPTER 10

FURTHER RESEARCH FOR CRP40 IN NEUROLOGICAL DISEASE

10.0 Current and on going projects

10.0.1 Human Parkinson's blood collection and analysis

Drs. Gabriele and Mishra of McMaster University have been awarded a grant and partnership with the Quebec Consortium for Drug Discovery (CQDM) for the on going collection of blood samples from PD patients and control subjects. This project incorporates collaboration with Dr. DiPaolo of the University of Laval, as well as Dr. Blanchet of the University of Montreal. The collaborative application between Ontario and Québec research teams is to foster the recently developed CRP40 technology to stimulate the growth and development of a young biotechnology company called CRP40 Inc.

The overall objective of the CQDM project is to build on the work described in Chapter 7 of this manuscript. Specifically, the goal is to fully establish and strengthen the diagnostic utility of CRP40 as a biomarker for PD by comparing the steady state concentrations of CRP40 mRNA among platelets from patient and control groups as follows: a) patients newly diagnosed with PD (drug naive) with healthy age-matched controls; b) patients newly diagnosed with PD with patients currently receiving dopaminergic drugs for the treatment of PD with healthy age-matched controls; c) AD patients with healthy age-matched controls and d) stroke patients with healthy age-matched controls.

10.0.2 Primate blood collection and analysis

Under the partneship with CQDM and in collaboration with Dr. DiPaolo (Laval), blood samples from a primate model of PD will also be analyzed for CRP40 expression.

In order to strengthen the biomarker technology, validation studies will be performed in the well-established MPTP primate model of PD. Specifically, animals will be tested for CRP40 steady state mRNA to investigate whether they corroborate human findings of reduced CRP40 expression in platelets.

10.0.3 Standardized RT-PCR test for Parkinson's disease diagnosis

Current diagnostic methods for PD, which are based on clinical interviews, are often unreliable and flawed. Diagnosis of PD by current methods may result in misdiagnosis of up to 25% of patients (Tolosa et al., 2006)

As discussed in Chapter 7, CRP40 mRNA is significantly decreased in blood platelet samples from patients with PD (Lubarda et al., 2013). These findings have led to the development of a Real Time RT-PCR-based diagnostic test. Blood studies in collaboration with CQDM, under the sponsorship of Merck, Pfizer and Astra-Zeneca, are on going. The objective is to standardize this test for PD diagnosis by proving that it is highly reliable, reproducible and affordable, and when introduced in clinical laboratories, it will facilitate the early identification, intervention and prevention efforts for PD. Confirming the correct diagnosis of PD will allow appropriate medication with L-DOPA or other drugs. In fact, diagnosis of PD in its early stages may allow for earlier therapeutic intervention, which may mitigate progress of the disease.

10.1 Future directions

10.1.1 CRP40 as a therapeutic in animal models of Parkinson's disease

Since CRP40 is a relatively large protein (~40kDa), it cannot cross the blood-brain barrier. For this reason, various projects have been set in motion to elucidate the active region of CRP40 protein for use as a potential therapeutic. The pilot study, presented in Chapter 5 of this manuscript, suggests that a 7kDa peptide fragment of the full-length CRP40 exhibits efficacy in alleviating behavioural symptoms in the 6-OHDA hemi-lesioned rat model of PD.

Using bioinformatics, even smaller fragments of this 7kDa (2,4) peptide will be designed to incorporate potentially functional motifs (β-strands and/or α-helices) that may form a structure with the ability to bind either to a ligand or to another protein in order to confer some function. These new fragments will then be investigated for their therapeutic efficacy and biological function in the 6-OHDA, as well as MPTP and genetic, animal models of PD.

MANUSCRIPTS ARISING FROM THIS RESEARCH PROJECT:

In preparation:

Groleau, S.E., Lubarda, J., Ferro, M.A., Thomas, N., Mishra, R.K., Gabriele, J.P. CRP40 Alleviates Behavioural Symptoms in the 6-OHDA Rat Model of Parkinson's. In preparation for submission to MOVEMENT DISORDERS.

Published findings:

Lubarda, J., **Groleau, S.E.,** Thomas, N., Ferro, M.A., Pristupa, Z.B., Mishra, R.K., Gabriele, J.P. Dysregulation of novel catecholamine-regulated protein 40 (CRP40) in Parkinson's disease patients. Mov Disord. 2013 [Epub ahead of print].

Groleau, S.E., Lubarda, J., Thomas, N., Ferro, M.A., Pristupa, Z.B., Mishra, R.K., Gabriele, J.P. Human blood analysis reveals differences in gene expression of catecholamine-regulated protein 40 (CRP40) in schizophrenia. Schizophr Res. 2013;143(1):203-6.

Review publications:

Groleau, S.E., Lubarda, J., Thomas, N., Pristupa, Z.B., Mishra, R.K., Gabriele, J.P. The Novel Catecholamine-Regulated Protein 40: A crucial protein for understanding and diagnosing neurological disorders? Integrated Healthcare Practitioners Magazine. 2013.

Lubarda, J., **Groleau, S.E.,** Thomas, N., Pristupa, Z.B., Mishra, R.K., Gabriele, J.P. Molecular Chaperones as 21st Century Solutions for Neurodegenerative Disorders: A Look at Catecholamine-Regulated Protein 40 (CRP40). Integrated Healthcare Practitioners Magazine. 2013;6(1):65-70.

Gabriele, J.P., **Groleau, S.E.,** Daya, R.P., Pristupa, Z.B., Mishra, R.K. "Catecholamine Regulated Protein (CRP40), a splice variant of Mortalin-2: Functional Role in CNS Disorders". In *Mortalin Biology: Stress, Life and Death.* Springer publishing; 2012.

Reference List

Abi-Dargham, A., Rodenhiser, J., Printz, D., Zea-Ponce, Y., Gil, R., Kegeles, L. S., Weiss, R., et al. (2000). Increased baseline occupancy of D2 receptors by dopamine in schizophrenia. *Proceedings of the National Academy of Sciences of the United States of America*, *97*(14), 8104–9.

Adriano, F., Caltagirone, C., & Spalletta, G. (2012). Hippocampal volume reduction in first-episode and chronic schizophrenia: a review and meta-analysis. *The Neuroscientist : a review journal bringing neurobiology, neurology and psychiatry*, *18*(2), 180–200.

Amar, S., Shamir, A., Ovadia, O., Blanaru, M., Reshef, A., Kremer, I., Rietschel, M., et al. (2007). Mitochondrial DNA HV lineage increases the susceptibility to schizophrenia among Israeli Arabs. *Schizophrenia research*, *94*(1-3), 354–8.

Bai, O., Wei, Z., Lu, W., Bowen, R., Keegan, D., & Li, X.M. (2002). Protective effects of atypical antipsychotic drugs on PC12 cells after serum withdrawal. *Journal of neuroscience research*, *69*(2), 278–83.

Bayer, T. A., Wirths, O., Majtényi, K., Hartmann, T., Multhaup, G., Beyreuther, K., & Czech, C. (2001). Key factors in Alzheimer's disease: beta-amyloid precursor protein processing, metabolism and intraneuronal transport. *Brain pathology (Zurich, Switzerland)*, *11*(1), 1–11.

Becker, J., & Craig, E. A. (1994). Heat-shock proteins as molecular chaperones. *European journal of biochemistry / FEBS*, *219*(1-2), 11–23.

Ben-Shachar, D., Zuk, R., Gazawi, H., & Ljubuncic, P. (2004). Dopamine toxicity involves mitochondrial complex I inhibition: implications to dopamine-related neuropsychiatric disorders. *Biochemical pharmacology*, *67*(10), 1965–74.

Betarbet, R., Sherer, T. B., & Greenamyre, J. T. (2002). Animal models of Parkinson's disease. *BioEssays : news and reviews in molecular, cellular and developmental biology*, *24*(4), 308–18.

Binder, V., Albert, M. H., Kabus, M., Bertone, M., Meindl, A., & Belohradsky, B. H. (2006). The genotype of the original Wiskott phenotype. *The New England journal of medicine*, *355*(17), 1790–3.

Bitanihirwe, B. K. Y., & Woo, T. U. W. (2011). Oxidative stress in schizophrenia: an integrated approach. *Neuroscience and biobehavioral reviews*, *35*(3), 878–93.

Blandini, F., Nappi, G., Fancellu, R., Mangiagalli, A., Samuele, A., Riboldazzi, G., Calandrella, D., et al. (2003). Modifications of plasma and platelet levels of L-DOPA and its direct metabolites during treatment with tolcapone or entacapone in patients with Parkinson's disease. *Journal of neural transmission (Vienna, Austria : 1996)*, *110*(8), 911–22.

Blum, D., Torch, S., Lambeng, N., Nissou, M., Benabid, A. L., Sadoul, R., & Verna, J. M. (2001). Molecular pathways involved in the neurotoxicity of 6-OHDA, dopamine and MPTP: contribution to the apoptotic theory in Parkinson's disease. *Progress in neurobiology*, *65*(2), 135–72. Retrieved from

Bossy-Wetzel, E., Schwarzenbacher, R., & Lipton, S. A. (2004). Molecular pathways to neurodegeneration. *Nature medicine*, *10 Suppl*, S2–9.

Böttger, S., Jerszyk, E., Low, B., & Walker, C. (2008). Genotoxic stress-induced expression of p53 and apoptosis in leukemic clam hemocytes with cytoplasmically sequestered p53. *Cancer research*, *68*(3), 777–82.

Bowen, D. M., Smith, C. B., White, P., & Davison, A. N. (1976). Neurotransmitter-related enzymes and indices of hypoxia in senile dementia and other abiotrophies. *Brain : a journal of neurology*, *99*(3), 459–96.

Buchsbaum, M. S., Yang, S., Hazlett, E., Siegel, B. V, Germans, M., Haznedar, M., O'Flaithbheartaigh, S., et al. (1997). Ventricular volume and asymmetry in schizotypal personality disorder and schizophrenia assessed with magnetic resonance imaging. *Schizophrenia research*, *27*(1), 45–53.

Burbulla, L. F., Schelling, C., Kato, H., Rapaport, D., Woitalla, D., Schiesling, C., Schulte, C., et al. (2010). Dissecting the role of the mitochondrial chaperone mortalin in Parkinson's disease: functional impact of disease-related variants on mitochondrial homeostasis. *Human molecular genetics*, *19*(22), 4437–52.

Burke, W. J., Li, S. W., Chung, H. D., Ruggiero, D. A., Kristal, B. S., Johnson, E. M., Lampe, P., et al. (2004). Neurotoxicity of MAO metabolites of catecholamine neurotransmitters: role in neurodegenerative diseases. *Neurotoxicology*, *25*(1-2), 101–15.

Busse, S., Busse, M., Schiltz, K., Bielau, H., Gos, T., Brisch, R., Mawrin, C., et al. (2012). Different distribution patterns of lymphocytes and microglia in the hippocampus of patients with residual versus paranoid schizophrenia: further evidence for disease course-related immune alterations? *Brain, behavior, and immunity*, *26*(8), 1273–9.

Buttarelli, F. R., Fanciulli, A., Pellicano, C., & Pontieri, F. E. (2011). The dopaminergic system in peripheral blood lymphocytes: from physiology to pharmacology and potential applications to neuropsychiatric disorders. *Current neuropharmacology*, *9*(2), 278–88.

Castañeda, E., Whishaw, I. Q., & Robinson, T. E. (1990). Changes in striatal dopamine neurotransmission assessed with microdialysis following recovery from a bilateral 6-OHDA lesion: variation as a function of lesion size. *The Journal of neuroscience : the official journal of the Society for Neuroscience*, *10*(6), 1847–54.

Castle, D., Wessely, S., Der, G., & Murray, R. M. (1991). The incidence of operationally defined schizophrenia in Camberwell, 1965-84. *The British journal of psychiatry : the journal of mental science*, *159*, 790–4.

Chiasserini, D., Tozzi, A., De Iure, A., Tantucci, M., Susta, F., Orvietani, P. L., Koya, K., et al. (2011). Mortalin inhibition in experimental Parkinson's disease. *Movement disorders : official journal of the Movement Disorder Society*, *26*(9), 1639–47.

Choi, J., Forster, M. J., McDonald, S. R., Weintraub, S. T., Carroll, C. A., & Gracy, R. W. (2004). Proteomic identification of specific oxidized proteins in ApoE-knockout mice: relevance to Alzheimer's disease. *Free radical biology & medicine*, *36*(9), 1155–62.

Ciobica, A., Padurariu, M., Dobrin, I., Stefanescu, C., & Dobrin, R. (2011). Oxidative stress in schizophrenia - focusing on the main markers. *Psychiatria Danubina*, *23*(3), 237–45.

Clay, H. B., Sillivan, S., & Konradi, C. (2011). Mitochondrial dysfunction and pathology in bipolar disorder and schizophrenia. *International journal of developmental neuroscience : the official journal of the International Society for Developmental Neuroscience*, *29*(3), 311–24.

Clinton, L. K., Billings, L. M., Green, K. N., Caccamo, A., Ngo, J., Oddo, S., McGaugh, J. L., et al. (2007). Age-dependent sexual dimorphism in cognition and stress response in the 3xTg-AD mice. *Neurobiology of disease*, *28*(1), 76–82.

Cowan, W. M., Südhof, T. C., & Stevens, C. F. (2001). *Synapses*. Johns Hopkins press.

Creese, I., Burt, D. R., & Snyder, S. H. (1977). Dopamine receptor binding enhancement accompanies lesion-induced behavioral supersensitivity. *Science (New York, N.Y.)*, *197*(4303), 596–8.

Creese, I., & Snyder, S. H. (1979). Nigrostriatal lesions enhance striatal ^{3}H-apomorphine and ^{3}H-spiroperidol binding. *European journal of pharmacology*, *56*(3), 277–81.

Csernansky, J. G. (2007). Neurodegeneration in schizophrenia: evidence from *in vivo* neuroimaging studies. *TheScientificWorldJournal*, *7*, 135–43.

Culver, K. E., Rosenfeld, J. M., & Szechtman, H. (2002). Monoamine oxidase inhibitor-induced blockade of locomotor sensitization to quinpirole: role of striatal dopamine uptake inhibition. *Neuropharmacology*, *43*(3), 385–93.

Cummings, J. L., Vinters, H. V, Cole, G. M., & Khachaturian, Z. S. (1998). Alzheimer's disease: etiologies, pathophysiology, cognitive reserve, and treatment opportunities. *Neurology*, *51*(1 Suppl 1), S2–17; discussion S65–7.

D'Souza, S. M., & Brown, I. R. (1998). Constitutive expression of heat shock proteins Hsp90, Hsc70, Hsp70 and Hsp60 in neural and non-neural tissues of the rat during postnatal development. *Cell stress & chaperones*, *3*(3), 188–99.

Dauer, W., & Przedborski, S. (2003). Parkinson's disease: mechanisms and models. *Neuron*, *39*(6), 889–909.

Davies, P., & Maloney, A. J. (1976). Selective loss of central cholinergic neurons in Alzheimer's disease. *Lancet*, *2*(8000), 1403.

De Mena, L., Coto, E., Sánchez-Ferrero, E., Ribacoba, R., Guisasola, L. M., Salvador, C., Blázquez, M., et al. (2009). Mutational screening of the mortalin gene (HSPA9) in Parkinson's disease. *Journal of neural transmission (Vienna, Austria : 1996)*, *116*(10), 1289–93.

Deocaris, C. C., Kaul, S. C., & Wadhwa, R. (2008). From proliferative to neurological role of an hsp70 stress chaperone, mortalin. *Biogerontology*, *9*(6), 391–403.

Deshaies, R. J., Koch, B. D., Werner-Washburne, M., Craig, E. A., & Schekman, R. (1988). A subfamily of stress proteins facilitates translocation of secretory and mitochondrial precursor polypeptides. *Nature*, *332*(6167), 800–5.

Djordjević, V. V, Ristić, T., Lazarević, D., Cosić, V., Vlahović, P., & Djordjević, V. B. (2012). Schizophrenia is associated with increased levels of serum Fas and FasL. *Clinical chemistry and laboratory medicine : CCLM / FESCC*, *50*(6), 1049–54.

Domanico, S. Z., DeNagel, D. C., Dahlseid, J. N., Green, J. M., & Pierce, S. K. (1993). Cloning of the gene encoding peptide-binding protein 74 shows that it is a new member of the heat shock protein 70 family. *Molecular and cellular biology*, *13*(6), 3598–610.

Dunkley, P. R., Bobrovskaya, L., Graham, M. E., Von Nagy-Felsobuki, E. I., & Dickson, P. W. (2004). Tyrosine hydroxylase phosphorylation: regulation and consequences. *Journal of neurochemistry*, *91*(5), 1025–43.

Dupuis, L., Spreux-Varoquaux, O., Bensimon, G., Jullien, P., Lacomblez, L., Salachas, F., Bruneteau, G., et al. (2010). Platelet serotonin level predicts survival in amyotrophic lateral sclerosis. *PloS one*, *5*(10), e13346.

Edmondson, D. E., Mattevi, A., Binda, C., Li, M., & Hubálek, F. (2004). Structure and mechanism of monoamine oxidase. *Current medicinal chemistry*, *11*(15), 1983–93.

Ellis, J. (1987). Proteins as molecular chaperones. *Nature*, *328*(6129), 378–9.

Emdadul Haque, M., Asanuma, M., Higashi, Y., Miyazaki, I., Tanaka, K., & Ogawa, N. (2003). Apoptosis-inducing neurotoxicity of dopamine and its metabolites via reactive quinone generation in neuroblastoma cells. *Biochimica et biophysica acta*, *1619*(1), 39–52.

Farlow, M. R., Graham, S. M., & Alva, G. (2008). Memantine for the treatment of Alzheimer's disease: tolerability and safety data from clinical trials. *Drug safety : an international journal of medical toxicology and drug experience*, *31*(7), 577–85.

Faull, R. L., & Laverty, R. (1969). Changes in dopamine levels in the corpus striatum following lesions in the substantia nigra. *Experimental neurology*, *23*(3), 332–40.

Fitzgerald, P. A. (2011). Chapter 11. Adrenal Medulla and Paraganglia. In D. G. Gardner & D. Shoback (Eds.), *Greenspan's Basic & Clinical Endocrinology (9th ed.)*. New York: McGraw-Hill.

Foroud, T., Pankratz, N., & Martinez, M. (2006). Chromosome 5 and Parkinson disease. *European journal of human genetics : EJHG*, *14*(10), 1106–10.

Förstl, H., & Kurz, A. (1999). Clinical features of Alzheimer's disease. *European archives of psychiatry and clinical neuroscience*, *249*(6), 288–90.

Francis, P. T., Palmer, A. M., Snape, M., & Wilcock, G. K. (1999). The cholinergic hypothesis of Alzheimer's disease: a review of progress. *Journal of neurology, neurosurgery, and psychiatry*, *66*(2), 137–47.

Francis, P. T., Sims, N. R., Procter, A. W., & Bowen, D. M. (1993). Cortical pyramidal neuron loss may cause glutamatergic hypoactivity and cognitive impairment in Alzheimer's disease: investigative and therapeutic perspectives. *Journal of neurochemistry*, *60*(5), 1589–604.

Fujimaki, K., Takahashi, T., & Morinobu, S. (2012). Association of typical versus atypical antipsychotics with symptoms and quality of life in schizophrenia. *PloS one*, *7*(5), e37087.

Gabriele, J., Culver, K., Sharma, S., Zhang, B., Szechtman, H., & Mishra, R. (2003). Asymmetric modulation of a catecholamine-regulated protein in the rat brain, following quinpirole administration. *Synapse (New York, N.Y.)*, *49*(4), 261–9.

Gabriele, J. P., Chong, V. Z., Pontoriero, G. F., & Mishra, R. K. (2005). Decreased expression of a 40-kDa catecholamine-regulated protein in the ventral striatum of schizophrenic brain specimens from the Stanley Foundation Neuropathology Consortium. *Schizophrenia research*, *74*(1), 111–9.

Gabriele, J. P., Pontoriero, G. F., Thomas, N., Ferro, M. a, Mahadevan, G., MacCrimmon, D. J., Pristupa, Z. B., et al. (2010b). Antipsychotic drug use is correlated with CRP40/mortalin mRNA expression in the dorsolateral prefrontal cortex of human postmortem brain specimens. *Schizophrenia research*, *119*(1-3), 228–31.

Gabriele, J., Pontoriero, G. F., Thomas, N., Thomson, C. a, Skoblenick, K., Pristupa, Z. B., & Mishra, R. K. (2009). Cloning, characterization, and functional studies of a human 40-kDa catecholamine-regulated protein: implications in central nervous system disorders. *Cell stress & chaperones*, *14*(6), 555–67.

Gabriele, J., Rajaram, M., Zhang, B., Sharma, S., & Mishra, R. K. (2002). Modulation of a 40-kDa catecholamine-regulated protein following D-amphetamine treatment in discrete brain regions. *European journal of pharmacology*, *453*(1), 13–9.

Gabriele, J., Thomas, N., N-Marandi, S., & Mishra, R. (2007). Differential modulation of a 40 kDa catecholamine regulated protein in the core and shell subcompartments of the nucleus accumbens following chronic quinpirole and haloperidol administration in the rat. *Synapse (New York, N.Y.)*, *61*(10), 835–42.

Gabriele, N., Pontoriero, G. F., Thomas, N., Shethwala, S. K., Pristupa, Z. B., & Gabriele, J. P. (2010a). Knockdown of mortalin within the medial prefrontal cortex impairs normal sensorimotor gating. *Synapse (New York, N.Y.)*, *64*(11), 808–13.

Giménez-Llort, L., Blázquez, G., Cañete, T., Johansson, B., Oddo, S., Tobeña, A., LaFerla, F. M., et al. (2007). Modeling behavioral and neuronal symptoms of Alzheimer's disease in mice: a role for intraneuronal amyloid. *Neuroscience and biobehavioral reviews*, *31*(1), 125–47.

Girault, J. A., & Greengard, P. (2004). The neurobiology of dopamine signaling. *Archives of neurology*, *61*(5), 641–4.

Goto, A., Doering, L., Nair, V. D., & Mishra, R. K. (2001). Immunohistochemical localization of a 40-kDa catecholamine regulated protein in the nigrostriatal pathway. *Brain research*, *900*(2), 314–9.

Graham, D. G., Tiffany, S. M., Bell, W. R., & Gutknecht, W. F. (1978). Autoxidation versus covalent binding of quinones as the mechanism of toxicity of dopamine, 6-hydroxydopamine, and related compounds toward C1300 neuroblastoma cells *in vitro*. *Molecular pharmacology*, *14*(4), 644–53.

Groleau, S. E., Lubarda, J., Thomas, N., Ferro, M. A., Pristupa, Z. B., Mishra, R. K., & Gabriele, J. P. (2013). Human blood analysis reveals differences in gene expression of catecholamine-regulated protein 40 (CRP40) in schizophrenia. *Schizophrenia research*, *143*(1), 203–6.

Gupta, R. S., & Sneath, P. H. A. (2007). Application of the character compatibility approach to generalized molecular sequence data: branching order of the proteobacterial subdivisions. *Journal of molecular evolution*, *64*(1), 90–100.

Häfner, H., & an der Heiden, W. (1997). Epidemiology of schizophrenia. *Canadian journal of psychiatry. Revue canadienne de psychiatrie*, *42*(2), 139–51.

Hardy, J., & Selkoe, D. J. (2002). The amyloid hypothesis of Alzheimer's disease: progress and problems on the road to therapeutics. *Science (New York, N.Y.)*, *297*(5580), 353–6.

Hastings, T. G. (2009). The role of dopamine oxidation in mitochondrial dysfunction: implications for Parkinson's disease. *Journal of bioenergetics and biomembranes*, *41*(6), 469–72.

Hattoria, N., Wanga, M., Taka, H., Fujimura, T., Yoritaka, A., Kubo, S. I., & Mochizuki, H. (2009). Toxic effects of dopamine metabolism in Parkinson's disease. *Parkinsonism & related disorders*, *15 Suppl 1*, S35–8.

Hayes, S. A., & Dice, J. F. (1996). Roles of molecular chaperones in protein degradation. *The Journal of cell biology*, *132*(3), 255–8.

Hendrick, J. P., & Hartl, F. U. (1993). Molecular chaperone functions of heat-shock proteins. *Annual review of biochemistry*, *62*, 349–84.

Hughes, A. J., Daniel, S. E., & Lees, A. J. (2001). Improved accuracy of clinical diagnosis of Lewy body Parkinson's disease. *Neurology*, *57*(8), 1497–9.

Jeyasingham, R. A., Baird, A. L., Meldrum, A., & Dunnett, S. B. (2001). Differential effects of unilateral striatal and nigrostriatal lesions on grip strength, skilled paw reaching and drug-induced rotation in the rat. *Brain research bulletin*, *55*(4), 541–8.

Jin, J., Hulette, C., Wang, Y., Zhang, T., Pan, C., Wadhwa, R., & Zhang, J. (2006). Proteomic identification of a stress protein, mortalin/mthsp70/GRP75: relevance to Parkinson disease. *Molecular & cellular proteomics : MCP*, *5*(7), 1193–204.

Jin, J., Li, G. J., Davis, J., Zhu, D., Wang, Y., Pan, C., & Zhang, J. (2007). Identification of novel proteins associated with both alpha-synuclein and DJ-1. *Molecular & cellular proteomics : MCP*, *6*(5), 845–59.

Jorm, A. F., Korten, A. E., & Henderson, A. S. (1987). The prevalence of dementia: a quantitative integration of the literature. *Acta psychiatrica Scandinavica*, *76*(5), 465–79.

Kandel, E., Swartz, J., & Jessell, T. (Eds.). (2000). *Principles of Neural Science, 4TH Edition.* New York: McGraw Hill.

Karreman, M., & Moghaddam, B. (1996). The prefrontal cortex regulates the basal release of dopamine in the limbic striatum: an effect mediated by ventral tegmental area. *Journal of neurochemistry*, *66*(2), 589–98.

Kasai, K., Iwanami, A., Yamasue, H., Kuroki, N., Nakagome, K., & Fukuda, M. (2002). Neuroanatomy and neurophysiology in schizophrenia. *Neuroscience research*, *43*(2), 93–110.

Kaul, S. C., Deocaris, C. C., & Wadhwa, R. (2007). Three faces of mortalin: a housekeeper, guardian and killer. *Experimental gerontology*, *42*(4), 263–74.

Kelly, C. A., Harvey, R. J., & Cayton, H. (1997). Drug treatments for Alzheimer's disease. *BMJ (Clinical research ed.)*, *314*(7082), 693–4.

Kempton, M. J., Stahl, D., Williams, S. C. R., & DeLisi, L. E. (2010). Progressive lateral ventricular enlargement in schizophrenia: a meta-analysis of longitudinal MRI studies. *Schizophrenia research*, *120*(1-3), 54–62.

Keshavan, M. S. (1999). Development, disease and degeneration in schizophrenia: a unitary pathophysiological model. *Journal of psychiatric research*, *33*(6), 513–21.

Kim, J. J., Mandelli, L., Lim, S., Lim, H. K., Kwon, O. J., Pae, C. U., Serretti, A., et al. (2008). Association analysis of heat shock protein 70 gene polymorphisms in schizophrenia. *European archives of psychiatry and clinical neuroscience*, *258*(4), 239–44.

Kopin, I. J. (1968). Biosynthesis and metabolism of catecholamines. *Anesthesiology*, *29*(4), 654–60.

Kumar, A. M., Sevush, S., Kumar, M., Ruiz, J., & Eisdorfer, C. (1995). Peripheral serotonin in Alzheimer's disease. *Neuropsychobiology*, *32*(1), 9–12.

Kuroda, Y., Mitsui, T., Kunishige, M., & Matsumoto, T. (2006). Parkin affects mitochondrial function and apoptosis in neuronal and myogenic cells. *Biochemical and biophysical research communications*, *348*(3), 787–93.

Lang, A. E., & Lozano, A. M. (1998). Parkinson's disease. First of two parts. *The New England journal of medicine*, *339*(15), 1044–53.

Lewis, D. a, & Lieberman, J. a. (2000). Catching up on schizophrenia: natural history and neurobiology. *Neuron*, *28*(2), 325–34.

Lim, K. O., Tew, W., Kushner, M., Chow, K., Matsumoto, B., & DeLisi, L. E. (1996). Cortical gray matter volume deficit in patients with first-episode schizophrenia. *The American journal of psychiatry*, *153*(12), 1548–53.

Liu, Y., Liu, W., Song, X. D., & Zuo, J. (2005). Effect of GRP75/mthsp70/PBP74/mortalin overexpression on intracellular ATP level, mitochondrial membrane potential and ROS accumulation following glucose deprivation in PC12 cells. *Molecular and cellular biochemistry*, *268*(1-2), 45–51.

Londono, C., Osorio, C., Gama, V., & Alzate, O. (2012). Mortalin, Apoptosis, and Neurodegeneration. *Biomolecules*, *2*(4), 143–164.

Lubarda, J., **Groleau, S.E.,** Thomas, N., Ferro, M.A., Pristupa, Z.B., Mishra, R.K., Gabriele, J.P. Dysregulation of novel catecholamine-regulated protein 40 (CRP40) in Parkinson's disease patients. Mov Disord. 2013 [Epub ahead of print].

Luo, W.I., Dizin, E., Yoon, T., & Cowan, J. A. (2010). Kinetic and structural characterization of human mortalin. *Protein expression and purification*, *72*(1), 75–81.

Marksteiner, J., Hinterhuber, H., & Humpel, C. (2007). Cerebrospinal fluid biomarkers for diagnosis of Alzheimer's disease: beta-amyloid (1-42), tau, phospho-tau-181 and total protein. *Drugs of today (Barcelona, Spain : 1998)*, *43*(6), 423–31.

Marras, C., & Tanner, C. (2004). Epidemiology of Parkinson's disease. In R. Watts & W. Koller (Eds.), *Movement disorders, neurologic principles and practice, 2nd ed.* (pp. 177–196). New York, McGraw Hill.

Martins-de-Souza, D., Harris, L. W., Guest, P. C., & Bahn, S. (2011). The role of energy metabolism dysfunction and oxidative stress in schizophrenia revealed by proteomics. *Antioxidants & redox signaling*, *15*(7), 2067–79.

Maschietto, M., Silva, A. R., Puga, R. D., Lima, L., Pereira, C. B., Nakano, E. Y., Mello, B., et al. (2012). Gene expression of peripheral blood lymphocytes may discriminate patients with schizophrenia from controls. *Psychiatry research*, *200*(2-3), 1018–21.

Matsumoto, M., Weickert, C. S., Akil, M., Lipska, B. K., Hyde, T. M., Herman, M. M., Kleinman, J. E., et al. (2003). Catechol O-methyltransferase mRNA expression in human and rat brain: evidence for a role in cortical neuronal function. *Neuroscience*, *116*(1), 127–37.

Michel, P. P., & Hefti, F. (1990). Toxicity of 6-hydroxydopamine and dopamine for dopaminergic neurons in culture. *Journal of neuroscience research*, *26*(4), 428–35.

Mitelman, S. A., Canfield, E. L., Brickman, A. M., Shihabuddin, L., Hazlett, E. A., & Buchsbaum, M. S. (2010). Progressive ventricular expansion in chronic poor-outcome schizophrenia. *Cognitive and behavioral neurology : official journal of the Society for Behavioral and Cognitive Neurology*, *23*(2), 85–8.

Modi, P. I., Kashyap, A., Nair, V. D., Ross, G. M., Fu, M., Savelli, J. E., Marcotte, E. R., et al. (1996). Modulation of brain catecholamine absorbing proteins by dopaminergic agents. *European journal of pharmacology*, *299*(1-3), 213–20.

Mohs, R. C., Schmeidler, J., & Aryan, M. (2000). Longitudinal studies of cognitive, functional and behavioural change in patients with Alzheimer's disease. *Statistics in medicine*, *19*(11-12), 1401–9.

Moore, D. J., West, A. B., Dawson, V. L., & Dawson, T. M. (2005). Molecular pathophysiology of Parkinson's disease. *Annual review of neuroscience*, *28*, 57–87.

Munakata, K., Iwamoto, K., Bundo, M., & Kato, T. (2005). Mitochondrial DNA 3243A>G mutation and increased expression of LARS2 gene in the brains of patients with bipolar disorder and schizophrenia. *Biological psychiatry*, *57*(5), 525–32.

Nagata, K., Saga, S., & Yamada, K. M. (1988). Characterization of a novel transformation-sensitive heat-shock protein (HSP47) that binds to collagen. *Biochemical and biophysical research communications*, *153*(1), 428–34.

Nair, V. D., & Mishra, R. K. (2001). Molecular cloning, localization and characterization of a 40-kDa catecholamine-regulated protein. *Journal of neurochemistry*, *76*(4), 1142–52.

Nelson, M. D., Saykin, A. J., Flashman, L. A., & Riordan, H. J. (1998). Hippocampal volume reduction in schizophrenia as assessed by magnetic resonance imaging: a meta-analytic study. *Archives of general psychiatry*, *55*(5), 433–40.

Nilsson, L., Nordberg, A., Hardy, J., Wester, P., & Winblad, B. (1986). Physostigmine restores ^{3}H-acetylcholine efflux from Alzheimer brain slices to normal level. *Journal of neural transmission*, *67*(3-4), 275–85.

North, C., & Cadoret, R. (1981). Diagnostic discrepancy in personal accounts of patients with “schizophrenia”. *Archives of general psychiatry*, *38*(2), 133–7.

Nutt, J. G., & Wooten, G. F. (2005). Clinical practice. Diagnosis and initial management of Parkinson’s disease. *The New England journal of medicine*, *353*(10), 1021–7.

Oddo, S., Caccamo, A., Shepherd, J. D., Murphy, M. P., Golde, T. E., Kayed, R., Metherate, R., et al. (2003). Triple-transgenic model of Alzheimer’s disease with plaques and tangles: intracellular Abeta and synaptic dysfunction. *Neuron*, *39*(3), 409–21.

Osorio, C., Sullivan, P. M., He, D. N., Mace, B. E., Ervin, J. F., Strittmatter, W. J., & Alzate, O. (2007). Mortalin is regulated by APOE in hippocampus of AD patients and by human APOE in TR mice. *Neurobiology of aging*, *28*(12), 1853–62.

Pae, C. U., Drago, A., Kim, J. J., Mandelli, L., De Ronchi, D., & Serretti, A. (2009). The impact of heat shock protein 70 gene variations on clinical presentation and outcome in schizophrenic inpatients. *Neuropsychobiology*, *59*(3), 135–41.

Pae, C. U., Kim, T. S., Kwon, O. J., Artioli, P., Serretti, A., Lee, C. U., Lee, S. J., et al. (2005). Polymorphisms of heat shock protein 70 gene (HSPA1A, HSPA1B and HSPA1L) and schizophrenia. *Neuroscience research*, *53*(1), 8–13.

Park, S. W., Lee, C. H., Lee, J. G., Kim, L. W., Shin, B. S., Lee, B. J., & Kim, Y. H. (2011). Protective effects of atypical antipsychotic drugs against MPP (+)-induced oxidative stress in PC12 cells. *Neuroscience research*, *69*(4), 283–90.

Pasternak, O., Westin, C. F., Bouix, S., Seidman, L. J., Goldstein, J. M., Woo, T. U. W., Petryshen, T. L., et al. (2012). Excessive extracellular volume reveals a neurodegenerative pattern in schizophrenia onset. *The Journal of neuroscience : the official journal of the Society for Neuroscience*, *32*(48), 17365–72.

Patten, D. A., Germain, M., Kelly, M. A., & Slack, R. S. (2010). Reactive oxygen species: stuck in the middle of neurodegeneration. *Journal of Alzheimer's disease : JAD*, *20 Suppl 2*, S357–67.

Pérez-Neri, I., Ramírez-Bermúdez, J., Montes, S., & Ríos, C. (2006). Possible mechanisms of neurodegeneration in schizophrenia. *Neurochemical research*, *31*(10), 1279–94.

Perry, E. K., Gibson, P. H., Blessed, G., Perry, R. H., & Tomlinson, B. E. (1977). Neurotransmitter enzyme abnormalities in senile dementia. Choline acetyltransferase and glutamic acid decarboxylase activities in necropsy brain tissue. *Journal of the neurological sciences*, *34*(2), 247–65.

Perry, E. K., Tomlinson, B. E., Blessed, G., Bergmann, K., Gibson, P. H., & Perry, R. H. (1978). Correlation of cholinergic abnormalities with senile plaques and mental test scores in senile dementia. *British medical journal*, *2*(6150), 1457–9.

Pifl, C., Reither, H., & Hornykiewicz, O. (1992). Functional sensitization of striatal dopamine D1 receptors in the 6-hydroxydopamine-lesioned rat. *Brain research*, *572*(1-2), 87–93.

Pirger, Z., Rácz, B., & Kiss, T. (2009). Dopamine-induced programmed cell death is associated with cytochrome c release and caspase-3 activation in snail salivary gland cells. *Biology of the cell / under the auspices of the European Cell Biology Organization*, *101*(2), 105–16.

Pongrac, J. L., Middleton, F. A., Peng, L., Lewis, D. A., Levitt, P., & Mirnics, K. (2004). Heat shock protein 12A shows reduced expression in the prefrontal cortex of subjects with schizophrenia. *Biological psychiatry*, *56*(12), 943–50.

Prabakaran, S., Wengenroth, M., Lockstone, H. E., Lilley, K., Leweke, F. M., & Bahn, S. (2007). 2-D DIGE analysis of liver and red blood cells provides further evidence for oxidative stress in schizophrenia. *Journal of proteome research*, *6*(1), 141–9.

Pretorius, E. (2008). The role of platelet and fibrin ultrastructure in identifying disease patterns. *Pathophysiology of haemostasis and thrombosis*, *36*(5), 251–8.

Qu, M., Zhou, Z., Xu, S., Chen, C., Yu, Z., & Wang, D. (2011). Mortalin overexpression attenuates beta-amyloid-induced neurotoxicity in SH-SY5Y cells. *Brain research*, *1368*, 336–45.

Rajput, A. H., Rozdilsky, B., & Rajput, A. (1991). Accuracy of clinical diagnosis in Parkinsonism--a prospective study. *The Canadian journal of neurological sciences. Le journal canadien des sciences neurologiques*, *18*(3), 275–8.

Ritchie, K., & Touchon, J. (1992). Heterogeneity in senile dementia of the Alzheimer type: individual differences, progressive deterioration or clinical sub-types? *Journal of clinical epidemiology*, *45*(12), 1391–8.

Ross, G. M., McCarry, B. E., & Mishra, R. K. (1995). Covalent affinity labeling of brain catecholamine-absorbing proteins using a high-specific-activity substituted tetrahydronaphthalene. *Journal of neurochemistry*, *65*(6), 2783–9.

Ross, G. M., McCarry, B. E., Thakur, S., & Mishra, R. K. (1993). Identification of novel catecholamine absorbing proteins in the central nervous system. *Journal of molecular neuroscience : MN*, *4*(3), 141–8.

Rubin, D. B. (1987). *Multiple Imputation for Nonresponse in Surveys*. Wiley Classics.

Rylett, R. J., Ball, M. J., & Colhoun, E. H. (1983). Evidence for high affinity choline transport in synaptosomes prepared from hippocampus and neocortex of patients with Alzheimer's disease. *Brain research*, *289*(1-2), 169–75.

Sajjad, M. U., Samson, B., & Wyttenbach, A. (2010). Heat shock proteins: therapeutic drug targets for chronic neurodegeneration? *Current pharmaceutical biotechnology*, *11*(2), 198–215.

Sakić, B., Szechtman, H., Denburg, S., Carbotte, R., & Denburg, J. A. (1993). Spatial learning during the course of autoimmune disease in MRL mice. *Behavioural brain research*, *54*(1), 57–66.

Schapira, A. H. V. (2009). Neurobiology and treatment of Parkinson's disease. *Trends in pharmacological sciences*, *30*(1), 41–7.

Schlesinger, M. J. (1990). Heat shock proteins. *The Journal of biological chemistry*, *265*(21), 12111–4.

Schober, A. (2004). Classic toxin-induced animal models of Parkinson's disease: 6-OHDA and MPTP. *Cell and tissue research*, *318*(1), 215–24.

Schon, E. A., & Manfredi, G. (2003). Neuronal degeneration and mitochondrial dysfunction. *The Journal of clinical investigation*, *111*(3), 303–12.

Schultz, W. (1998). Predictive Reward Signal of Dopamine Neurons Predictive Reward Signal of Dopamine Neurons. *J Neurophysiol*, 80(1):1–27.

Schwarting, R. K., & Huston, J. P. (1996). The unilateral 6-hydroxydopamine lesion model in behavioral brain research. Analysis of functional deficits, recovery and treatments. *Progress in neurobiology*, *50*(2-3), 275–331.

Schwarz, E., Prabakaran, S., Whitfield, P., Major, H., Leweke, F. M., Koethe, D., McKenna, P., et al. (2008). High throughput lipidomic profiling of schizophrenia and bipolar disorder brain tissue reveals alterations of free fatty acids, phosphatidylcholines, and ceramides. *Journal of proteome research*, *7*(10), 4266–77.

Schwarz, M. J., Riedel, M., Gruber, R., Ackenheil, M., & Müller, N. (1999). Antibodies to heat shock proteins in schizophrenic patients: implications for the mechanism of the disease. *The American journal of psychiatry*, *156*(7), 1103–4.

Seeman, P., & Kapur, S. (2000). Schizophrenia: more dopamine, more D2 receptors. *Proceedings of the National Academy of Sciences of the United States of America*, *97*(14), 7673–5.

Sharan, N, Nair, V. D., & Mishra, R. K. (2001). Modulation of a 40-kDa catecholamine regulated protein by dopamine receptor antagonists. *European journal of pharmacology*, *413*(1), 73–9.

Sharan, Niki, Chong, V. Z., Nair, V. D., Mishra, R. K., Hayes, R. J., & Gardner, E. L. (2003). Cocaine treatment increases expression of a 40 kDa catecholamine-regulated protein in discrete brain regions. *Synapse (New York, N.Y.)*, *47*(1), 33–44.

Sherer, T. B., Betarbet, R., Testa, C. M., Seo, B. B., Richardson, J. R., Kim, J. H., Miller, G. W., et al. (2003). Mechanism of toxicity in rotenone models of Parkinson's disease. *The Journal of neuroscience : the official journal of the Society for Neuroscience*, *23*(34), 10756–64.

Shi, M., Jin, J., Wang, Y., Beyer, R. P., Kitsou, E., Albin, R. L., Gearing, M., et al. (2008). Mortalin: a protein associated with progression of Parkinson disease? *Journal of neuropathology and experimental neurology*, *67*(2), 117–24.

Shi, M., Zabetian, C. P., Hancock, A. M., Ginghina, C., Hong, Z., Yearout, D., Chung, K. A., et al. (2010). Significance and confounders of peripheral DJ-1 and alpha-synuclein in Parkinson's disease. *Neuroscience letters*, *480*(1), 78–82.

Shinkai, T., Zhang, L., Mathias, S. a, & Roth, G. S. (1997). Dopamine induces apoptosis in cultured rat striatal neurons; possible mechanism of D2-dopamine receptor neuron loss during aging. *Journal of neuroscience research*, *47*(4), 393–9.

Shrivastava, M., & Vivekanandhan, S. (2011). An insight into ultrastructural and morphological alterations of platelets in neurodegenerative diseases. *Ultrastructural pathology*, *35*(3), 110–6.

Siegel, G. J., Arganoff, B. W., Albers, R. W., & Molinoff, P. B. (1994). *Basic Neurochemistry, Fifth Edition*. Raven Press.

Sim, K., DeWitt, I., Ditman, T., Zalesak, M., Greenhouse, I., Goff, D., Weiss, A. P., et al. (2006). Hippocampal and parahippocampal volumes in schizophrenia: a structural MRI study. *Schizophrenia bulletin*, *32*(2), 332–40.

Simantov, R., Blinder, E., Ratovitski, T., Tauber, M., Gabbay, M., & Porat, S. (1996). Dopamine-induced apoptosis in human neuronal cells: inhibition by nucleic acids antisense to the dopamine transporter. *Neuroscience*, *74*(1), 39–50.

Sims, N. R., Bowen, D. M., Allen, S. J., Smith, C. C., Neary, D., Thomas, D. J., & Davison, A. N. (1983). Presynaptic cholinergic dysfunction in patients with dementia. *Journal of neurochemistry*, *40*(2), 503–9.

Sirk, D., Zhu, Z., Wadia, J. S., Shulyakova, N., Phan, N., Fong, J., & Mills, L. R. (2007). Chronic exposure to sub-lethal beta-amyloid (Abeta) inhibits the import of nuclear-encoded proteins to mitochondria in differentiated PC12 cells. *Journal of neurochemistry*, *103*(5), 1989–2003.

Sklar, P., Pato, M. T., Kirby, A., Petryshen, T. L., Medeiros, H., Carvalho, C., Macedo, A., et al. (2004). Genome-wide scan in Portuguese Island families identifies 5q31-5q35 as a susceptibility locus for schizophrenia and psychosis. *Molecular psychiatry*, *9*(2), 213–8.

Stargardt, T., Weinbrenner, S., Busse, R., Juckel, G., & Gericke, C. A. (2008). Effectiveness and cost of atypical versus typical antipsychotic treatment for schizophrenia in routine care. *The journal of mental health policy and economics*, *11*(2), 89–97.

Sterniczuk, R., Antle, M. C., Laferla, F. M., & Dyck, R. H. (2010). Characterization of the 3xTg-AD mouse model of Alzheimer's disease: part 2. Behavioral and cognitive changes. *Brain research*, *1348*, 149–55.

Stokes, A. H., Hastings, T. G., & Vrana, K. E. (1999). Cytotoxic and genotoxic potential of dopamine. *Journal of neuroscience research*, *55*(6), 659–65.

Südhof, T. C. (1995). The synaptic vesicle cycle: a cascade of protein-protein interactions. *Nature*, *375*(6533), 645–53.

Sun, Y., Ouyang, Y. B., Xu, L., Chow, A. M. Y., Anderson, R., Hecker, J. G., & Giffard, R. G. (2006). The carboxyl-terminal domain of inducible Hsp70 protects from ischemic injury *in vivo* and *in vitro*. *Journal of cerebral blood flow and metabolism : official journal of the International Society of Cerebral Blood Flow and Metabolism*, *26*(7), 937–50.

Swerdlow, N. R., Braff, D. L., & Geyer, M. A. (2000). Animal models of deficient sensorimotor gating: what we know, what we think we know, and what we hope to know soon. *Behavioural pharmacology*, *11*(3-4), 185–204.

Taira, T., Saito, Y., Niki, T., Iguchi-Ariga, S. M. M., Takahashi, K., & Ariga, H. (2004). DJ-1 has a role in antioxidative stress to prevent cell death. *EMBO reports*, *5*(2), 213–8.

Thompson, T. L., & Moss, R. L. (1995). *In vivo* stimulated dopamine release in the nucleus accumbens: modulation by the prefrontal cortex. *Brain research*, *686*(1), 93–8.

Tolosa, E., Wenning, G., & Poewe, W. (2006). The diagnosis of Parkinson's disease. *Lancet neurology*, *5*(1), 75–86.

Torres, G. E., Gainetdinov, R. R., & Caron, M. G. (2003). Plasma membrane monoamine transporters: structure, regulation and function. *Nature reviews. Neuroscience*, *4*(1), 13–25.

Ungerstedt, U. (1968). 6-Hydroxy-dopamine induced degeneration of central monoamine neurons. *European journal of pharmacology*, *5*(1), 107–10.

Ungerstedt, U., & Arbuthnott, G. W. (1970). Quantitative recording of rotational behavior in rats after 6-hydroxy-dopamine lesions of the nigrostriatal dopamine system. *Brain research*, *24*(3), 485–93.

Vallone, D., Picetti, R., & Borrelli, E. (2000). Structure and function of dopamine receptors. *Neuroscience and biobehavioral reviews*, *24*(1), 125–32.

Van Den Eeden, S. K., Tanner, C. M., Bernstein, A. L., Fross, R. D., Leimpeter, A., Bloch, D. A., & Nelson, L. M. (2003). Incidence of Parkinson's disease: variation by age, gender, and race/ethnicity. *American journal of epidemiology*, *157*(11), 1015–22.

Van Laar, V. S., Dukes, A., Casco, M., & Hastings, T. G. (2008). Proteomic analysis of rat brain mitochondria following exposure to dopamine quinone: implications for Parkinson disease. *Neurobiology of disease*, *29*(3), 477–89.

Volobоueva, L., Duane, M., Ouyang, Y., Emery, J. F., Story, C., & Giffard, R. G. (2008). Overexpression of mitochondrial Hsp70/Hsp75 protects astrocytes against ischemic injury *in vitro*. *Journal of cerebral blood flow and metabolism : official journal of the International Society of Cerebral Blood Flow and Metabolism*, *28*(5), 1009–16.

Volobоueva, L. A., Such, S. W., Swanson, R. A., & Giffard, R. G. (2007). Inhibition of mitochondrial function in astrocytes: implications for neuroprotection. *Journal of neurochemistry*, *102*(4), 1383–94.

Walker, C., Böttger, S., & Low, B. (2006). Mortalin-based cytoplasmic sequestration of p53 in a nonmammalian cancer model. *The American journal of pathology*, *168*(5), 1526–30.

Walsh, D., Li, K., Crowther, C., Marsh, D., & Edwards, M. (1991). Thermotolerance and heat shock response during early development of the mammalian embryo. *Results and problems in cell differentiation*, *17*, 58–70.

Wei, Z., Bai, O., Richardson, J. S., Mousseau, D. D., & Li, X. M. (2003). Olanzapine protects PC12 cells from oxidative stress induced by hydrogen peroxide. *Journal of neuroscience research*, *73*(3), 364–8.

Wei, Z., Mousseau, D. D., Richardson, J. S., Dyck, L. E., & Li, X. M. (2003). Atypical antipsychotics attenuate neurotoxicity of beta-amyloid (25-35) by modulating Box and Bbl.-X(l/s) expression and localization. *Journal of neuroscience research*, *74*(6), 942–7.

Weiss, M. L., Medicetty, S., Bledsoe, A. R., Rachakatla, R. S., Choi, M., Merchav, S., Luo, Y., et al. (2006). Human umbilical cord matrix stem cells: preliminary characterization and effect of transplantation in a rodent model of Parkinson's disease. *Stem cells (Dayton, Ohio)*, *24*(3), 781–92.

Wilcock, G. K., Esiri, M. M., Bowen, D. M., & Smith, C. C. (1982). Alzheimer's disease. Correlation of cortical choline acetyltransferase activity with the severity of dementia and histological abnormalities. *Journal of the neurological sciences*, *57*(2-3), 407–17.

Wood, S. J., Yücel, M., Pantelis, C., & Berk, M. (2009). Neurobiology of schizophrenia spectrum disorders: the role of oxidative stress. *Annals of the Academy of Medicine, Singapore*, *38*(5), 396–6.

Wood-Kaczmar, A., Gandhi, S., & Wood, N. W. (2006). Understanding the molecular causes of Parkinson's disease. *Trends in molecular medicine*, *12*(11), 521–8.

Xu, L., Volobouevа, L. A., Ouyang, Y., Emery, J. F., & Giffard, R. G. (2009). Overexpression of mitochondrial Hsp70/Hsp75 in rat brain protects mitochondria, reduces oxidative stress, and protects from focal ischemia. *Journal of cerebral blood flow and metabolism : official journal of the International Society of Cerebral Blood Flow and Metabolism*, *29*(2), 365–74.

Yaari, R., & Corey-Bloom, J. (2007). Alzheimer's disease. *Seminars in neurology*, *27*(1), 32–41.

Yang, H., Zhou, X., Liu, X., Yang, L., Chen, Q., Zhao, D., Zuo, J., et al. (2011). Mitochondrial dysfunction induced by knockdown of mortalin is rescued by Parkin. *Biochemical and biophysical research communications*, *410*(1), 114–20.

Yao, J K, Reddy, R. D., & Van Kammen, D. P. (2001). Oxidative damage and schizophrenia: an overview of the evidence and its therapeutic implications. *CNS drugs*, *15*(4), 287–310.

Yao, Jeffrey K, Dougherty, G. G., Reddy, R. D., Keshavan, M. S., Montrose, D. M., Matson, W. R., McEvoy, J., et al. (2010). Homeostatic imbalance of purine catabolism in first-episode neuroleptic-naïve patients with schizophrenia. *PloS one*, *5*(3), e9508.

Yao, Jeffrey K, & Keshavan, M. S. (2011). Antioxidants, redox signaling, and pathophysiology in schizophrenia: an integrative view. *Antioxidants & redox signaling*, *15*(7), 2011–35.

Yu, W., Sun, Y., Guo, S., & Lu, B. (2011). The PINK1/Parkin pathway regulates mitochondrial dynamics and function in mammalian hippocampal and dopaminergic neurons. *Human molecular genetics*, *20*(16), 3227–40.

Zhang, J., Price, J. O., Graham, D. G., & Montine, T. J. (1998). Secondary excitotoxicity contributes to dopamine-induced apoptosis of dopaminergic neuronal cultures. *Biochemical and biophysical research communications*, *248*(3), 812–6.

Zhang, X. Y., Chen, D. C., Xiu, M. H., Wang, F., Qi, L. Y., Sun, H. Q., Chen, S., et al. (2009). The novel oxidative stress marker thioredoxin is increased in first-episode schizophrenic patients. *Schizophrenia research*, *113*(2-3), 151–7.